1-1-2016

A Petrographic Analysis of the Microbial Thrombolite Buildup in the Oxfordian Smackover Formation, Little Cedar Creek Field, Alabama

Natalie Samaidegaarden

A petrographic analysis of the microbial thrombolite buildup in the Oxfordian Smackover Formation, Little Cedar Creek Field, Alabama

By

Natalie Samai-Odegaarden

A Thesis
Submitted to the Faculty of
Mississippi State University
in Partial Fulfillment of the Requirements
for the Degree of Master of Science
in Geology
in the Department of Geosciences

Mississippi State, Mississippi

May 2016

A petrographic analysis of the microbial thrombolite buildup in the Oxfordian Smackover Formation, Little Cedar Creek Field, Alabama

By

Natalie Samai-Odegaarden

Approved:

_____

Brenda L. Kirkland
(Major Professor)

_____

Adam Skarke
(Committee Professor)

_____

Darrel W. Schmitz
(Committee Member)

_____

Ezat Heydari
(Committee Member)

_____

Michael E. Brown
(Graduate Coordinator)

_____

Rick Travis
Interim Dean
College of Arts & Sciences

Name: Natalie Samai-Odegaarden

Date of Degree: May 7, 2016

Institution: Mississippi State University

Major Field: Geology

Major Professor: Dr. Brenda Kirkland

Title of Study: A petrographic analysis of the microbial thrombolite buildup in the Oxfordian Smackover Formation, Little Cedar Creek Field, Alabama

Pages in Study 124

Candidate for Degree of Master of Science

The Jurassic (Oxfordian) Smackover Formation in Little Cedar Creek Field, Alabama is composed of microbial thrombolitic buildups. Core description, petrography, SEM, and isotopic analysis were used to identify the succession of organisms, microbial carbonate deposition, and diagenesis that contributed to formation of these thrombolitic buildups. The microbial thrombolite reef facies in this study accounts for 38.5% of the total Smackover Formation. This facies was deposited 0.5 to 6.75 miles from the paleo-coastline. Today it is located 10,225 to 11,750 feet in the subsurface and contains buildups 26 to 50 feet thick. Four microfacies were defined: A- Black *Renalcis*-like layers, B- Digitate, C- Chaotic and D- Brown laminated centimeter-scale cycles. In most of the buildup, distinct layers of microbially precipitated micrite forms in succession. Microfacies A (Black *Renalcis*-like Layer) is the relatively least porous and permeable, acting as a potential barrier to flow in contrast to the other more porous microfacies.

DEDICATION

As a self-funded graduate student my original plan was to get in, get out and socialize as little as possible. However, after meeting all the wonderful students, professors and staff at the Geosciences Department who eventually became my friends, I would like to dedicate this thesis to them. To all of my past and present "basement" friends Jonney, Taryn, Brookes, Asa, Aleks, Courtney, Patrick, Dora, and Mehnaz, thank you for the priceless memories and for being the best group of friends anyone could ever ask for. Jonney Mitchell and Taryn Smith, without your help it would have taken me forever to map and polish my cores. I will always have fond memories of the time we spent working at Buckner. To the most patient and helpful geosciences office staff, thank you especially Tina Davis, for always answering my numerous questions with a happy smile. I would also like to give dedication to my precious family in Trinidad Ramlakhan, Brenda, Samantha and Gary Samai whose persistent question of, "are you done yet?" kept me going.

ACKNOWLEDGEMENTS

I would like to first and foremost thank my advisor, Dr. Brenda Kirkland for continuously guiding me through my project and opening my eyes to the importance of microbes and the role they play in carbonates. Her enthusiasm was infectious. To my committee members also a big thank you, to Dr. Ezat Heydari for locating the cores for this study and also Dr. Darrel Schmitz and Dr. Adam Skarke for the courses they taught that helped me prepare for the work ahead.

I would also like to thank the staff at the Alabama State Oil and Gas Board and the Alabama Stable Isotope lab at Tuscaloosa for allowing me unlimited access to the cores and for analyzing my isotope samples free of charge.

Finally, I'd like to thank the Geosciences Department for use of equipment such as the micro miller, microscopes, core polishing equipment and Petra software. Also, thank you so very much for paying for my thin sections and for allowing me to print posters for various conventions.

TABLE OF CONTENTS

LIST OF TABLES

LIST OF FIGURES

CHAPTER I

INTRODUCTION

The Gulf of Mexico Basin is one of the most productive hydrocarbon basins in the world, with a history stretching more than 100 years and the discovery of more than 230 billion barrels of oil equivalent since the early 1990's (Salvador, 1987 and Galloway, 2009). Based on geologic age, Cenozoic sediments are the most prolific reservoirs, yielding 130 billion barrels of oil equivalent, followed by Cretaceous sediments, with more than 85 billion barrels of oil equivalent and, lastly the oldest rocks in the basin, the Jurassic sediments, with 15 billion barrels of oil equivalent (Galloway, 2009).

The Upper Jurassic (Oxfordian) Smackover Formation today, occurs in the subsurface as a belt of limestone deposited on a carbonate ramp. It extends across the northern rim of the Gulf of Mexico from Florida to South Texas and as far north as southern Arkansas (Oehler, 1981) (Figure 1). It consists of carbonate, evaporite, and clastic rocks (Oehler, 1981). It does not outcrop at the surface in the northern Gulf Coast and is a prolific hydrocarbon source and reservoir with production coming from a variety of structural, stratigraphic, diagenetic, and combination traps (Lieber, 1989).

The Little Cedar Creek Field (LCCF) is an onshore oil field located in southwestern Alabama, in the northeastern Gulf of Mexico. The Smackover Formation was deposited during a major marine transgression and highstand on a ramp-like platform across the northern rim of the Gulf of Mexico during the Late Jurassic after tensional

deformation of the continental crust ceased and basinal subsidence followed. The Smackover oil pool in Little Cedar Creek Field consists of two reservoirs separated from one another by inter-buildups of non-porous and non-permeable horizons based on lithofacies analysis (Heydari and Baria, 2006). A lower and upper reservoir of microbial carbonate facies and associated nearshore ooid-grainstone carbonate bank facies that overlie conglomerate and sandstone facies of the Norphlet Formation and underlie argillaceous, anhydrite and carbonaceous facies of the Haynesville Formation (Haddad and Mancini, 2013a).

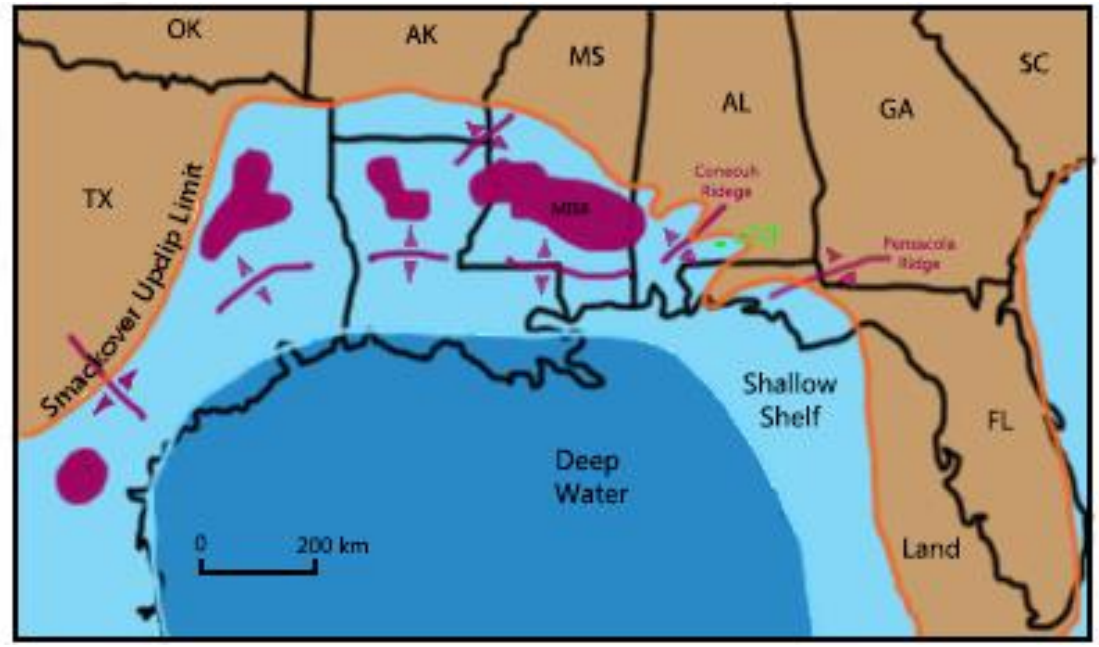

Figure 1 The map shows the updip limit of the Smackover Formation and location of the Little Cedar Creek field.

(It also shows salt basins and structural elements in the southeastern United States, modified from Wade and Moore, 1993).

Depositional facies, along with diagenesis and dolomitization, control the quality of reservoir rocks. The microbial buildups that formed in the Smackover Formation occur

as clusters and belts that influence the heterogeneity of the reservoirs. The exploration strategy used to find hydrocarbon-productive microbial and high-energy, nearshore carbonate facies in the Smackover of the Little Cedar Creek Field requires refinement to increase the probability of identifying and delineating these potential reservoir facies (Mancini et al., 2006).

Refinement through microfacies analysis of cores can provide information that can aid in understanding other heterogeneous Upper Jurassic hydrocarbon productive microbial facies associated with stratigraphic traps. Because the arrangement of the framework of the thrombolitic Smackover Formation in the Little Cedar Creek Field form pore types that are mainly vuggy and intercrystalline, connectivity evaluation studies were undertaken on Holocene microbialites from Brazil and compared to Smackover microbialites to make refined depositional models for better subsurface prediction. It was shown that the primary pore network is related to textural changes in microbialite successions driven by environmental changes, which can reduce or enhance reservoir quality by diagenesis (Rezende *et. al*., 2013, Tonietto *et. al*., 2014).

A microbial origin of the framework is based on the distribution, texture, fossil content, and order of microstratigraphic succession (Kirkland *et. al*., 1998). Textural changes are formed by the arrangement of pellets, peloids, ostracods and benthic foraminifera making up the framework. Depositional textures control structure size, packing and framework fabric, which in turn influence the pore volume and number of pore throat, therefore, large structures with open packing, and chaotic framework fabric had a good connected pore network (Rezende *et al*., 2013). Dolomitized textures have intercrystalline porosity resulting in hydrocarbon reservoirs with a homogeneous pore

system. Identification of microbial successions in the sub-facies from the thrombolitic cores in my study area will further enhance understanding of these complex textural changes in microbial buildups

Statement of Problem/Hypothesis

The hypothesis is that the Little Cedar Creek Field Smackover Formation buildups can be divided into microfacies and that their distribution is therefore to some extent predictable.

Objectives

The Little Cedar Creek Field is located near the up dip limit of the Smackover Formation in Conecuh County, Alabama. The field produces oil from dual microbial carbonate reservoirs (ooid grainstone and thrombolite boundstone) i.e. there are seven litho- facies that make up the Smackover Formation and of these, two are permeable and porous thus forming reservoirs, whilst the other facies sandwiching them are not porous and permeable therefore acting as vertical seals. Diagenesis though dissolution, re-precipitation, and dolomitization has allowed for the preservation of the original carbonate fabric. Good porosity and permeability along with preservation makes this field a rich oil producer and ideal for studying microbial buildups.

The objective of this study is to 1) establish the microstratigraphic succession of events that led to the formation of these buildups in the lower, thrombolitic boundstone reservoir; and 2) to determine if freshwater or seawater influenced the distribution of the buildups. This ultimately aids in understanding the complexity of reservoir heterogeneity as well as deepens understanding of the origin of these enigmatic buildups.

Ten cores retrieved from wells that run parallel to the up dip limit of the Smackover Formation and well logs were used for correlation (Figure 2). Each core will be described using the Dunham classification scheme to construct stratigraphic columns. Descriptions of lithologies will be made to define microfacies and assess distribution. Based on the descriptions, the cores will be grouped into microfacies and thin sections will be made from each representative microfacies in order to document evidence of microbial fabrics. A scanner will be used to image a representative core of each microfacies and Photoshop software will be used for mapping the succession of events that led to the microbial buildup. SEM will help confirm evidence of microbes. Lastly, isotopic analysis for carbon and oxygen isotope ratios will determine if fresh water or seawater influenced the buildups.

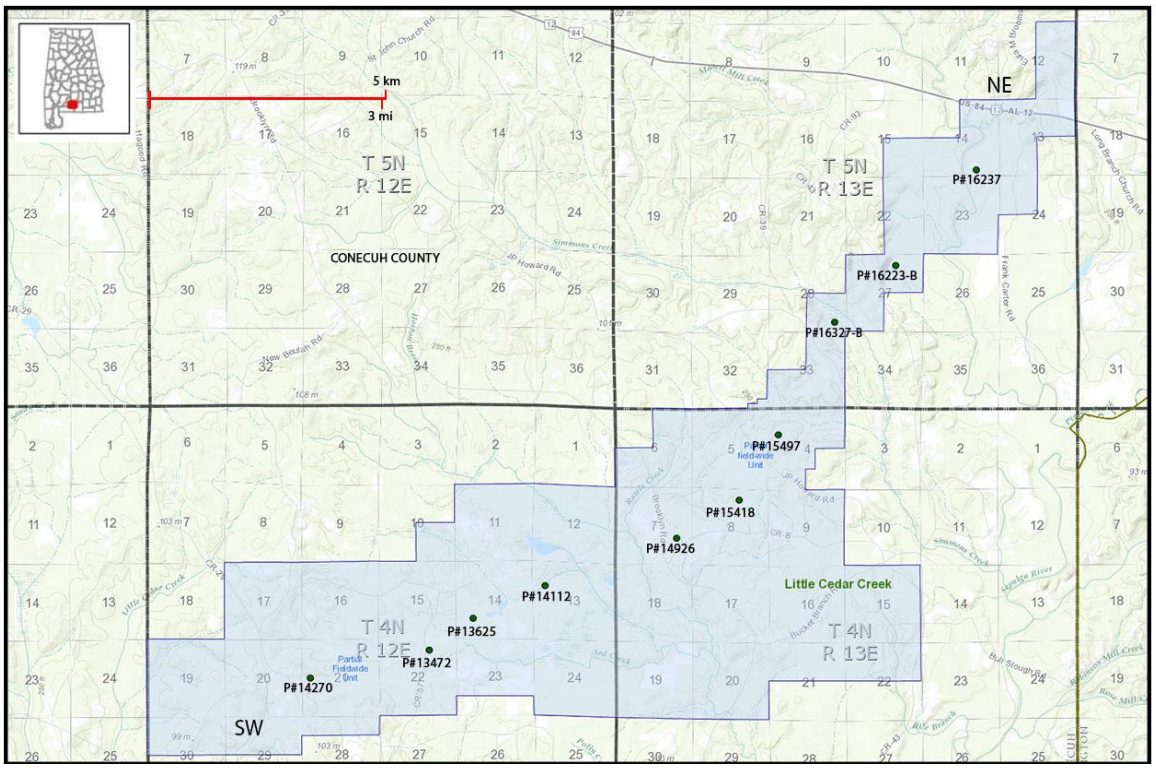

Figure 2 Cores for this study were retrieved from these ten wells in the Little Cedar Creek Field, Alabama.

Literature Review

History and Field Location

The Smackover Formation was first discovered in Union County, Arkansas around 1936 when the Phillips Petroleum Company drilled a discovery well, Reynolds No. 1 intercepting an oil and gas limestone reservoir at 1,493 meters (4,897 feet), it was aptly named the Reynolds Oolite. In literature, the Reynolds's Oolite is now commonly referred to as an ooid grainstone. The Smackover Formation's name was derived from a small agricultural and sawmill community in Arkansas that had been first settled by French fur trappers in 1844 called, "Sumac-Couvert" meaning covered with sumac or shumate bushes (Alabama Oil and Gas Historical Society, 2015). However, it was D.H.

Bingham, a petroleum geologist who coined the term Smackover in 1937 on account of the Phillips Petroleum Company discovery well in limestone and a mispronunciation of the town's name, "Sumac-Couvert" where the limestone was first discovered.

In Alabama, oil was first discovered in the Smackover Formation in 1967 at the Toxey Field in Choctaw County when, the wildcat well #1 Scott Paper Co.-S.H.Bolinger 4-8 intercepted the top of the formation at a depth of 10,461 feet. The Little Cedar Creek Field was discovered in 1994 by the Hunt Oil Company after drilling the Cedar Creek Land & Timber Company 30-1 No.1 well, Permit No. 10560 in Conecuh County, Alabama. The Upper Jurassic (Oxfordian) Smackover Formation was perforated at a depth of 3,618 to 3,622 meters (11,870 to 11,883 feet) and was completed as an oil producer at a total depth of 3,658 meters (12,000 feet) (Geological Survey of Alabama, 2012).

The Conecuh Embayment in southwestern Alabama encompasses the counties of Escambia, Covington, and Conecuh hosting several oil fields that produce from the Smackover Oil Pool. The Little Cedar Creek Field is located in Conecuh County, spans 27.4 kilometers (17 miles) paralleling the up dip limit of the Smackover Formation in a southwestern-northeastern trend in blocks 4N12E, 4N13E, 5N13E, and 5N15E respectively (Figure 2). According to the Alabama State Oil and Gas Board database, as of 2013, approximately 134 fields have been developed with the Little Cedar Creek Field and the Brooklyn Field being the largest oil field discoveries in the state. As of July 2014, the Smackover Pool in the Little Cedar Creek Field has produced 18,417,638 barrels of oil or condensate and 22,285,312 thousand cubic feet of gas. It is now considered a

mature field that was unitized in part in 2005. Secondary recovery through gas injection began in 2007 (GSA, 2012).

Geologic Setting

The Gulf of Mexico (GOM) is a divergent-margin basin created by the breakup of Pangea and is defined by extensional rift tectonics and wrench faulting (Mancini et al., 2001, Salvador, 1987). The evolution of the basin spans from the Late Triassic to Cretaceous and is characterized by two tectono-stratigraphic periods (Salvador, 1991). The two periods include, the Late Triassic to the end of the Middle Jurassic defined by active rifting/tensional deformation and the Late Jurassic to Cretaceous tectonic stability defined by subsidence and vertical deformation from plastic salt flow (Salvador, 1987).

Late Paleozoic collision of the Afro-South American Plate into North America produced the Appalachian-Ouachita-Marathon orogeny during the final stages of assembly of the supercontinent Pangea. Initial Mesozoic rifting of Pangea produced the zone that was to become the passive margin of the North American plate and the Yucatan microplate, characterized by peripheral horst and graben structures in the Gulf of Mexico basin. Thick non-marine red-bed clastics derived from bounding horst blocks accumulated in the rapidly subsiding grabens and were deposited as alluvial fans and fluvial, delta-plain, or freshwater-lake deposits (Salvador, 1991). The red-beds were named the Eagle Mills Formation and are commonly associated volcanics relating to continental crustal stretching (Figure 3).

The latter rifting stage in the late Middle Jurassic (Callovian) resulted in thick, extensive deposition of the Louann Salt and the Werner Anhydrite. This period marked the intermittent influx of seawater from the Pacific to the Gulf of Mexico basin where it

filled shallow depressions of the continental surface produced by the graben systems of the Late Triassic. The restricted shallow embayments compounded by the arid climate at the time produced large hypersaline water bodies that allowed for the accumulation of large quantities of halite in the central basin and anhydrite the periphery. After salt deposition ended, postsalt crustal stretching occurred from continued rifting until sea-floor spreading of oceanic crust divided the salt into two pieces on opposite sides of the ocean basin (Hudec et al., 2013). The once shallow, hypersaline water bodies of the Callovian were replaced during the Oxfordian by an increasingly larger and deeper body of water with unrestricted circulation and normal salinity commonly known as the ancestral Gulf of Mexico.

The second phase of the basin's evolution began in the Late Jurassic (Oxfordian) and was a stable tectonic phase marked by basinal subsidence and salt flow. The Oxfordian sequence was deposited at this time and consisted predominantly of deep shelf marine sediments composed of carbonates, calcareous shales, and siliciclastic shales. The Norphlet Formation a conglomerate and sandstone unit at the base of this sequence is included in the Oxfordian (Hazzard, 1939). It is interpreted as representing fluvial and eolian deposits (Mancini *et al*., 1985). The upper Oxfordian sequence is called the Smackover Formation and is divided into two units, a lower dark carbonate mudstone formed in a low-energy environment and an upper grain-supported microbial carbonate, formed in a high-energy shallow water environment. This upper unit provides the reservoir rock for numerous oil and gas fields in the U.S Gulf Coast. Lateral gradations are also recognized in the upper Oxfordian, with coarser clastic landward deposits grading into grainstones and packstones typical of a shallow shelf or ramp, then into

shales and shaley limestones indicating deposition in a deeper shelf. The coarse terrigenous clastics indicate that a proximal fluvial system, likely the ancestral Mississippi River, was draining the North American continental interior. Generally, after the mid-Oxfordian tectonic activity shifted southward to the Caribbean region (Salvador, 1991). The Late Jurassic is characterized as tectonically stable, allowing for the predominantly marine Upper Jurassic section to be deposited on broad stable ramps and shelves (Salvador, 1991).

During the Kimmeridgian stage, marine invasion continued overstepping the Oxfordian and pinching out farther landward reflecting deposition in a marine or shallower marine environment (Salvador, 1991). It is characterized by evaporitic deposits (mainly anhydrite) and associated red-beds formed in hypersaline coastal lagoons or sabkhas and is named the Buckner Anhydrite, which is the evaporitic member of the Haynesville Formation. Oolitic grainstones deposited as elongated offshore bars and shoals formed a restrictive barrier environment behind which the evaporites formed. By the end of the Jurassic the basic structural, stratigraphic and geographic features of the Gulf of Mexico known today, were virtually present.

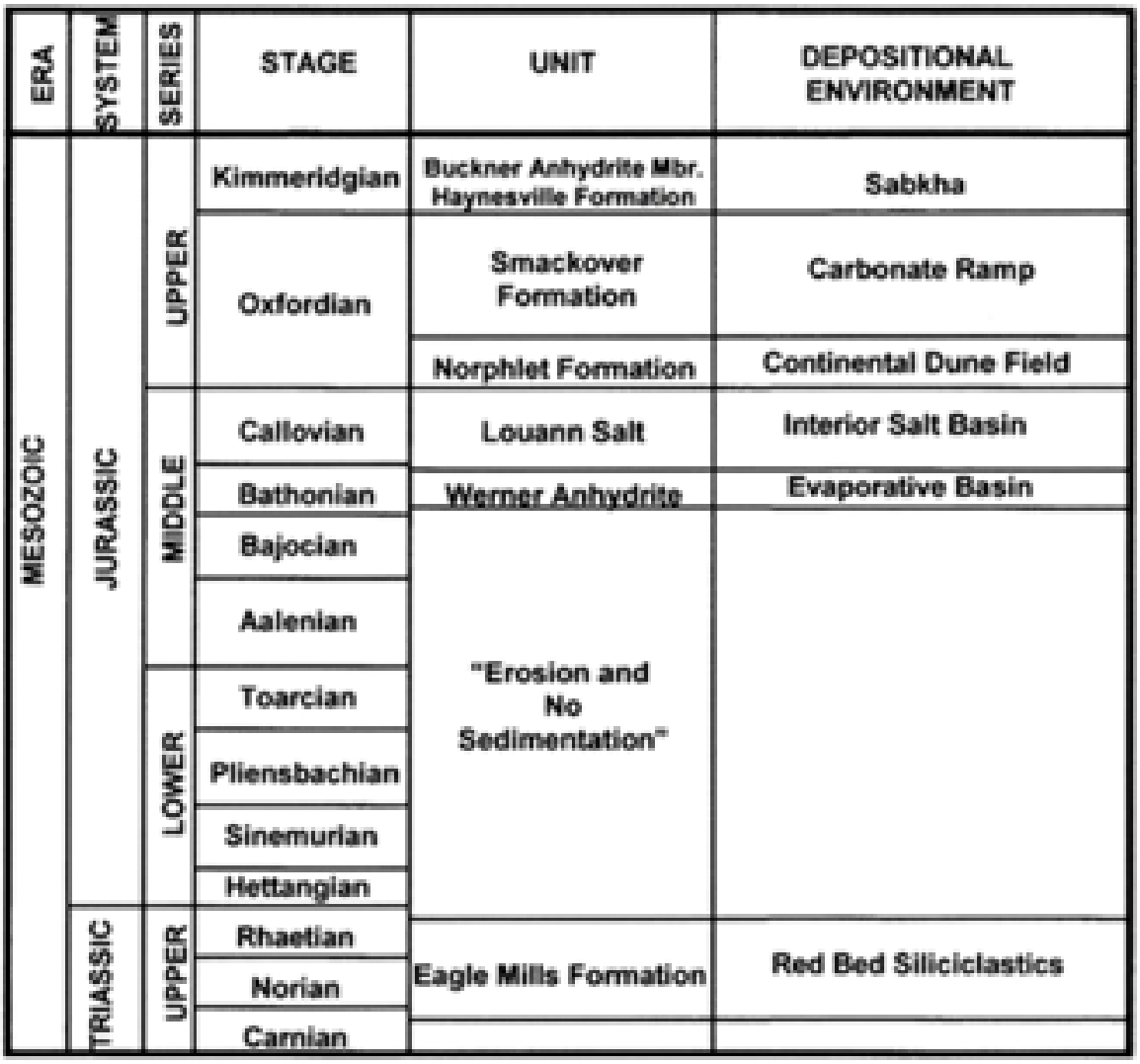

Figure 3 Stratigraphic record of the units and possible depositional environment during the evolution of the Gulf of Mexico

(Tedesco, 2003)

Regional Structure and Stratigraphy

The Conecuh Embayment is located in a relatively tectonically stable area approximately 70 by 80 km in dimension and is a broad paleotopographic low within the western prong of the South Georgia rift system (Prather, 1992). It is bounded to the west and east by the Conecuh Ridge complex and Pensacola Ridge respectively and, to the

south by the Pollard Foshee Fault Zone, the northern margin represents the updip limit of deposition of the Smackover Formation (Figure 4). The geologic history of the Little Cedar Creek Field is directly related to the evolution of the Conecuh Embayment, because the Paleozoic ridge represents a continuation of the Appalachian structural trend. These ridges were topographic highs at the time of Smackover deposition (Haddad and Mancini, 2013a). The ridges acted as barriers from ocean currents and wave energy producing a protected and sometimes restricted embayment area near the Smackover shoreline in the northern part of the Conecuh embayment (Haddad and Mancini, 2013a).

The embayment is essentially the inner part of the ramp where growth of the microbial buildups occurred. The climate during the Jurassic (Oxfordian) was arid. Ramps are an important carbonate depositional setting for microbial reef buildup because ramps offer an extensive, stable area with shallow seas allowing for photosynthesis and low to no sediment influx from land. Crevello and Harris (1984) classified Smackover reefs as developing on a wave-agitated ramp setting. In the northeastern Gulf Coast, the ramp system the Smackover Formation was deposited on, is partitioned by underlying basement topography, mainly the Wiggins Arch, and local structures such as the Conecuh Embayment.

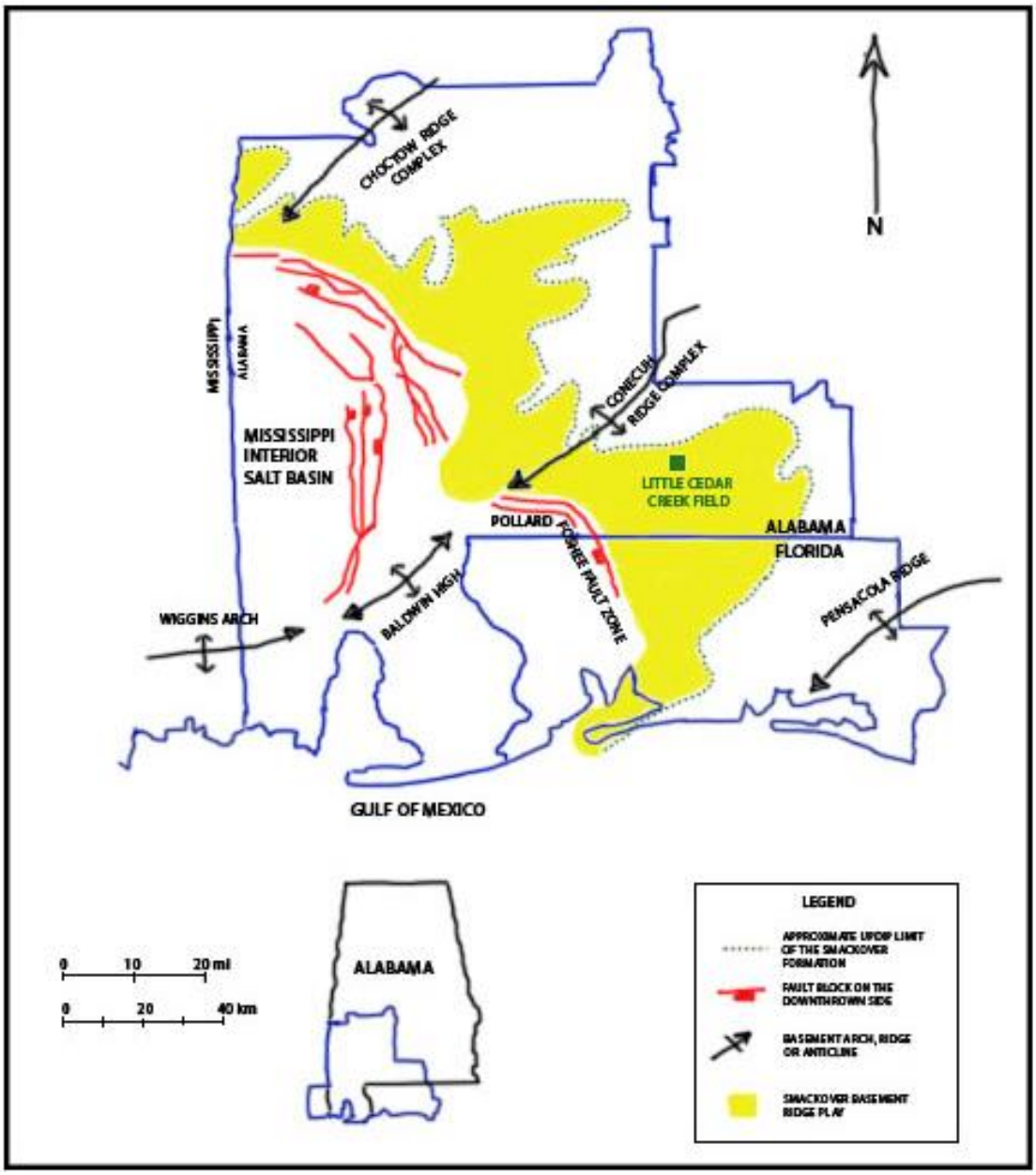

Figure 4 The location of the Little Cedar Creek Field within the Conecuh Embayment (redrawn and modified from Haddad and Mancini, 2013b)

The Wiggins Arch separates the ramp into an inner ramp associated with onshore basins from an outer ramp in offshore areas (Parcell, 1999). In Alabama, the embayments in the inner ramp north of the Wiggins Arch were created by the sea encroaching on the south end of the Appalachian Mountains upon which reefs developed in a shallow sea (Parcell, 1999). The Late Jurassic represents a major period of extensive reef development. A period of relatively high sea-level stand created shallow epeiric seas and attached ramp shelves. Microbial buildups in the Upper Jurassic (Oxfordian) Smackover Formation northeastern Gulf Coast represent microbial-dominated reef growth on a carbonate ramp (Parcell, 1999).

The Smackover Formation in the Little Cedar Creek Field is unique compared to other producing Smackover fields in southwest Alabama because, it does not possess a Buckner anhydrite top seal, lacks structural closure, and is composed of limestone rather than dolomite. In this field, the formation unconformably overlies Norphlet conglomeratic sandstone, and is disconformably overlain by the argillaceous Haynesville Formation (Figure 5). The Smackover within the Little Cedar Creek Field in the Conecuh Embayment is only 80-100 ft (24-30 m) thick. It consists of seven distinct lithofacies (S1-S7) that range in depositional environment from mid-ramp to tidal flat deposits (Heydari and Baria, 2005; 2006) (Figures 6). Other authors though have established six lithofacies by grouping S1 and S2 as one lithofacies (Mancini, et al., 2006). The seven lithofacies from base to top are: S1 a transgressive laminated peloid wackestone; S2 bioturbated, peloid packstone; S3 microbial (thrombolite) boundstone; S4 laminated peloid wackestone- packstone; S5 bioturbated peloid packstone; S6 peloid-ooid grainstone; and S7 wackestone, shale, and siltstone (Heydari and Baria, 2006)

(Figure 6). The formation in southwest Alabama is substantially thin compared to those found in the four marginal salt basins (Wade and Moore, 1993). Parcell (1999) observed that the Smackover reefs developed during a transgressive event, and growth ceased during the time of maximum water depth.

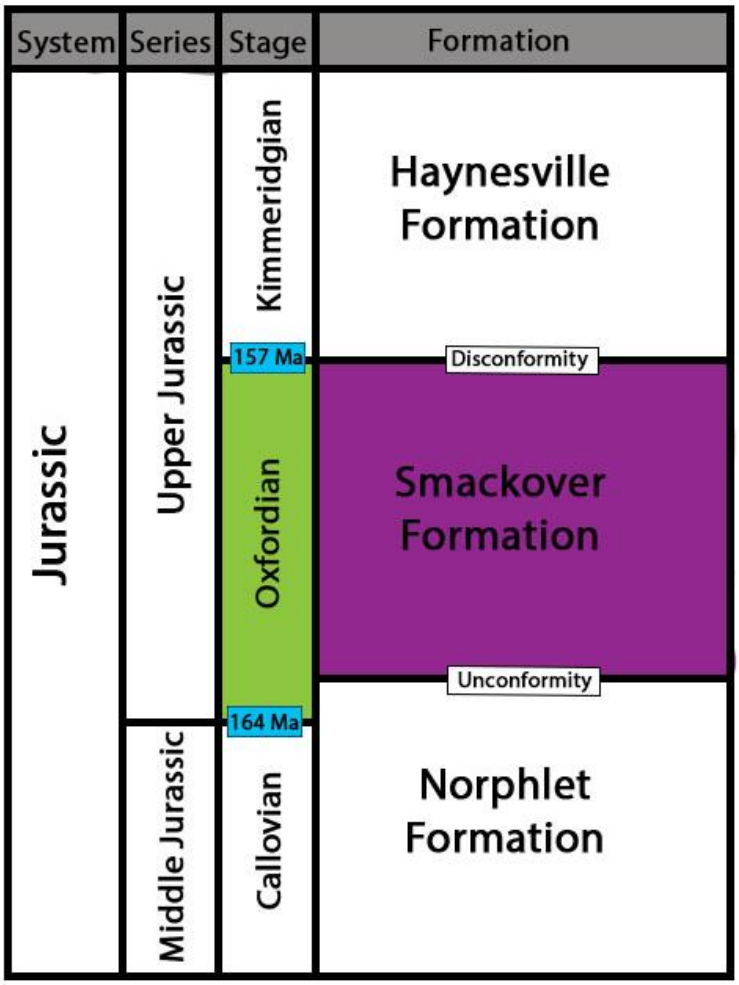

Figure 5 Jurassic (Oxfordian) stratigraphy in the Little Cedar Creek Field, Alabama

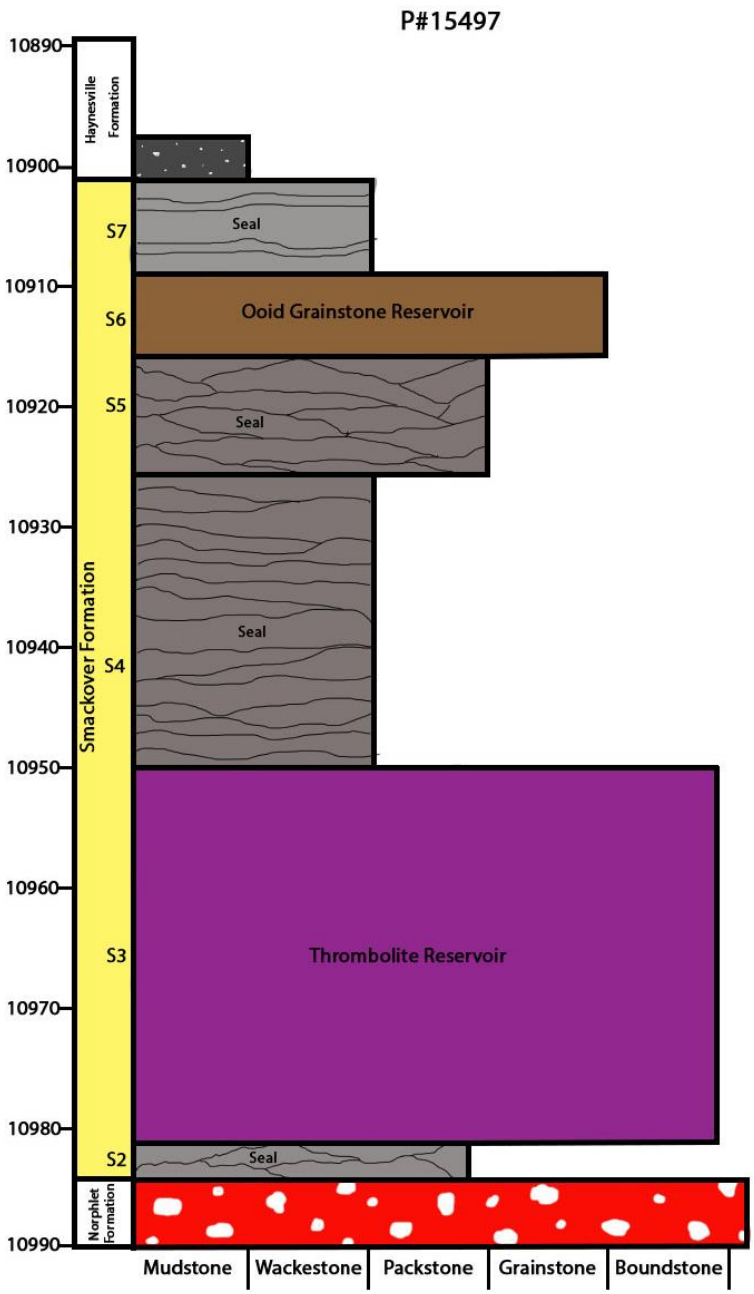

Figure 6 Stratigraphic column for the well P#15497 shows six of the seven lithofacies that make up the Smackover Formation in the Little Cedar Creek Field, Alabama

The lithofacies sequence and respective depositional environments indicate a shoaling upward cycle formed by the southward progradation following a rapid transgression (Heydari and Baria, 2005). Nearly every lithofacies of the Smackover Formation exhibits microbial features, making the entire thickness of the formation microbial in origin. The microbial origin of this unit is interpreted as a result of harsh environmental conditions imposed by the geometry of the embayment, the ramp, low energy conditions, and poor seawater circulation (Heydari and Baria, 2005).

The petroleum trap in the Little Cedar Creek Field is stratigraphic. It is characterized by microbial boundstone and packstone and nearshore grainstone and packstone reservoirs that are underlain and overlain by lime mudstone and dolomudstone to wackestone that grades into lime mudstone and dolomudstone near the depositional updip limit of the Smackover Formation (Mancini, *et al*., 2008). These facies are interpreted to have accumulated in water depths of approximately 3m (10 ft) and in 5 km (3 mi) from the paleo-shoreline (Mancini, *et al*., 2008). These reservoir rocks trend from southwest to northeast and the thrombolites did not grow directly on paleohighs associated with Paleozoic crystalline rocks in contrast to other thrombolites identified in the Gulf coastal plain (Mancini, *et al*., 2008). Instead, the microbial buildups developed on mudstone facies and retained a large percentage of primary depositional fabrics (Day and Parcell, 2013). The seven lithofacies (S1-S7 in ascending order) previously mentioned are responsible for forming reservoir and seal because the Buckner Anhydrite seal is lacking. The Buckner Anhydrite is a member of the Haynesville Formation. The S3 microbial boundstone and the S6 peloid-ooid grainstone form excellent reservoirs and are separated by S4 and S5 and sealed by the S7 facies respectively (Figure 6). The

excellent porosity and permeability of the microbial lithofacies of the Smackover Formation makes it an important unit to study.

What are Microbial Buildups?

According to Riding (2000), microbial carbonate (microbialites) is biologically stimulated and the principal organisms involved in microbial carbonate buildups are bacteria, particularly cyanobacteria (benthic), small algae and fungi, that participate in the growth of microbial biofilms and mats. Cyanobacteria are alga-like bacteria that have a long geologic history, can be benthic or planktonic allowing for their occurrence in a wide realm of environments and conditions, and can perform photosynthesis and nitrogen fixation (Riding, 2011a). Microbial growth predominantly occurs in seas and lakes, producing micro-fabrics that are heterogeneous. The three main processes involved in the formation of microbial carbonates are 1) grain-trapping, 2) biomineralization of organic tissue and, 3) surficial precipitation of minerals on organisms and sediments, producing reefal accumulations of calcified microbes and enhancing mat accretion and preservation. Biomineralization preserves the most information concerning the organisms involved, trapping preserves the least and surface mineralization is intermediate preserving only the exterior size and shape of the organisms. Carbonate precipitation can occur through various metabolic processes such as, photosynthetic uptake of CO_2 and/or HCO_3 by cyanobacteria, and ammonification, denitrification and sulphate reduction by other bacteria increasing alkalinity.

Microbial buildups are biological in origin, i.e. the sediments are biotically induced/stimulated rather than biotically controlled or abiotically precipitated. Stimulated biomineralization in microbial carbonates refer to the secretion of metabolic byproducts

by bacteria extracellularly such as on the cell walls or exopolymers (slimes, sheaths, biofilms), which reacts with ions or compounds in the environment to precipitate minerals randomly on the external cell walls (Frankel and Bazylinski, 2003) e.g. the induced precipitation of $CaCO_3$ from bacteria, which is deposited as accumulations of microbial micrite after the microbes die and their soft tissue disintegrates.

Calcified microbes or calcimicrobes involve calcification of the microbe's external sheath or thallus mainly cyanobacteria e.g. *Giravanella* preserving a mold of their tiny tube morphology comprised of micritc walls. The fabric of the limestone will be clotted and finely peloidal (Flügel, 2010). The significance of calcimicrobes in microfacies analysis is the reconstruction of paleoenvironmental and ecological conditions, biostratigraphy, and their ability to form carbonate sediments, which can act as hydrocarbon source and reservoirs (Flügel, 2010).

Intracellular biomineralization has been recently recognized from work done by the discovery of a rare carbonate mineral benstonite, calcified in the cyanobacteria *Candidatus Gloeomargarita lithophora* in an alkaline lake in Mexico (Cordeau et al., 2012). The benstonite occurs as inclusions in the cyanobacteria in the form of spheres less than 0.5 μm across, can act as ballast, and may help understand the geologic record of cyanobacteria in rocks older than 1200 million years old if barium and strontium are present in the benstonite inclusions.

Calcified cyanobacteria fossil's distribution through the geologic record shows a scarcity in rocks older than 1200 million years ago, becoming discernible during the Neoproterozoic, when the first well-calcified cyanobacteria were recognized. They are found in the Paleozoic and Mesozoic, and became vanishingly scarce in the Cenozoic and

present-day seas, but locally abundant in fresh water. During the Mesozoic, calcimicrobes were common in restricted, lagoons and on an open-marine carbonate platform contributing towards the formation of reefs and mud mounds (Flügel, 2010). Today only 10% of carbonate production takes place in shallow seas. Because microbial buildups are induced biologically, environmental factors such as light, water temperature, sedimentary influx, and paleoenvironmental settings influence the distribution and frequency of organisms that produce carbonates. The two crucial environmental influences in cyanobacteria calcification are the carbonate saturation state of ambient waters, which affects precipitation of calcium carbonate minerals, and the availability of dissolved carbon dioxide, which affects photosynthesis (Riding, 2012). When levels of CO_2 decline, sheath calcification is promoted by increased bicarbonate uptake.

Cyanobacteria, cyanophytes or blue-green are procaryotes i.e. organisms lacking a discrete nucleus and membrane-bounded organelles within the cell. The cells are arranged in colonies or threads, which can be branched and enclosed in exopolymers. When the branches are calcified the microfossil exhibits microfabric morphologies such as tubes or irregular bodies, laminated or massive amalgamated masses or microbushes. The structure of the macrofabric formed by microbial buildups is determined by the assemblage geometry of the calcified microbes. The various macrofabric textures include shapes such as thrombolite (clotted), stromatolite (laminated), dendrolite (dendritic), and leolite (aphanitic) (Figure 7). The first two are most common when it comes to microbial reservoirs for hydrocarbons. Preserved microfabrics can also pinpoint environmentally-related depositional fabrics (Ahr, 2009).

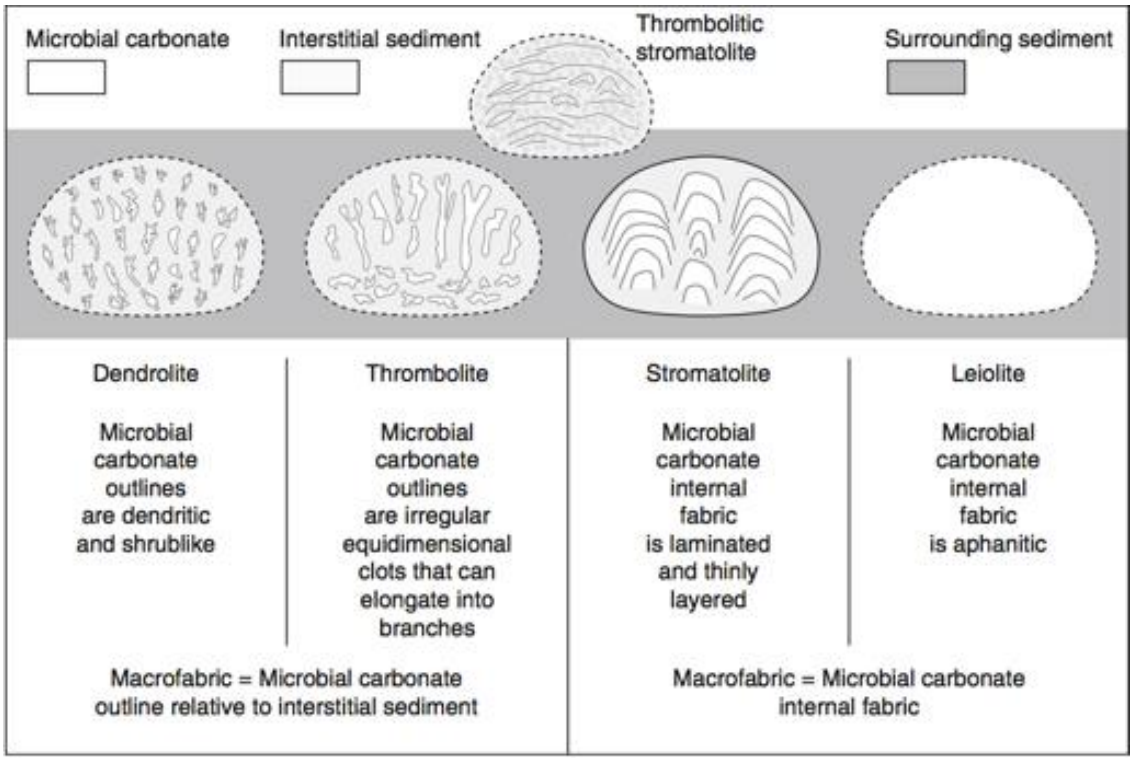

Figure 7 Macrofabrics of microbial carbonates

(Riding, 2011b)

Clots in thrombolite buildups can occur in different patterns. They can be prostrate and irregular and also vertical forming amalgamated elongate branches. Thrombolites were common in the mid-late Jurassic and the last recorded major peak of calcified marine cyanobacteria's abundance coincided with this time period (Arp et al., 2001). According to Riding (2011b) thrombolites are benthic microbial carbonates with macroclotted fabrics and the two main types of thrombolite buildups are calcified microbes and coarse agglutinated (Riding, 2011b). The metabolism mechanism of the microbes, which results in microbial carbonate deposits evolved as a response to changes in seawater and atmospheric chemistry throughout the ages. The occurrence of certain associations of cyanobacteria along with different skeletal components would be typified

of that time period therefore influencing the macro and microfabric of the buildups. For example, microbial fabrics found during the Permo-Caboniferous were microbial mud-cementstones whereas peloidal thrombolites are found in the Jurassic.

The Smackover Formation in the Little Cedar Creek Field was deposited during the Jurassic (Oxfordian) on the inner shallow (subtidal) continental shelf or ramp (Figure 8). The formation trends southwest to northeast and consists of two separate carbonate lithofacies that form hydrocarbon reservoirs. The lower reservoir is comprised of microbial buildups of subtidal thrombolitic boundstone while the upper reservoir consists of a series of progradational ooid and peloidal sand bodies in a carbonate bank setting (Haddad and Mancini, 2013).

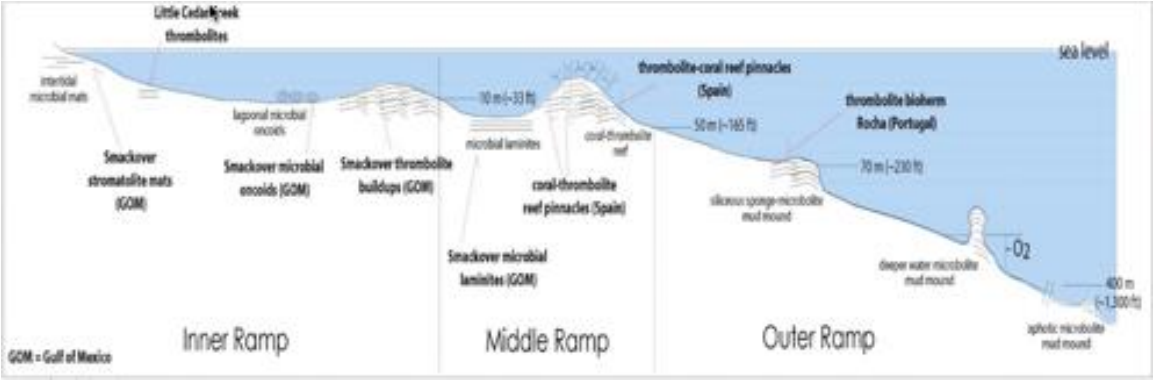

Figure 8 Depositional environments of the Smackover thrombolites (Al Haddad & Mancini, 2013a)

The trap for these reservoirs are purely stratigraphic separating the reservoirs from one another by interbuildups that act as potential barriers or baffles to the flow of hydrocarbons between reservoirs (Haddad and Mancini, 2013a). The interbuildups represent changes in depositional facies and comprise of non-porous, non-permeable

horizons of laminated and or peloidal wackestone or packstone (Heydari and Baria, 2006). In the case of the thrombolitic boundstone reservoir, the measurement of the hydrocarbon flow helped determine the distribution of the microbial boundstone (Haddad and Mancini, 2013a). It was found that the thrombolitic buildups developed as clusters in the western, central and northern part of the Little Cedar Creek Field. The thrombolite facies in the Little Cedar Creek Field has a clotted, mottled and nodular texture, with rare domal and branching structures that includes pellets, peloids, benthic foraminiferas and ostracods (Tonietto *et al*., 2014). The microbial peloids being formed as a result of precipitation of calcium carbonate by metabolizing cyanobacteria, with preserved shapes recognized as *Girvanella, Renalcis and Epiphyton.* Binding and cementation of the grains and skeletal fragments by a combination of microbial and abiotic processes helped formed the reef's fabric (Heydari and Baria, 2006).

Porosity and permeability in microbialites may be depositional, diagenetic or fractured (Ahr, 2009). Marine diagenesis along with microbial binding and cementation of the thrombolitic boundstone reservoir in the Smackover Formation are mainly responsible for preserving its porosity (Heydari and Baria, 2006). Dolomitization preserves porosity also. Dolomitization due to diagenesis occurs in the Little Cedar Creek Field however its distribution decreases gradually from south to north, being absent from near the center to the northeast portion of the field (Tonietto and Pope, 2013). According to Tonietto *et al* (2014) where dolomitization occurs pore geometry is simpler and is responsible for intercrystalline porosity. Generally, the pore system of the microbial boundstone consists of primary growth framework vugs and intergranular along with

secondary diagenetic vugs and microfractures. This pore system provides high permeability and connectivity.

Significance

The Little Cedar Creek Field is one of the largest Smackover field discoveries in the northern Gulf Coast with an oil column of 640 meters (2100 feet) (Baria, 2011). Because the stratigraphic framework has been established, improved understanding of the microbial origin of these buildups will result in more efficient development plan designs for other fields producing from microbial carbonate reservoirs. The recent discovery of hydrocarbon in Cretaceous microbialites off the coast of Brazil is a perfect example. Industry is particularly interested in the predictability of the spatial distribution of reservoir facies and their sedimentary, petrophysical, and hydrocarbon productivity characteristics and the ability to model trends in heterogeneous reservoirs (Haddad and Mancini, 2013b). Pore type characterization work and reservoir characterization of the microbial thrombolitic boundstone has found that the connectivity of the pore system leads to high permeability up to 7953 md and porosity up to 30%. Beyond their significance as a petroleum resource a greater understanding of the Smackover Formation buildups contributes to our understanding of global biochemical cycles.

Microbial bacteria's influence in extreme environments such as on the rocky planets and ocean floor cold methane seeps, has been recently gaining attention. Their metabolism process gives them the ability to survive in these environments and possibly altering it. This makes bacteria a new variable to be considered. The variables usually considered include: pH, temperature, and climate. Alteration of the environment due to microbial metabolism can pertain to a change in seawater geochemistry, biological

precipitation of minerals, and or breakdown of minerals, along with preferential use of certain isotopes. For example, mineral transformation of iron from extruded basalt on the seafloor by iron-oxidizing bacteria. Another example is bacteria's preferential reaction with compounds that contain lighter isotopes. The significance of understanding microbial bacteria's effect on the environment are mainly as paleoenvironmental indicators and in the near future their ability to produce commercial quantities of pure mineral deposits e.g. the production of 400,000 metric tons of zinc sulfide in Nevada by sulfate-reducing bacteria (Bawden et al., 2003).

CHAPTER II

METHODS

The cores used in this study were obtained from ten wells in the Little Cedar Creek Field. The cores, are stored at the Alabama State Oil and Gas Board warehouse in Tuscaloosa, Alabama. These were slab cores of varying lengths; 51.9 to 95.5 feet that were cut into thirds. The core from well P#14112, Pruet #1 Tisdale 13-5 was unavailable. The wells were drilled spanning a time period of 2005-2010 and are all producing oil from the Smackover Formation (Table 1). Dunham's (1962) classification system is useful for microfacies interpretation of carbonate depositional environment, thus it was used to describe the depositional texture of the cores. Folk's (1962) classification scheme was used for thin section. Stratigraphic columns will be constructed for each core with further sub-division of the Smackover Formation based on litho-facies. The thrombolite facies will be focused on for sub-dividing into microfacies.

Representative sections of cores, approximately 40, with possible microbial buildups were selected from each well for polishing and scanning, and were then grouped into microfacies. Ten sample pieces were taken to make thin sections and for Scanning Electron Microscope (SEM) imaging. These techniques help find evidence of microbes and record the succession of events that contributed towards the microbial buildup in the Smackover Formation. Further analysis be performed by micro-milling the component of

buildup fabric of the cores to determine the oxygen and carbon isotope ratio and thus whether freshwater or seawater influenced the buildups.

Table 1 Cores taken from wells producing oil in the Smacker Formation

Permit Number	Operator	Year Drilled	Core Length (ft)	Depth (ft)	Producing/ Status
14270	Pruet #1 Cedar Creek Land & Timber 21-12	2005-2006	57.9	11,703.2-11,761.1	Oil/Unitized
13472	Pruet #1 Pugh 22-2	2004	92.5	11,495-11,587.5	Oil/Unitized
13625	Pruet #1 Price 14-12	2004	51.9	11,390-11,441.9	Oil/Converted
14112	Pruet #1 Tisdale 13-5	2005	Core Unavailable	Core Unavailable	Oil
14926	Pruet #1 McCreary 7-9	2007	89.2	11,100- 11,189.2	Oil
15418	Sklar #1 Craft-Mack 8-2	2007-2008	91.8	11,044-11,135.8	Oil
15497	Sklar #1 Craft-Ralls 4-5	2008	90	10,897-10,987	Oil
16327-B	Sklar #1 Craft Rallls 28-16	2010	95.5	10,795-10,890.5	Oil
16223-B	Sklar #1 Craft-Soterra 27-2	2010	87	10,825- 10,912	Oil
16237	Pruet #1 Cedar Creek Land & Timber 14-15	2010	94	10,195-10,289	Oil

Polishing of the cores were done by hand using different grit sizes in trays with glass plates. Silicon carbide grit was used in sizes from coarsest to finest: 60/90, 120/220, 400 and, 500/600. Polishing was carried out to eliminate the saw marks and enhance evidence of the microbial buildups in the cores. These polished core slabs were used to

identify the different types of microfacies that make up the thrombolite. Mapping of the microfacies into subfacies was done using a Wacom tablet and Adobe Photoshop software. After determining the microfacies, Petra well log correlation software was used to construct cross sections to find trends. Permeability (k) and porosity (Ø) log plots of the thrombolite part of the cores were used to acquire k and Ø data for each microfacies in each well, which will be plotted on a graph to determine any trend.

Preparation for thin sections were made by cutting 2x6 cm size pieces from the back of the slab cores. The pieces were sent to National Petrographic Houston, Texas to be made into thin sections. A blue epoxy was used to identify the pore spaces within the calcite matrix when viewed under the microscope in polarized and cross polarized light.

Scanning Electron Microscopy (SEM) focuses an electron beam over the surface of a sample to create an image. It has a large depth of field, high resolution and magnification making it ideal for detecting microbial buildups. SEM imaging was performed at the Institute for Imaging and Analytical Technologies Facility (I^2AT) on Mississippi State University campus using the Joel JSM-6500F microscope, on core pieces less than 1 cm in size taken from the parts of the sample trimmed off to make the thin sections.

Sample preparation for SEM imaging involved breaking the sample pieces to reveal a fresh surface, mounting on aluminum stubs with carbon planchette tape and coating with 30 nm platinum using the Election Microscopy Sciences 150T ES sputter coater, which makes the sample conductive for proper imaging.

Computer controlled micromilling permits discrete sampling of carbonate specimens with micron-scale resolution, for the purpose of acquiring high-resolution $\delta^{13}C$

and $\delta^{18}O$ values, and other elemental chemistry (Wurster et al., 1999). Samples were collected in 4.5 ml borosilicate vials after milling specific areas of the cores to get a powder with a mass range of 50 to 100 μg (0.050 to 0.100 mg) which were sent to the Alabama Stable Isotope Laboratory, Tuscaloosa for ^{13}C and ^{18}O isotope ratio measurements. The location on the cores chosen for sampling were based on the areas mapped as primary framework or microbial building blocks. The samples were analyzed using a Thermo GasBench II coupled via continuous He flow to a Thermo Delta V isotope ratio mass spectrometer. The samples were be reacted in the vials with orthophosphoric acid at 50º C. Values are reported in parts per mil (‰) relative to the Vienna Pee Dee Belemnite (VPDB) standard. This is achieved by correcting to multiple (typically 14) NBS-19 standards throughout the sample set to correct to VPDB, detect and correct for drift, and assess precision.

New concepts, ideas and comparative data collected on modern and ancient carbonates has allowed for the application of new techniques in the study and of microfacies (Flügel, 2010). These include grain origin and distribution patterns, how carbonate sedimentation is influenced by a dominant biological control and by geological time, and lastly, new concepts on defining facies models. Apart from the use of microscopy in thin section analysis, other new techniques developed include scanning electron microscopy and EDS, stable isotope geochemistry, cathodluminescence, X-ray, and fluid inclusion. These techniques offer new possibilities for the interpretation of diagenetic pathways of carbonates (Flügel, 2010).

CHAPTER III

RESULTS

Stable Isotope ^{18}O- ^{13}C Analysis

Stable isotopic analysis was done to determine whether the thrombolite buildups in the Little Cedar Creek field were initially deposited in fresh water or in sea water. Oxygen and carbon isotopic data were compiled from milled samples taken from polished cores. The location of each sample was chosen by identifying the first component formed in the fabric. Either an organism that formed the primary framework (subfacies 1 in cores P#15497 and P#16327B- Sample Site 1) or from the first component of the series of microbial components that make up the thrombolite (peloids in P#14270 and crust in P#16327B- Sample Site 2). The isotopic results are presented in Table 2.

Table 2 Isotopic ratios of the established primary framework and microbial building blocks

Sample Name	Depth (ft)	Microfacies	Subfacies	^{13}C (‰ VPDB)	^{18}O (‰ VPDB)
P#14270	11755.8	A	Peloids	4.0	-4.0
P#15497	10962.0	A	Brown Micrite	3.8	-2.4
P#16327B- Sample Site 1	10853.3	C	Brown Micrite	3.1	-4.1
P#16327B- Sample Site 2	10853.3	D	Crust	3.2	-5.1

The isotopic composition of the initial event was plotted with the hope of determining the original environment of deposition. In this study the initial event or organism was determined based on cross-cutting relationships on a polished core slab. The presence of framework was identified in three microfacies: A, B and C. Four milled samples were retrieved for the compilation of the ^{18}O and ^{13}C isotopic data (Figure 9). The sample depth ranged from 10,853.3 to 11,755.8 feet and the distance between the two furthest wells were 17.5 km (11 miles) apart. Sampling focused on the micritic regions of the primary subfacies, which are peloidal in nature and avoided equant calcite, stylolites, and large (> 2 mm) calcite spar crystals, all features that may have formed due to late stage burial diagenesis that can alter or reset the primary carbon and oxygen isotope composition.

Figure 9 Orange dots show the locations where samples were milled for isotopic analysis.

The samples labeled: P#15497 & P#16327B were milled in micritic zones identified as the results of initial events. Primary framework: 1 and microbial building blocks: P#14270 & P#16327B-Sample Site 2.

The data was then plotted on a bivariate graph and also superimposed onto Hudson's (1977) ^{18}O- ^{13}C cross- plot to distinguish the depositional and/or diagenetic paleo-environments responsible for carbonate formation (Figures 10 and 11). Hudson's cross-plot has distinct carbonate fields for carbonates of different origin such as meteoric, marine.

The isotopic ratios of the samples are compared with the international PDB standard, which has values of 0‰. The isotopic values for the microfacies range from -2.4 to -5.1 ‰VPBD for ^{18}O and 3.1 to 4.0 ‰ VPBD for ^{13}C. All of the isotopic data points for this study cluster in region 8 of the diagram created by Hudson (1977) highlighted by the stippled red line on the diagram, as common marine limestone (Figure 11). The loose clustering of the data points on the graph suggests that some alteration by diagenesis occurred but was not significant. In effect, it can be said that the original sea water that was locked into the sediment pore space after deposition along with the CO_2 source (microbes and shells) for precipitation retained most of their primary isotopic signatures.

The ^{18}O and ^{13}C of precipitated carbonates depend on respectively, the composition and temperature of the water and the dissolved bicarbonate source (Hudson, 1977). The ^{18}O values according to table 2 are negative (-4.0, -2.4, -4.1, -5.1) or depleted, implying a relative increase in the lighter isotope ^{16}O, which according to Hudson is associated with decreasing salinity and increasingly higher temperatures.

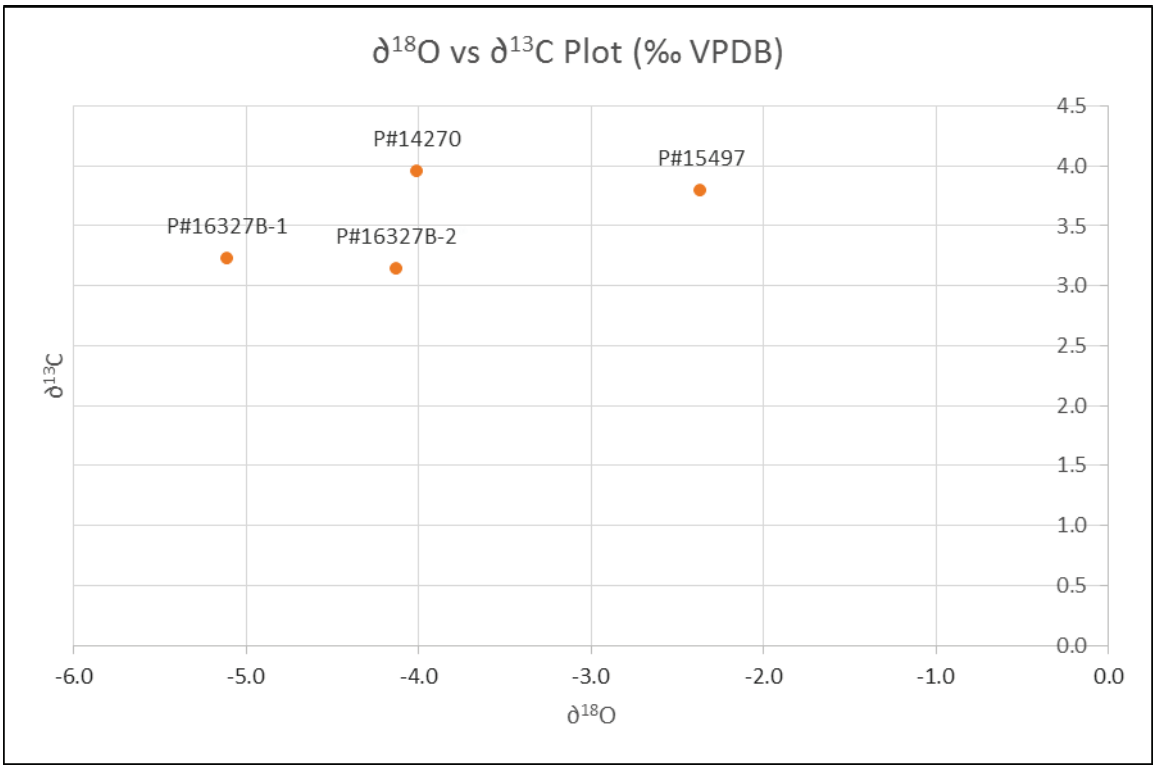

Figure 10 Bivariate graph of ^{18}O vs. ^{13}C shows the loose clustering of the data points.

Because it has been established that the limestone is of marine origin, and therefore not influenced by fresh water, the decrease in salinity can be due to microbial growth during a regional transgression whereby, the once restricted embayment experienced more mixing as regional sea-level rose due to oceanic crust emplacement, better connecting the embayment to the sea. Also, the negative or depleted values from the relative increase in the lighter ^{16}O isotope can be explained by higher temperatures since the climate during the Oxfordian was hot and arid so glaciers and ice sheets would have already deposited their melt water containing high quantities of ^{16}O into the oceans for circulation.

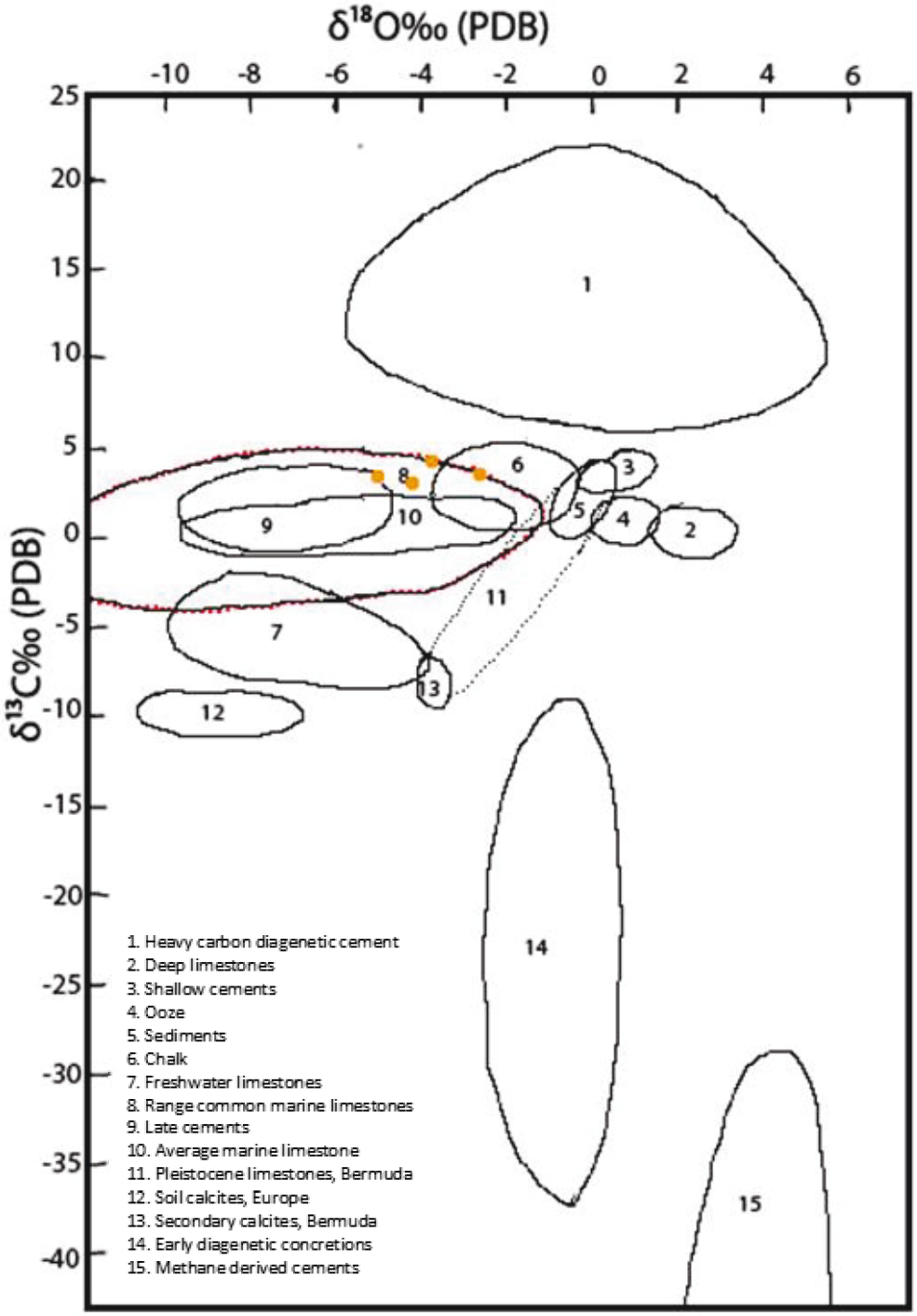

Figure 11 The orange dots are δ13C vs. 18O values for the thrombolite buildups in the Smackover Formation limestone, Little Cedar Creek Field, Al.

(The dots are superimposed onto Hudson's (1977) diagram of characteristic carbonate fields based on compiled isotopic data. The stippled red line shows that the carbonates are of marine origin redrawn from Hudson 1977 and Nagarajan et. al, 2008).

Sea water has a ^{13}C value of near 0‰, the data in the table show positive or enriched values close to sea water i.e. 3.1 to 4.0 ‰ VPBD. The primary microbial micrite precipitate retains the brown color, organic molecules, as imaged in SEM, and would therefore be inherently enriched with respect to ^{13}C. Small organisms with shell have been found useful for paleo-climate analysis since the isotope ratio of their diet can be passed on and deposited in the organism with greater preservation potential (Pickering and Owen, 1997).

During a transgression more organic matter is stored in the marginal areas, resulting in ^{13}C enrichment (Broecker, 1982). The thrombolite buildups in this study were deposited on the inner ramp, near the updip limit of the Smackover Formation or close to the paleo-coastline (0.5 to 6.75 miles (0.31 to 4.2 km) and contains organic matter such as peloidal micrite and thallasinoides microcoprolite which could also contribute to ^{13}C enrichment. Lastly, photosynthesis by living organisms favor the uptake of the lighter carbon isotope, ^{12}C leaving behind the heavier, ^{13}C as dissolved bicarbonates in seawater (Pickering and Owen, 1997). Calcimicrobes were identified in core and thin section. Since these microbes were photosynthetic it used up ^{12}C, thus explaining the positive or enriched ^{13}C values from the milled samples.

Overall, the characteristic range of ^{18}O and ^{13}C isotope values for the established primary framework of the thrombolites and its building blocks/ components suggest precipitation near isotopic equilibrium of the original sea water indicating good preservation, little alteration and retention of their primary isotopic signatures. Therefore, since the data points plotted in the “range of common marine limestone” along with the

presence of marine fossils (foraminiferas, sponge spicules) it is safe to conclude that the thrombolite buildups were initially precipitated in a marine environment.

Microfacies Delineation

It was determined from my study of cores and thin sections that the thrombolite facies of the Smackover Formation in the Little Cedar Creek Field, Alabama consists of a carbonate microbial-algal dominated reef preserved as a thrombolite boundstone. In the thrombolite facies four distinct microfacies were identified and are labelled A, B, C, D. The thrombolite facies is classified overall as a boundstone according to Dunham's (1964) classification scheme since calcite was precipitated *in situ* by organisms which, encrust and bind. The organisms in this case are algae and calcimicrobes sometimes referred to as cyanobacteria such as *Giravanella, Renalcis, Epiphyton, and Tubiphytes*, were the main frame-builders and frame-binders as evident from the clotted/ dendritic/ shrub-like, peloidal microfabric observed within the thrombolite buildup in cores and thin section. The framework built by microbes are not rigid initially like those of a coral reef but rather starts off as a colony of unicellular organisms surrounded by a mucilaginous sheath which eventually calcify.

The microbial reefs were deposited during a major transgression and are associated with maximum flooding events on a stable platform forming an epiric sea. This shallow sea probably promoted microbial growth since cyanobacteria are photosynthetic and can produce its own food. The Oxfordian microbial thrombolite reef facies in this study were deposited 0.5-6.75 miles (0.31-4.2 km) from the up-dip limit of the paleo-Smackover coastline on an inner ramp setting with water depths less than 10 feet (Figure 12). The climate during the Oxfordian was generally arid suggesting very

low to no sediment runoff from the terrestrial environment. No quartz or clay grains were observed in thin sections taken from the cores. However, one anhydrite/gypsum crystal was identified suggesting a very brief period of sub-aerial exposure.

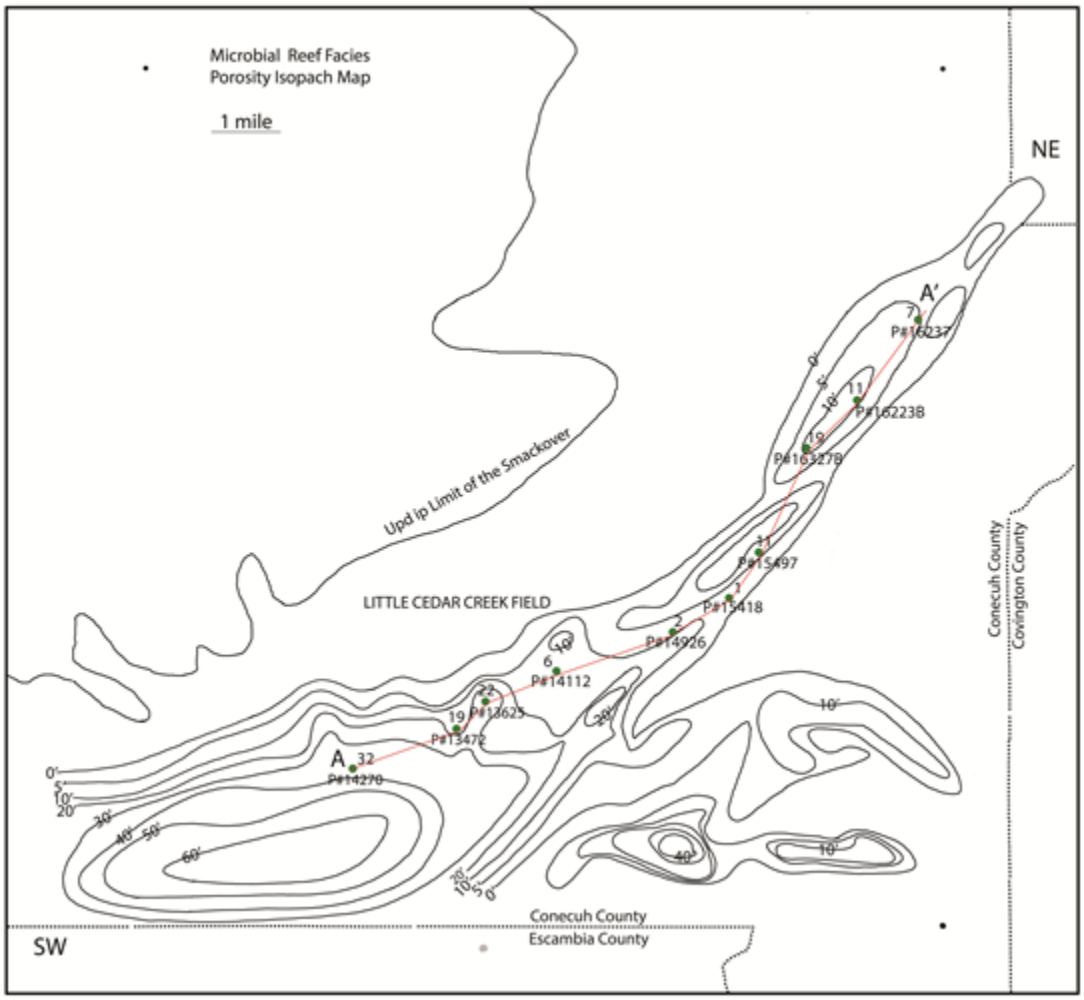

Figure 12 Porosity isopach map showing location of wells with porosity of the microbial reef and cross section line A-A'

(redrawn from Baria, 2012).

The microbial thrombolite facies was divided into four microfacies: A, B, C, and D based on distinctive characteristics such as color and pattern/fabric formed by the subfacies making up the microfacies. The depth of each microfacies in each well was recorded on a table (Table 3). The fabric describes the arrangement of the building blocks that make up individual subfacies or the overall microfacies such as dendritic, laminated and clotted. Building blocks include calcimicrobes, peloids, pellets, stromatoids, filaments and fossils. The colors observed refers to the individual subfacies such as dark brown for peloidal micrite, pinkish to light brown for cement, laminae or crust, black for *Renalcis*-like coating, and grey for micrite. As a result, the microfacies names are descriptive and are as follows: A is "Black *Renalcis*-like Layer", B is "Digitate", C is "Chaotic" and D is "Brown Laminated Centimeter Scale Cycle". It was found that the ratio of micrite to cement to crust to black *Renalcis*-like coating determined the formation of the different microfacies since variations of a single microfacies can occur as it progress through the core column (00).

In microfacies A (*Renalcis*- like Layer), the black *Renalcis*-like coating is very predominant forming in multiple layers that also encrust the dark brown peloidal micrite forming smooth edges. Voids are also present which has been infilled by a light brown calcite cement, no crust formation was evident. Microfacies B (Digitate) has negligible to no black *Renalcis*-like layer, no crust and is composed of dark brown peloidal micrite with jagged edges and light brown void filling calcite cement. Microfacies C (Chaotic) is made up entirely of a dark brown and grey peloidal micrite with no voids or crust and D (Brown Laminated Centimeter Scale Cycle) contains dark brown, peloidal micrite with crust formation on top of the micrite only, floating in a light brown cement with laminae.

All of the micrite contained well preserved, skeletal fossils. Subfacies can develop along with other subfacies or form one at a time. Micrite is brown calcite 0.004 mm or finer. The microfacies identified are not in order of occurrence since a single microfacies can occur multiple times through depth (Table 3).

Table 3 Table shows microfacies depth and thickness in feet for each well.

		Well Permit Number											
		14270	**13472**	**13625**	**14112**	**14926**	**15418**	**15497**	**16327**	**16223**	**16237**	Total (ft)	Percent of Total
Microfacies Depth (ft)	A	11750-11761 11768-11800	11534-11542	11408-11421 11428-11434	11285-11299 11306-11314	11140-11146 11147-11179		10950-10957 10965-10982	10818-10825 10841-10846	10862-10870 10878-10895	10225-10239 10246-10249	208	52.7%
	B		11542-11560	11421-11428 11434-11450	11299-11306 11314-11330		11132-11158			10874-10878	10249-10252	97	24.6%
	C								10848-10850 10851-10853 10854-10856	10895-10900 10903-10911	10257-10262	24	6.0%
	D	11761-11768				11146-11147		10957-10965	10815-10818 10825-10841 10846-10848 10850-10851 10853-10854 10856-10858	10870-10874 10895-10896 10900-10903	10239-10246 10252-10257 10262-10267	66	16.7%
Total (ft)		50	26	42	45	39	26	32	43	50	42	**395**	**100%**

The wells are arranged in order from southeast to northwest. The maroon colored numbers represents the base and top depths of the thrombolite facies.

The total thrombolite facies in each well was divided into microfacies A, B, C, D and the depths, thicknesses, and percentage of each microfacies were recorded (Table 3). According to the data, the total thickness of all the microfacies in the ten wells is 395 feet with a varied distribution of each microfacies. Microfacies A (Black *Renalcis*- like

Layer) is the most dominant accounting for 52.7% or 208 feet and microfacies C (Chaotic) is the least dominant accounting for 6% or 24 feet of the total thrombolite facies. The thrombolite facies in most wells with the exception of P#15418 are capped by/ends with microfacies A (Black *Renalcis*- like Layer), however the initial formation of the thrombolite can occur with microfacies A, B, C or D.

Structural and stratigraphic cross sections taken along the line A-A' in figure 12 and isopach maps highlight the thrombolite facies within the Smackover Formation and better display the structure of the thrombolite facies along with the distribution of the microfacies (Figures 13 and 14). The formation unconformably overlies the Norphlet Formation and disconformably underlies the Kimmeridgian Haynesville Formation. The thickness of the Smackover Formation ranges from 140 feet in well P#15418 to 85 feet in wells P#13625 and P#14112 respectively.

The formation top of the Smackover varies from 10,185 feet in well P#16237 in the northeastern part of the field and gets deeper further southwest to a depth of 11, 718 feet in well P#14270. The microbial thrombolite facies within the Smackover Formation ranges in thickness from 26 to 50 feet and also has shallower northeastern formation tops at 10,225 feet in well P#16237 to deeper tops in the southwest at 11,750 feet in well P#14270 (Figure 13). Overall, cross sections and isopach maps show that from northeast to southwest the thrombolite facies becomes deeper, has variable thickness throughout, and accounts for 38.5% of the total Smackover Formation based on the wells in this study.

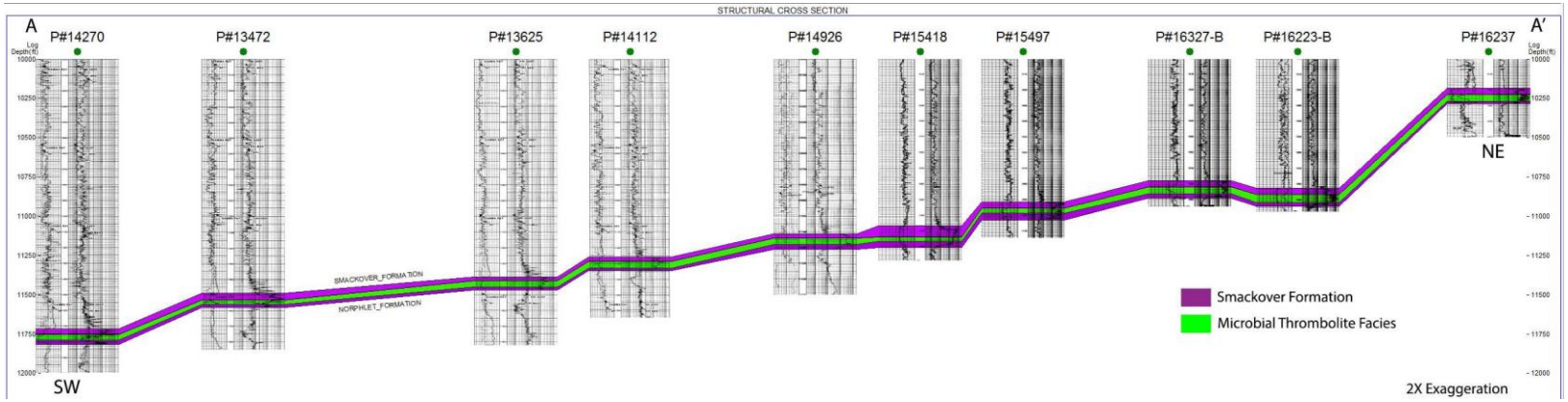

Figure 13 Structural cross sections of the wells in the Little Cedar Creek Field, Alabama.

The Smackover Formation and the thrombolite facies has the same trend deepening with depth from NE to SW. The Smackover Formation was deposited unconformably above the Norphlet Formation.

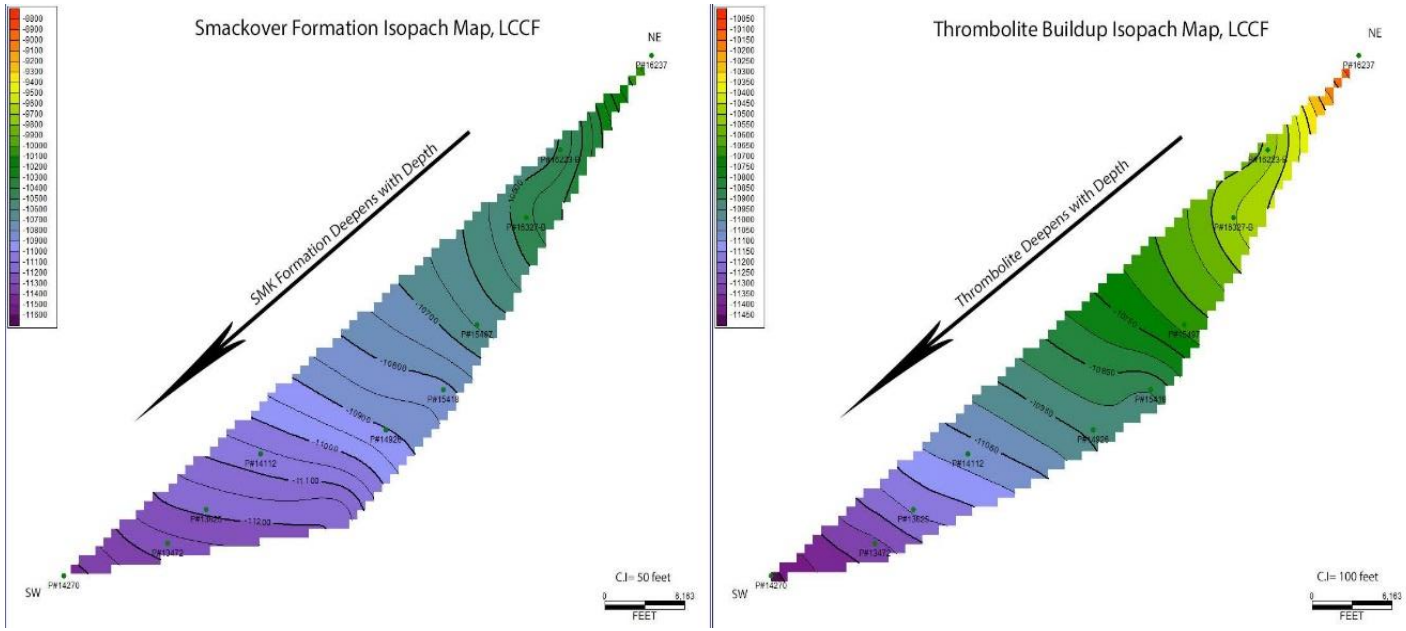

Figure 14 Subsurface isopach maps of the Smackover Formation and the thrombolite facies.

The thrombolite facies follows the same trend deepening with depth from NE to SW

The datum line used to construct the stratigraphic cross section (A-A') of the wells in the field was hung on the top of the Norphlet Formation and better display the structure of the thrombolite facies along with the distribution of the microfacies during the Oxfordian (Figures 15 and 16). The thrombolite facies is composed of individual mounds/ clusters at wells P#14270, P#14926, P#16223, and possibly at P#15497 with lower areas between the mounds (Figure 16). Overall, the thrombolitic buildups developed as clusters in the southwestern, central and northeastern part of the Little Cedar Creek Field (Figure 16). The mounds/ clusters are built up by microfacies A (Black *Renalcis*- like Layer) and microfacies D (Brown Laminated Centimeter Scale Cycles) with microfacies A forming more predominantly.

Generally, from northeast to southwest microfacies B (Digitate) becomes prevalent and seem to form in lower areas between the mounds. In the northeastern part of the field microfacies D forms more readily than in the southwest. Also, in the northeast there are more interbedding of the various microfacies (A, B, C, D) forming individual thinner buildups (as thin as 1 foot thick) compared to the southeast with individual thicker microfacies buildups (up to 32 feet thick) and less types of microfacies to form the buildups such as A and D forming mounds, and A and B in areas between mounds (Table 3 and Figure 16). Generally, the microfacies show a preference for formation depending on the high and low areas and from northeast to southwest.

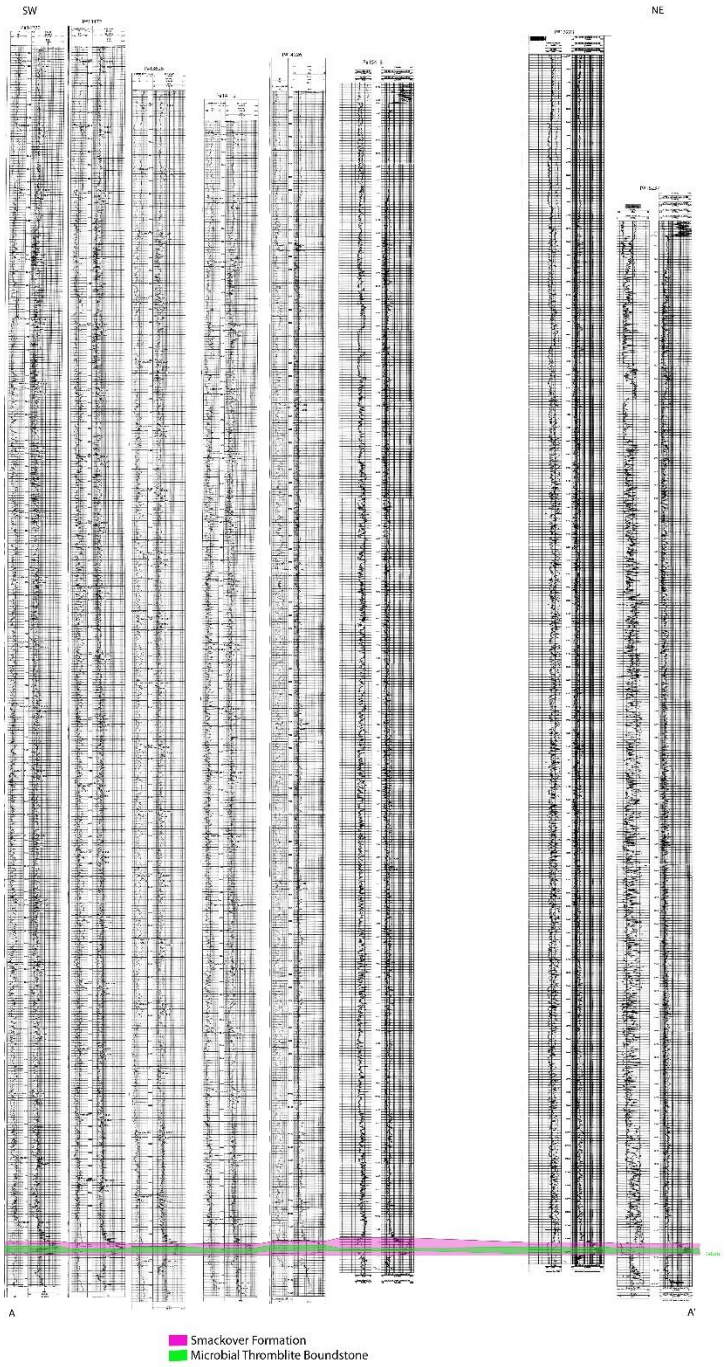

Figure 15 Stratigraphic cross section shows the Smackover Formation (pink) and the thrombolite reef facies (green) within it.

.

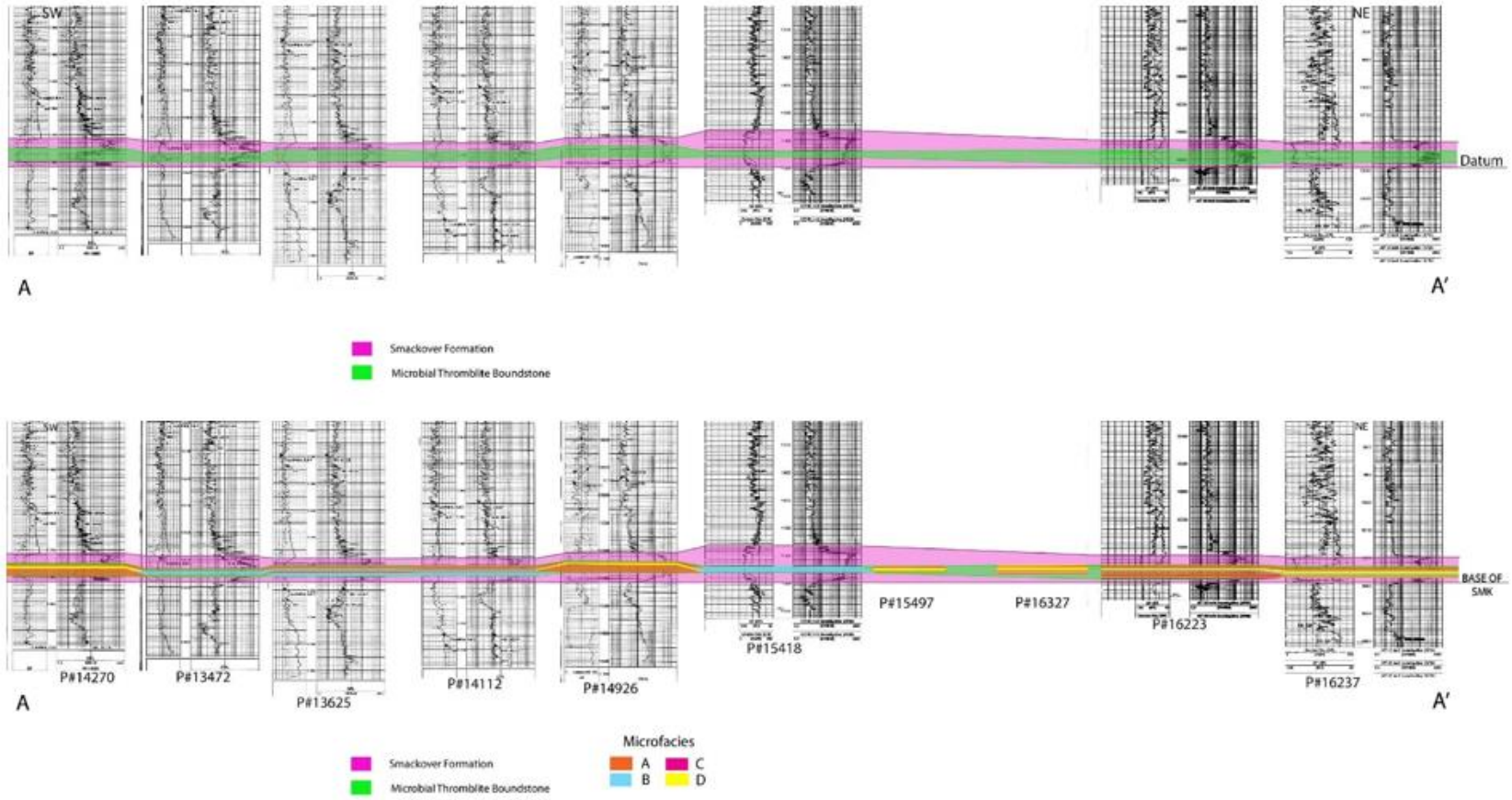

Figure 16 Stratigraphic cross section of the Smackover Formation shows the thrombolite buildup within the Smackover (above) and the distribution of the microfacies within the thrombolite (below).

Porosity and permeability log plots were available for six wells only and data was extracted from these for each microfacies (Table 4). The values were then plotted on a graph to determine a trend (Figure 4). Overall, porosity values range from 2% to 16.83% and permeability values range from 0.087 to 930 millidarcies (md). The majority of the data points on the graph are clustered below 100 millidarcies but has a wide range of porosity values, 2% to 16.83% (Figure 17). Microfacies A (Black *Renalcis*- like Layer) in all the wells mainly have < 6% porosity and very low permeability values ranging from 0.087 md to 17 md with the exception of A^2 in well P#16237 with porosity of 60 millidarcies. Microfacies D (Brown Laminated Centimeter Scale Cycle), in well P#16237 generally has the best porosity and permeability values ranging from 10.4% to 11.3% and 115 md to 592.5 md respectively, with the exception of D^1in well P#14926 which has a porosity value of 10% in line with other microfacies D values however, the permeability is relatively very low at 11.5 millidarcies.

It is interesting to note that in well P#16237 permeability values for microfacies $D^{1, 2, 3}$ increases with height in the thrombolite facies. The single highest porosity and permeability values was recorded in well P#13472 in microfacies B^1 at 16.83% and 930 md respectively. However, in other wells where microfacies B (Digitate) occurs permeability is <100 md and porosity widely vary from 2% to 10.4%.

Looking at each microfacies porosity and permeability values in individual wells, it seems as though microfacies A in all the wells presents itself as a potential baffler or barrier since it is relatively less porous and permeable, sandwiching microfacies that are relatively more porous and permeable (Table 4). For example, in table 4 well P#13625, microfacies B^1 and B^2 are relatively more porous (7.6%, 10.4%) and permeable

(10.41md, 71 md) compared to the interbedding buildup of microfacies A^1 and A^2 which are relatively less porous (3.4%, 4.5%) and permeable (0.087 md, 3.45 md) thereby acting as potential bafflers or barriers to flow. Each well shows this pattern with the microfacies.

Overall, using microfacies to determine a trend in porosity and permeability in a field can be somewhat difficult, however it is possible to look at the values of the various microfacies in individual wells to determine a trend. This is probably due to the fact that diagenesis acts differently on similar facies throughout a field.

Table 4 Permeability (k) and porosity (Ø) values of microfacies in six wells.

Wells/Microfacies/Depths	K	Ø
P#14270		
Microfacies A: 11754-11761 ft	17 md	9%
P#13472		
Microfacies A: 11534- 11542 ft	11.34 md	5.5%
Microfacies B: 11542- 11560 ft	930 md	16.83%
P#13625		
Microfacies A^1 : 11410-11421 ft	0.087 md	3.4%
Microfacies B^1 : 11421-11428 ft	10.41 md	7.6%
Microfacies A^2 : 11428-11434 ft	3.45 md	4.5%
Microfacies B^2 : 11434-11448 ft	71 md	10.4%
P#14112		
Microfacies A^1 : 11285- 11299 ft	0.1 md	2.2%
Microfacies B^1: 11299- 11306 ft	17.65 md	6.8%
Microfacies A^2: 11306- 11314 ft	1.10 md	4.75%
Microfacies B^2: 11314- 11330 ft	19.55 md	10%
P#14926		
Microfacies A^1: 11140-11146 ft	6.25 md	4.7%
Microfacies D : 11146-11147 ft	11.5 md	10%
Microfacies A^2: 11147- 11178 ft	1.47 md	4.3%
P#16237		
Microfacies A^1:10225- 10239 ft	4.26 md	4.87%
Microfacies D^1:10239- 10246 ft	592.5 md	10.4%
Microfacies A^2:10246- 10249 ft	60 md	4%
Microfacies B:10249- 10252 ft	5 md	2%
Microfacies D^2:10252- 10257 ft	350.1 md	10.5%
Microfacies C:10257- 10262 ft	0.17 md	6.25%
Microfacies D^3:10262-10267 ft	115 md	11.3%

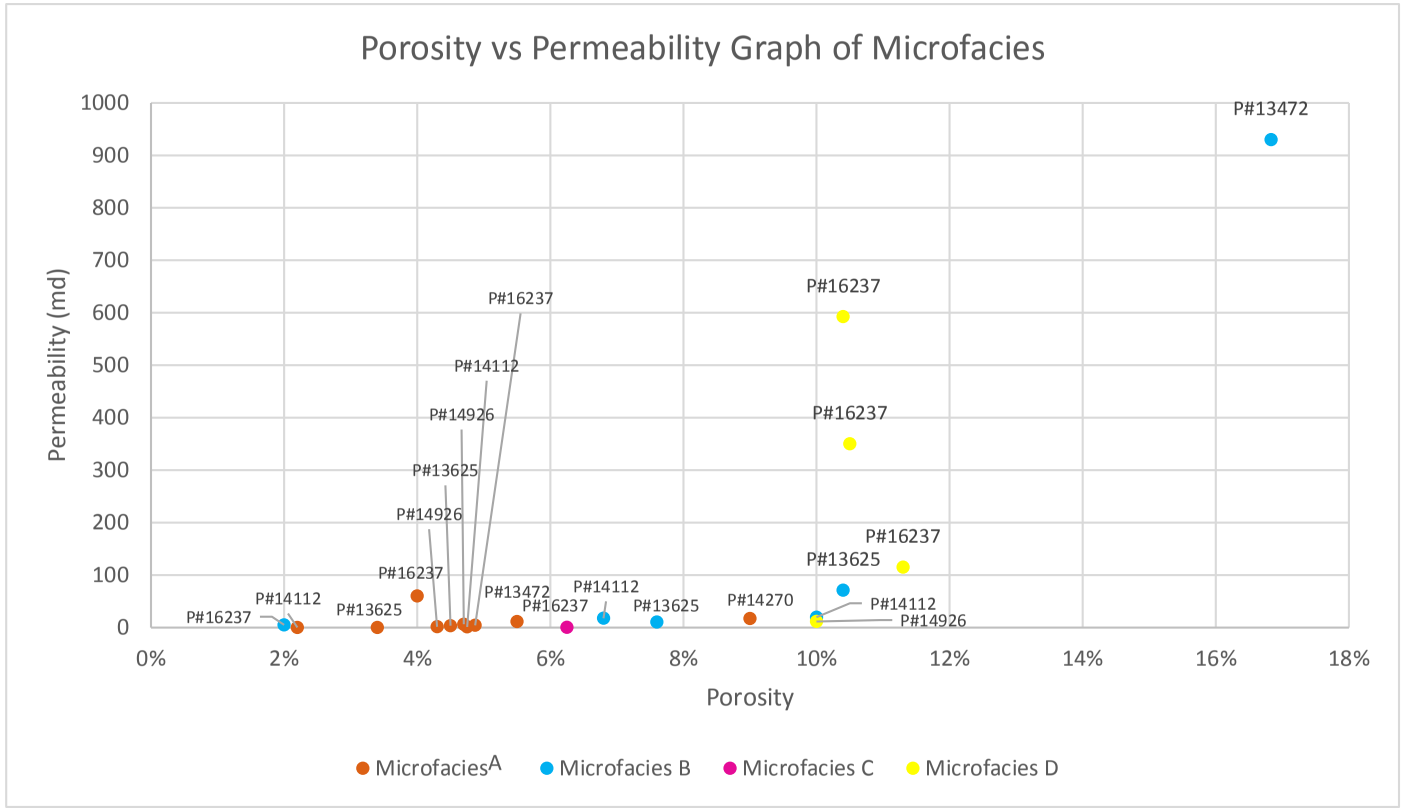

Figure 17 Porosity vs. permeability relationship of microfacies A, B, C, and D. Log data was available for only six wells.

Petrographic Analysis

Microfacies A: Black *Renalcis*-like Layer

Description

Microfacies A is dominated by three main subfacies (Figure 18). The most abundant of these is subfacies 1A composed of dark brown peloids (approximately 1mm in diameter) that form irregularly shaped accumulations reminiscent of billowing clouds at the centimeter-scale. It occurs as a very dense, brown micrite giving the polished slab a smooth to the touch feel, but the peloids form vaguely dendritic structures with more pore space in between near the top of this subfacies. Individual accumulations of this subfacies range from (1.5 to 8 cm). Micrite is brown calcite 0.004 mm or finer. Zones of subfacies 1A are bounded by layers less than 1 mm thick darker, more densely peloidal zone. The boundaries of 1A are sharp. The perimeter of the irregular shapes form definitive boundaries. Cement surrounding the peloids gives this subfacies a translucent appearance (Figure 19, 1Aa, 1Ab).

Layer 1A accounts for about 50% of this piece of core (Figure 20). Fossils and features in Subfacies 1A include, whole foraminifera less than 0.05 cm in size; shell fragments; ostracods; elongated skeletal shapes that are hollow and segmented measuring up to 1.50 mm long; filamentous strands; peloids; blocky calcite and infilled veins; round to irregular shaped molds/holes and vugs. Essentially, Subfacies 1A is a biomicrite according to Folk's (1962) classification. A particularly unusual fossil is found most often in subfacies 1A and is locally abundant.

Microfacies A
Renalcis-like Layers
P#14270/11755.8ft

Figure 18 Mapped core showing the order of succession that led to the thrombolite buildup.

The dark lens shapes that defines microfacies A (Black *Renalcis*- like Layer) is labeled 2A. The core is 9.5 inches (24 cm) long and 3.25 inches (8 cm) wide.

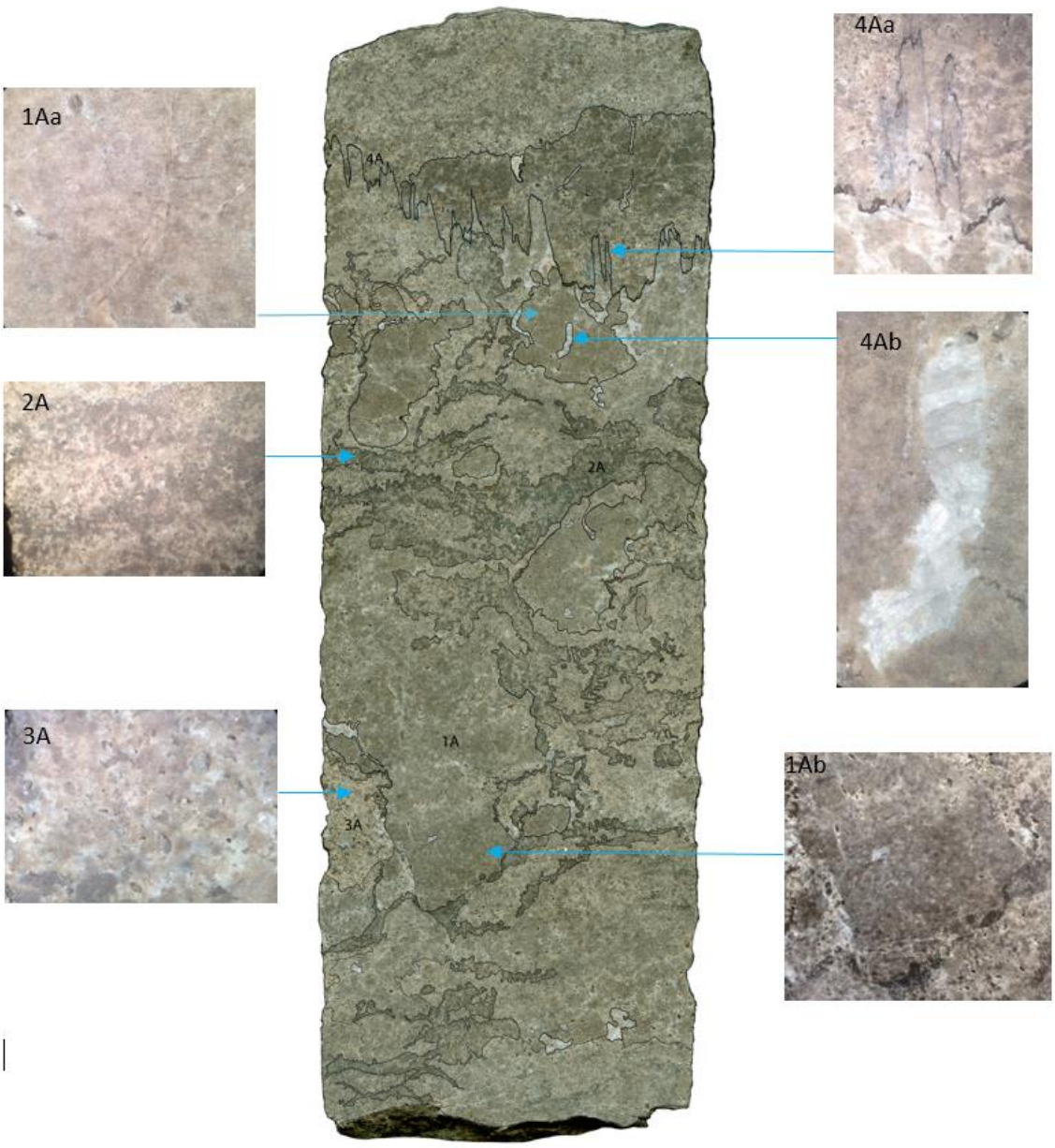

Figure 19 Photomicrographs showing the texture of the subfacies that make up microfacies A.

1Aa Dark brown, translucent, micritic calcite, peloids and branching bacteria.
1Ab Geopetal structure.
2A Renalcis-like, encrusting, layered, dendritic, black, coating.
3A Porous, medium to coarse grain calcite.
4Aa Stylolite, pressure solution feature.
4Ab Blocky calcite spar infill primary voids.

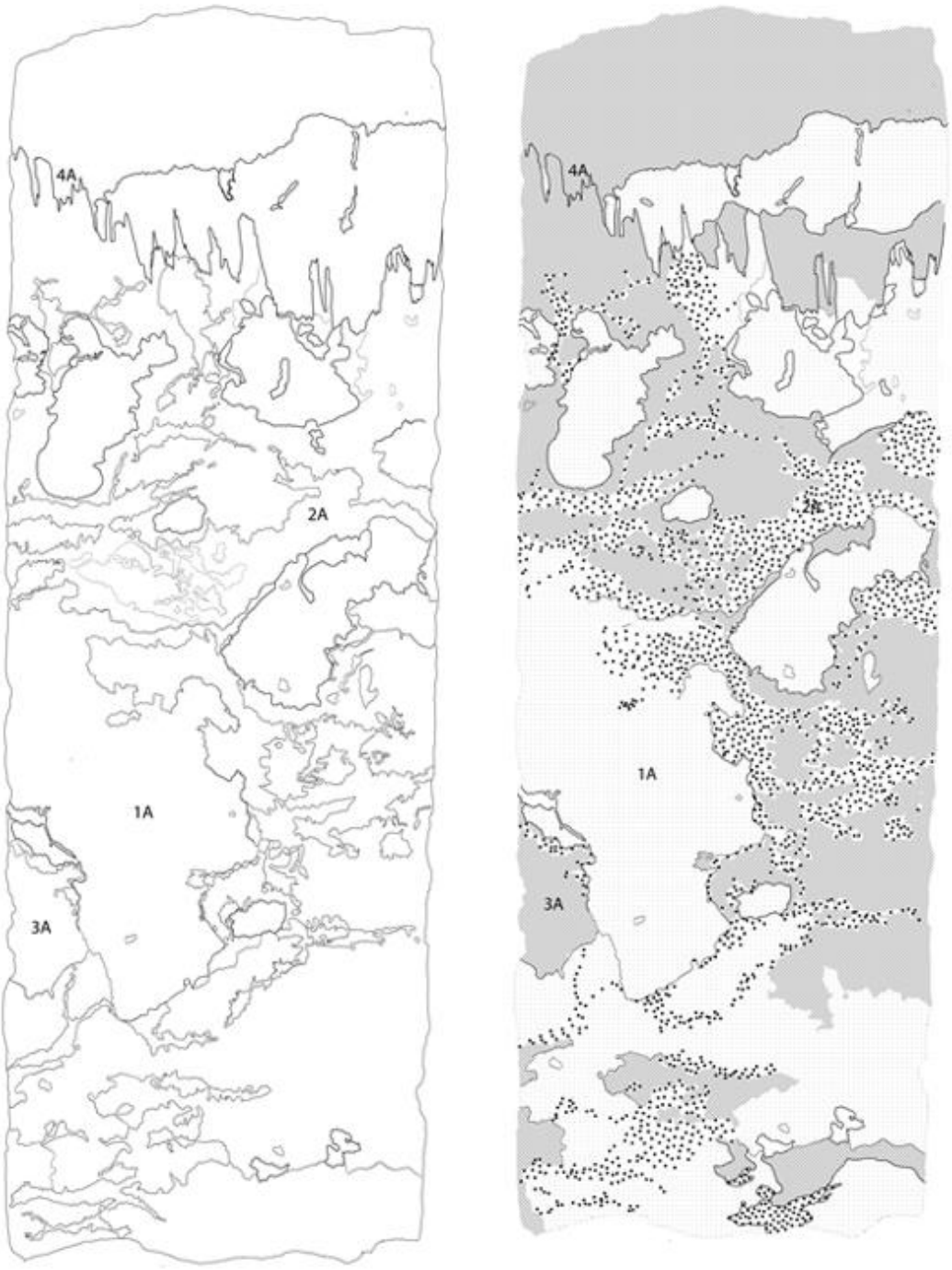

Figure 20 Mapped outline of core showing the order of succession formation for microfacies A.

The distribution of the subfacies are: 1A framework (50%), 2A primary encruster (40%), 3A cement (10%).

This fossil appears as slightly tapered, elongated tube shapes that vary in form from needle-like to curved. In polished surfaces and thin section the interior of the fossil appears to be segmented composed of individual, interconnected chambers. One end of the fossil tends to be wider than the other end which is slightly tapered. A cast of the interior tube shows that it was preserved as interconnected, segmented, elongated chambers. Another photomicrograph taken from microfacies A in core P#13625 shows a longitudinal view of one of these fossils with the interior chambers of the tube filled with light gray calcite surrounded by white calcite. Circular structures in thin sections of subfacies 1A are interpreted as cross sections through these skeletal tubes because they have a similar diameter (<0.25 mm). In some cases tubular fossils are dissolved in various stages resulting in secondary intraparticle and moldic porosity. Vugs and vuggy porosity occurs in this subfacies, but are smaller (1- 2 mm) and less abundant than in adjoining subfacies. White blocky calcite occurs in the vugs and stylolites cross this subfacies and others (Figure 19).

Subfacies 2A accounts for about 10% of this piece of core (Figure 20). It is composed of a layer of very dark brown to black structures (ranging from 0.5 to 2 mm tall and approximately 1 mm wide that branch or pile vertically upward (Figures 18 and 19). It is a primary encruster and was determined to be the second succession since it closely follows the perimeter of the irregular framework of 1A (Figure 19 2A). It was formed in close association with 3A or coeval (Figures 18 and 19 3A). In some places the very dark brown to black structures of subfacies 2A appear to be attached to or growing off of the brown peloids of subfacies 1A (Figure 19 2A).

Subfacies 3A accounts for about 40% of this piece of core (Figure 20). It is light brownish-pink, composed of small peloids (2mm) that form a vaguely dendritic pattern, medium to coarse grained calcite crystals (< 1mm) and fossils (Figure 19). The light colored peloids of subfacies 3A appear to fill in between the individual dark brown to black structures of subfacies 2A and to form thin undulose layers (approximately 1 mm in height and 1 to 2 cm in length) that are then partially encrusted again by subfacies 3A. The fossils identified are elongated tube shaped skeletons, foraminifera, peloids, and shell fragments. The fossils present are not very well preserved, with most being dissolved either partially or fully, leaving small voids forming secondary porosity. Some of the voids are infilled with blocky calcite.

Interpretation

The buildup order was determined based on cross-cutting relationships observed. 1A built the framework of the microbial reef, 2A encrusted the framework and 3A were cavities within the framework that later got infilled by sediment and cemented. Microfacies A (Black *Renalcis*- like Layer) formation is comparative to that of the Ledger microbialite in Pennsylvania. The Ledger Formation microbialite contains large open cavities indicating that it must have been at least semi-rigid to maintain such spaces (Monty 1995). Coeval cementation produced a semi-rigid structure, conducive to the formation and preservation of submarine cavities (Wet, et. al, 2004). The rigid structure is achieved from *Renalcis*-like microbes that are widely regarded as a relatively high-energy calcified microbial group (Riding 1991).

This is best visualized in another mapped core of microfacies A taken from well P#15497 (Figure 21). In this piece of core in plane/ longitudinal view, definite boundaries

amongst the three subfacies can be clearly seen. Subfacies 1A was originally a brown, fossiliferous, unfragmented micrite before being dissected by subfacies 3A creating individual, smaller pieces of subfacies 1A. At the top of the core, subfacies 2A originally encrusted subfacies 1A but disaggregation, dissolution and infilling replaced the brown micrite giving the appearance that subfacies 2A formed on subfacies 3A. A preserved, remnant piece of the brown micrite (1A) can still be seen encrusted by 3A. In cross section views of the same core, the brown micrite of subfacies 1A can be clearly seen enveloping 3A, further bolstering the interpretation that 1A formed first (Figure 21). Percentage distribution of the subfacies were: 1A- 75%, 2A- 5%, and 3A- 20%. Once more, the dark brown micrite of subfacies 1A is more abundant in this piece of core.

Subfacies 1A in core P#14270 represents the framework of the microbial reef. It was built by a colony of microbes and through the process of their metabolic activity allows for direct precipitation of calcium carbonate along with capturing and micritizing organisms and sediment in its biofilm, became calcified forming a semi-rigid structure with cavities (Figures 18 & 21).

The peloids in subfacies 1A are sparse, black and spherical forming a microfabric pattern building upwards that is vaguely dendritic to branching, this tells direction of growth (Figure 19). Since microbes in the buildup grow in colonies surrounded by a mucilaginous biofilm, it can catch, trap and suspend sediment and organisms in the water column eventually giving rise to the dendritic microfabric after degradation of the film. The spaces between the calcified biofilm produced cavities which later became infilled by sediment, producing succession 2A.

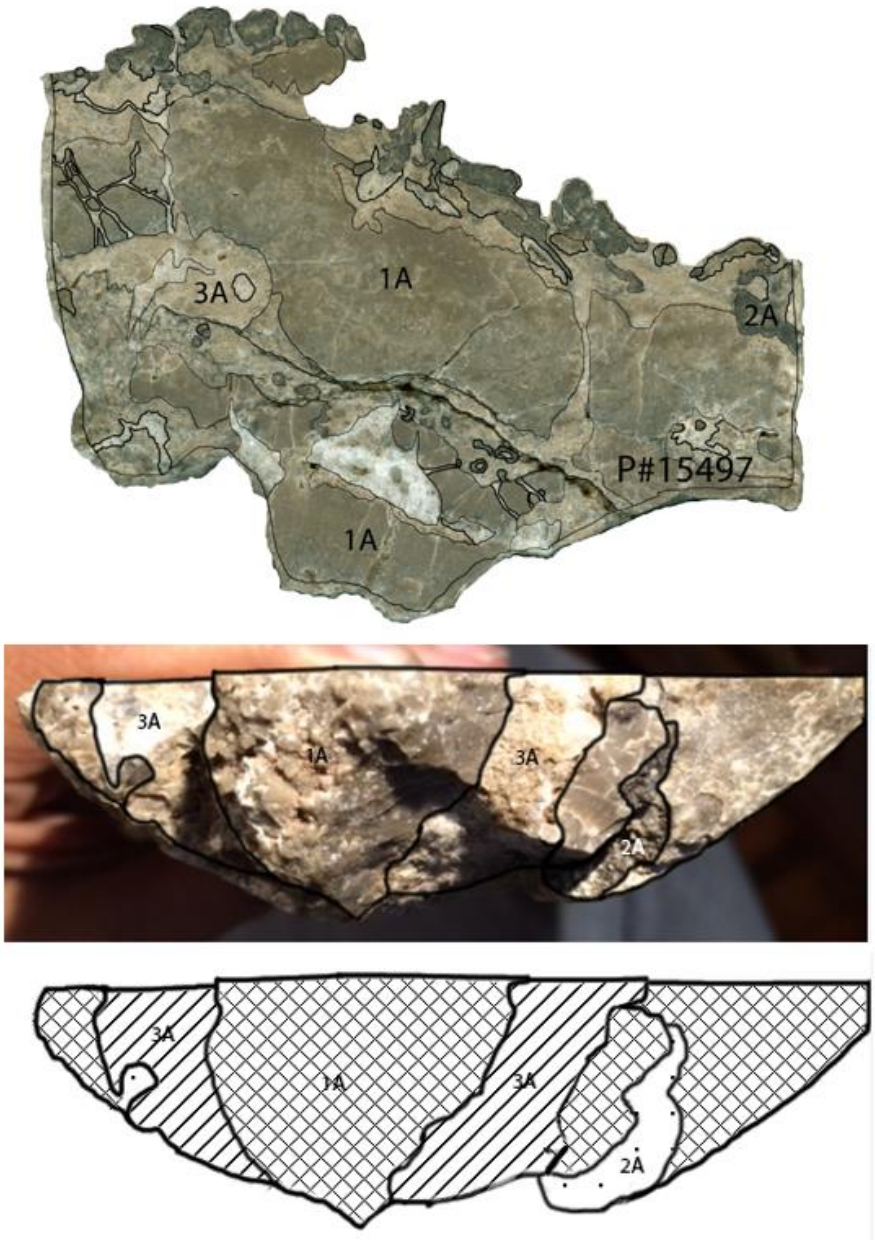

Figure 21 Cross cutting relationships in microfacies A-Black *Renalcis*-like layer.

Plane view (top) and cross section (middle) view of mapped core from well P#15497 showing subfacies. Bottom image shows percentage of subfacies distribution: 1A dark brown micrite (75%), 2A: black *Renalcis*- like layer (5%), and 3A cement (20%).

The skeletal tube-shaped organism identified in subfacies 1A seems to be of the rasping/syphoning variety, feeding on the microbial colony as evident from thin section (P#15497D) where a pathway through microbial micrite, highlighted by red arrows in figure 22a, terminated with the preservation of the organism enveloped in a thin membrane of micrite then by larger calcite grains (Figure 22). The slightly wider end of the tube-shaped fossil has a protrusion similar to a snout which can be used for feeding. The longest tube fossil identified has a tapered width and uniform wall thickness. When viewed in cross-section in cores and thin-section the skeleton appears as either an empty ring or as a ring with a solid ball in the center (Figure 22a). In varying degrees of longitudinal views the segmented chambers are visible. Microspar as referenced above is clear, carbonate cement crystals as fine as 0.001 mm in size. Sparry calcite is a primary, pore filling cement or generated secondarily by recrystallizing micrite (Prothero and Schwab, 2004).

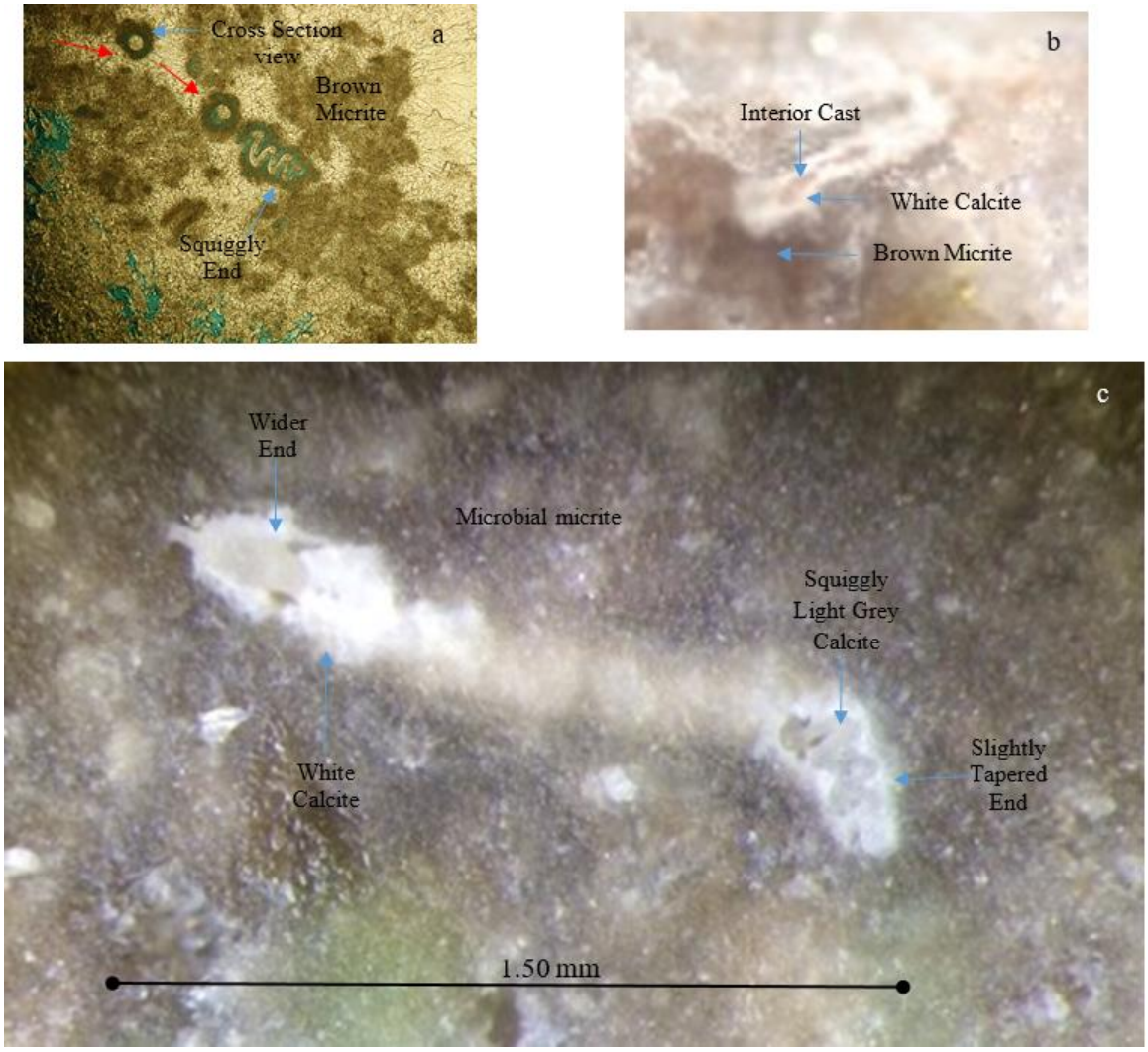

Figure 22 Thin section and photomicrograph of tube-shaped fossil.

Thin section (a) of the fossil in cross-section and longitudinal view surrounded by a shrub-like microfabric, the shell has been dissolved and replaced by micrite, however, the soft body of the organism was preserved by microspar. The photomicrograph (b) shows infilling of the interior chamber by brown micrite preserving a cast of the chambered interior. Skeletal fossil (c) with the morphology of the organism that lived within it suggested within the microspar in the interior of the organism.

Subfacies 2A is a dark brown to black, dense, layered, interconnected, clotted coating that appears to encrust subfacies 1A (Figure 19). Individual structures are (1.0-2.0 mm high) and (0.75- 1 mm wide) they are knob-like in cross section, some appear to have been hollow on the inside, and some branch upward. However, the core from well P#15497 in figure 21 above, individual knob-like structures are 7.0 mm high and 4.0 mm wide. In some places the dark brown to black knobby structures only form one layer. In most zones at least two layers are present and in some zones, it is possible that multiple layers grew, but they are difficult to distinguish. The morphology of this dark brown to black coating is reminiscent of, *Renalcis* and/or *Epiphyton* and interpreted as microbial in origin. Subfacies 2A contains peloids, fossils and sediment preserved in a dense, clotted to sparse, vaguely dendritic pattern.

A tangled mass of filamentous strands forming clumps is present within a few of the dark brown to black knob- like structures. The filaments are connected and compacted at the base then separates into individual, tangled strands away from the base with lengths ranging from 1-2 mm (Figure 23). The tangled strands are preserved within dark brown micrite which also forms a thin rim (<0.25 mm) around the clumps. These clumps may be preserved microbial colonies that are responsible for the formation of subfacies 1A since they are preserved in brown micrite or the clumps could be responsible for the sinuous, meandering form of the black *Renalcis*-like layer of subfacies 2A since it is made up of long, sinuous strands.

Subfacies 3A represents the fenestral cavities of the microbial buildup (Figure 18). The presence of cavities indicate a degree of rigidity formed by the framework and the calcifying *Renalcis*-like algae. The cavity was probably infilled by interstitial

sediment produced from the metabolic activity of the encrusting algae, fossils such as the tube-shaped rasper, and incoming new sediment which cemented and preserved the structure.

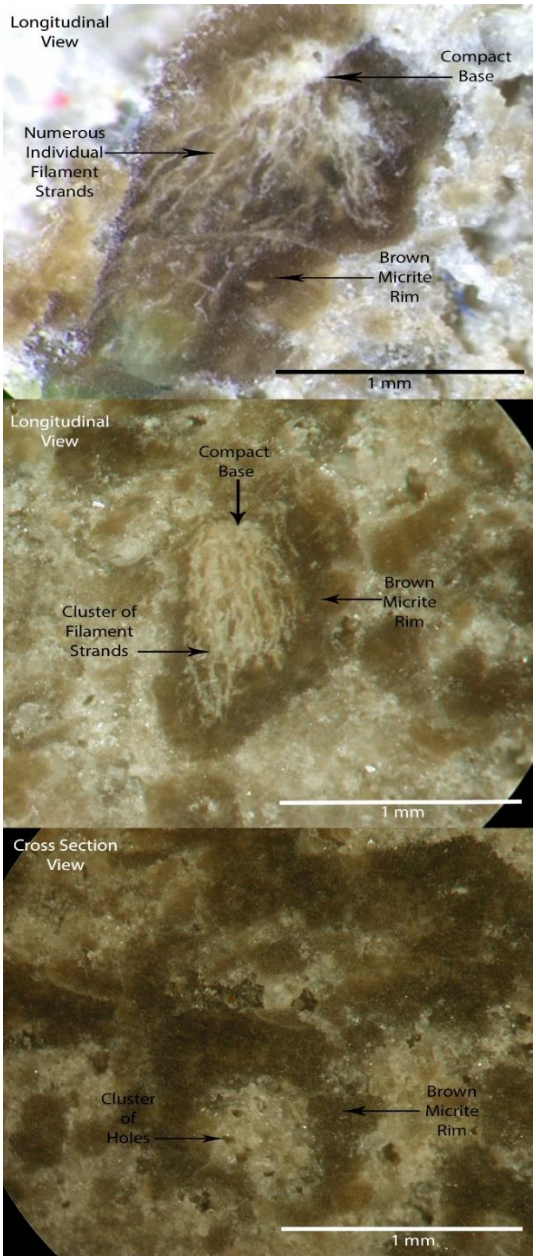

Figure 23 Tangled mass of filamentous, microspar strands surrounded by a <0.25 mm rim of dark brown micrite.

The thin section of Microfacies A was taken from the top of the core in subfacies 3A and is not representative of the whole core (Figure 24). According to Folk's (1962) classification scheme it is a biosparite or biomicrite. Peloids, foraminiferas and microbial buildups are supported by a grumeleuse micritic matrix i.e. a clotted micrite. In figures 25 and 26 evidence for microbial buildup is ample throughout the thin section occurring as clotted, peloidal, dendritic structures branching upwards (photo 3a); filamentous, layered, radiating structures (photos 4a, 6a, and 7a), and finally, groups of individual floating/ suspended foraminiferas in the grumeleuse matrix (photos 2a and 5a) (Figures 25 and 26). Of interest is the tangled, filamentous clump in photo 7a since it is similar in structure to the clumps identified in subfacies 2A. Preservation of these building blocks are good in a dense matrix.

Overall, the thin section shows good secondary porosity, formed after deposition such as fenestral (photo 1A), moldic (photos 6a, 8a), microfractures (7a) and vuggy (Figure 25 and 26). Thin section photographs of 1a, 3a, and 6a are good example of vuggy porosity. The vugs generally form separate-vug pores that are either grain or mud dominated. This means interconnectivity of the vugs are not good so permeability would be poor. Some vugs have been partially infilled by drusy calcite i.e. the calcite size increases towards the center of the void.

In photo 8a, an isopachous calcite ring can be seen in the mold of the partially dissolved fossil indicating early cementation and formation in a marine-phreatic environment. Late stage burial is evident in photo 5a showing stylolites cross cutting

foraminifera fossils to form a straightedge and photo 8a showing blocky calcite infilling the fossil's interior (Figure 26

Figure 24 Location the thin section was made from in core P#14270.

The labelled thin section are areas of microbial buildup evidence (see figure 7). Note, the thin section is not representative of the whole core, it was taken from the mapped area, 2A outlined in the blue box.

.

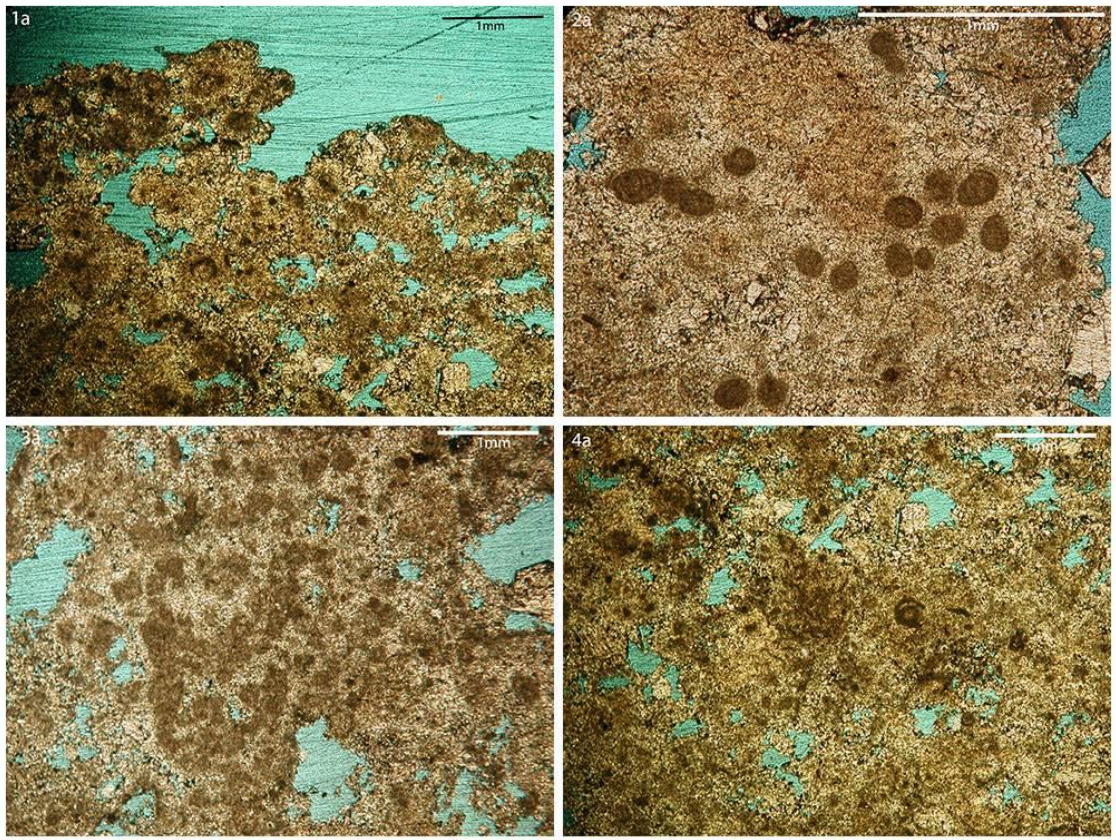

Figure 25 Thin section images showing good secondary porosity

1a. Fenestral porosity, vugs appear as windows within a dark micritic calcite
2a. Dense, microcrystalline calcite with micritized foraminifera
3a. Dendritic, branching upwards structure in microcrystalline calcite surrounded by partial vug to vug porosity
4a. A dendritic cluster of short strands forming a clump. Separate vug porosity. Vugs occluded by calcite.

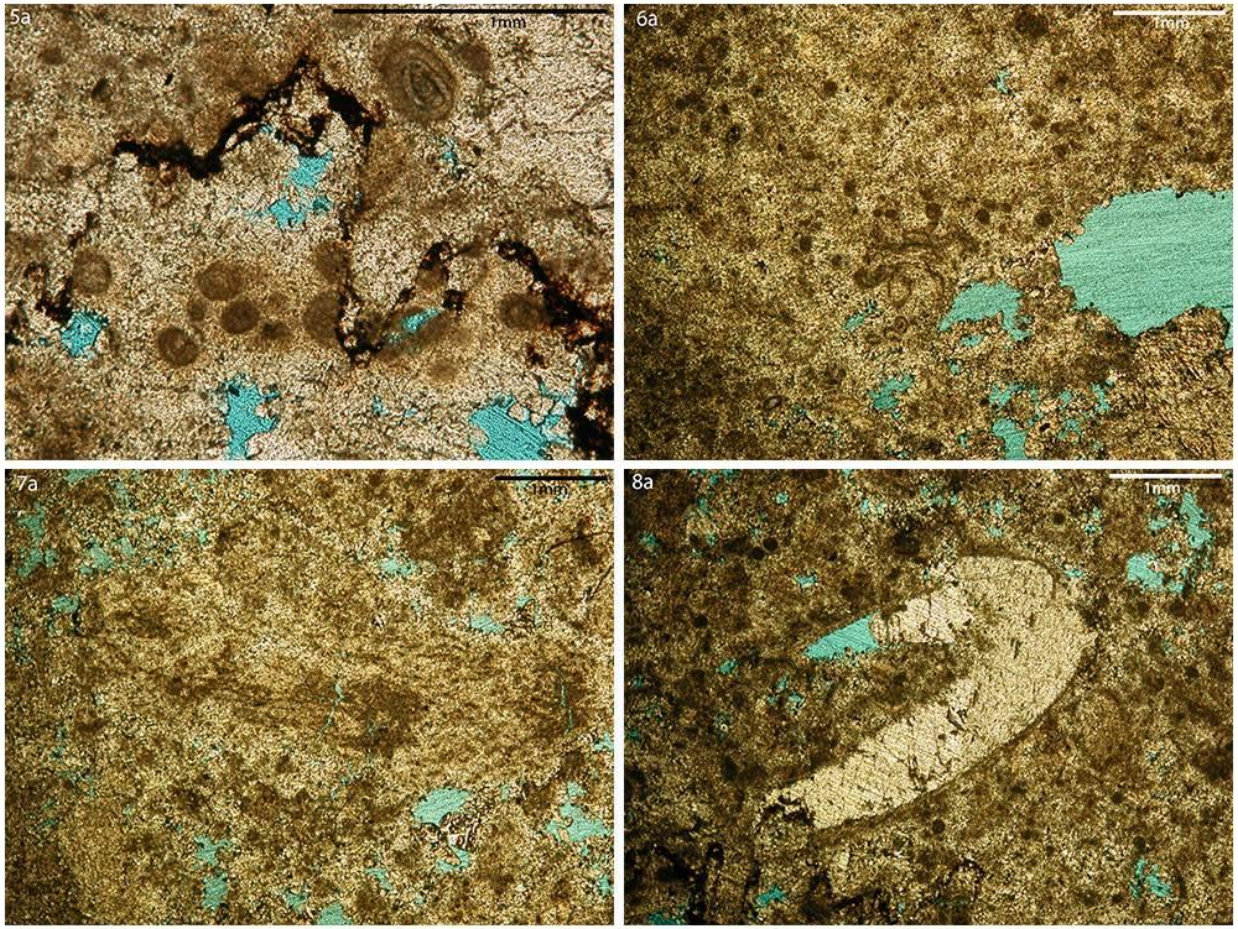

Figure 26 Thin section images show moderate secondary porosity

5a. Stylolite cross cutting foraminifera
6a. Separate vug pores in a dense microcrystalline calcite
7a. Filamentous clumps
8a. Partially dissolved bivalve forming moldic porosity

Scanning Electron Microscope (SEM) images also show evidence of microbial influence by the presence of calcimicrobe spheres, filaments and segmented tubule shape (Figure 27). The rough texture of the radiating calcite wedges and the mottled texture of the calcimicrobe spheres usually indicate microbially induced precipitation. The calcimicrobe spheres are approximately 1μm in length, are clustered at the center of the radiating pattern, and lay on the surface (Figure 28). The filaments and segmented tubule shape are <1 μm and 3μm in length respectively, and occur within the rough calcite (Figure 28 and 29). Small, round holes seen throughout the images are similar in diameter to the filaments (0.2 μm). In core P#14270, individual filament strands and filament clumps have been identified in thin section and core (Figures 23 and 26). The segmented tubule shape appears to be a mold of the original organism. It could also represent calcite filled tubules that formed from endolithic borings by algal tubules. Algal tubules are indicative of the photic zone and forms by precipitating a sheath of calcite around filament. Therefore, both the tubules and filaments maybe one of the same.

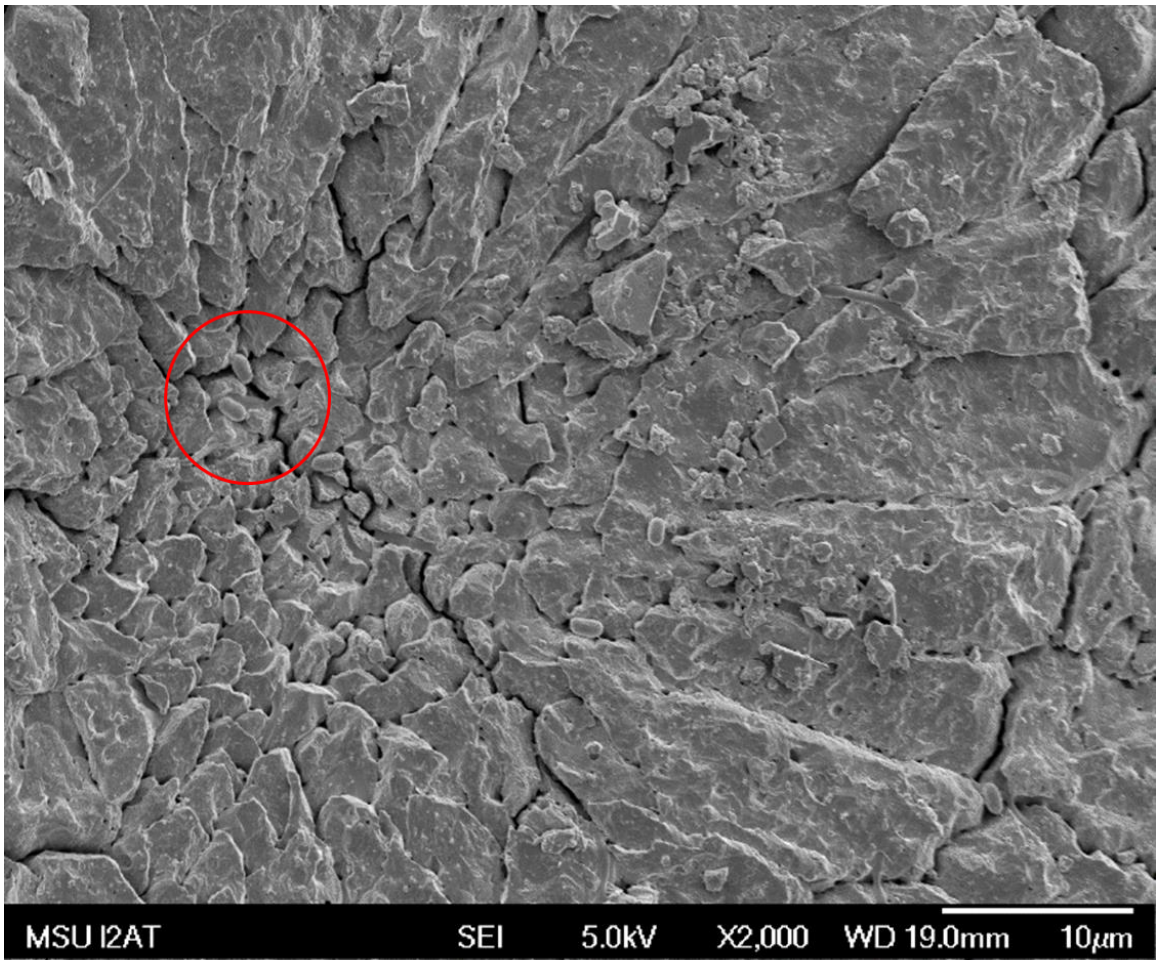

Figure 27 SEM image of calcite arranged in a radial pattern with numerous holes throughout.

The red circle highlights preserved mottled, oval-shaped spheres resembling bacteria along with, smooth, ribbon-like sheets, preserved tube shapes, and elongated, segmented shapes. The sample was taken from mapped area 2A.

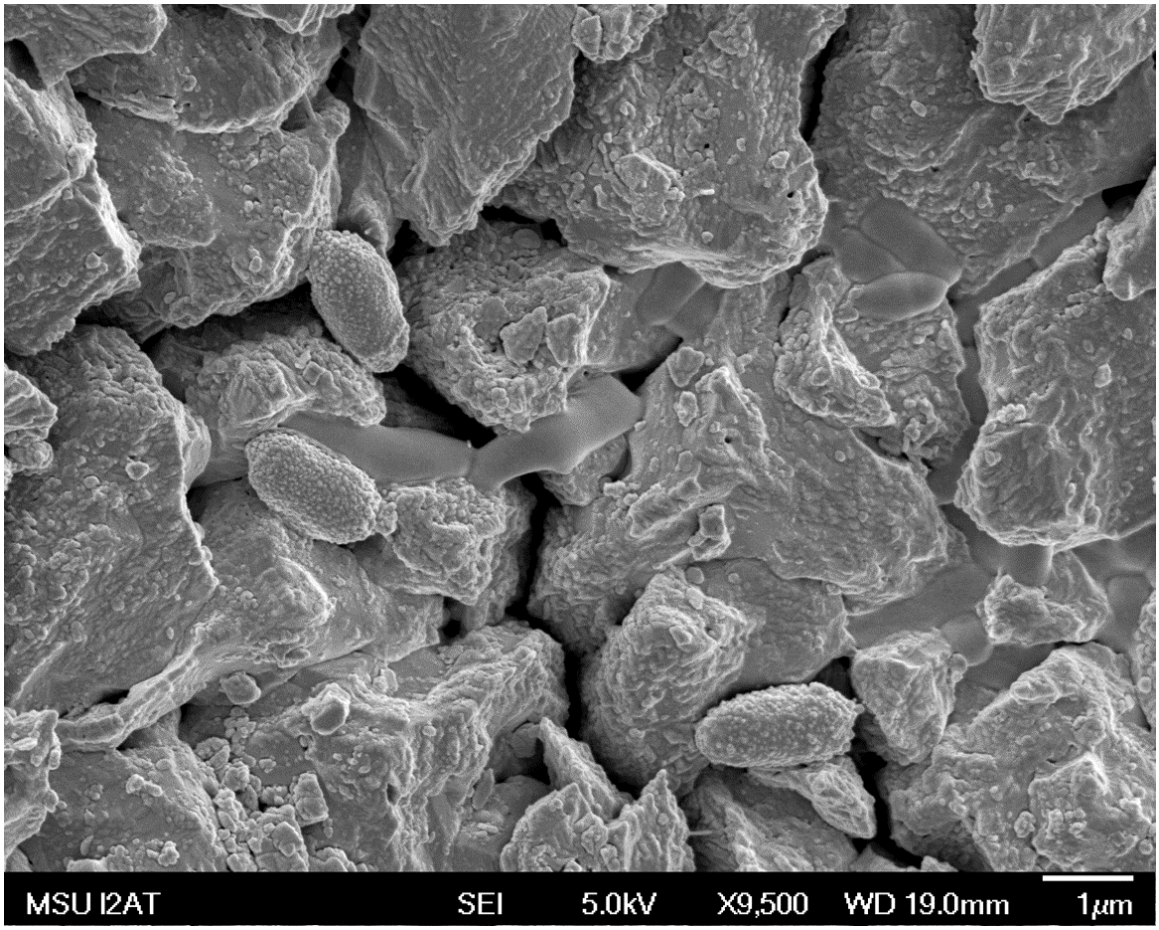

Figure 28 Magnification of area within the red circle shows spherical calcified microbes or calcimicrobes.

The relation of the spheres to the surrounding matrix shows that it is attached at some areas, its shape seems independent. Also, shown are elongated, segmented shape, and the distribution of the smooth, ribbon-like sheets throughout the calcite blocks

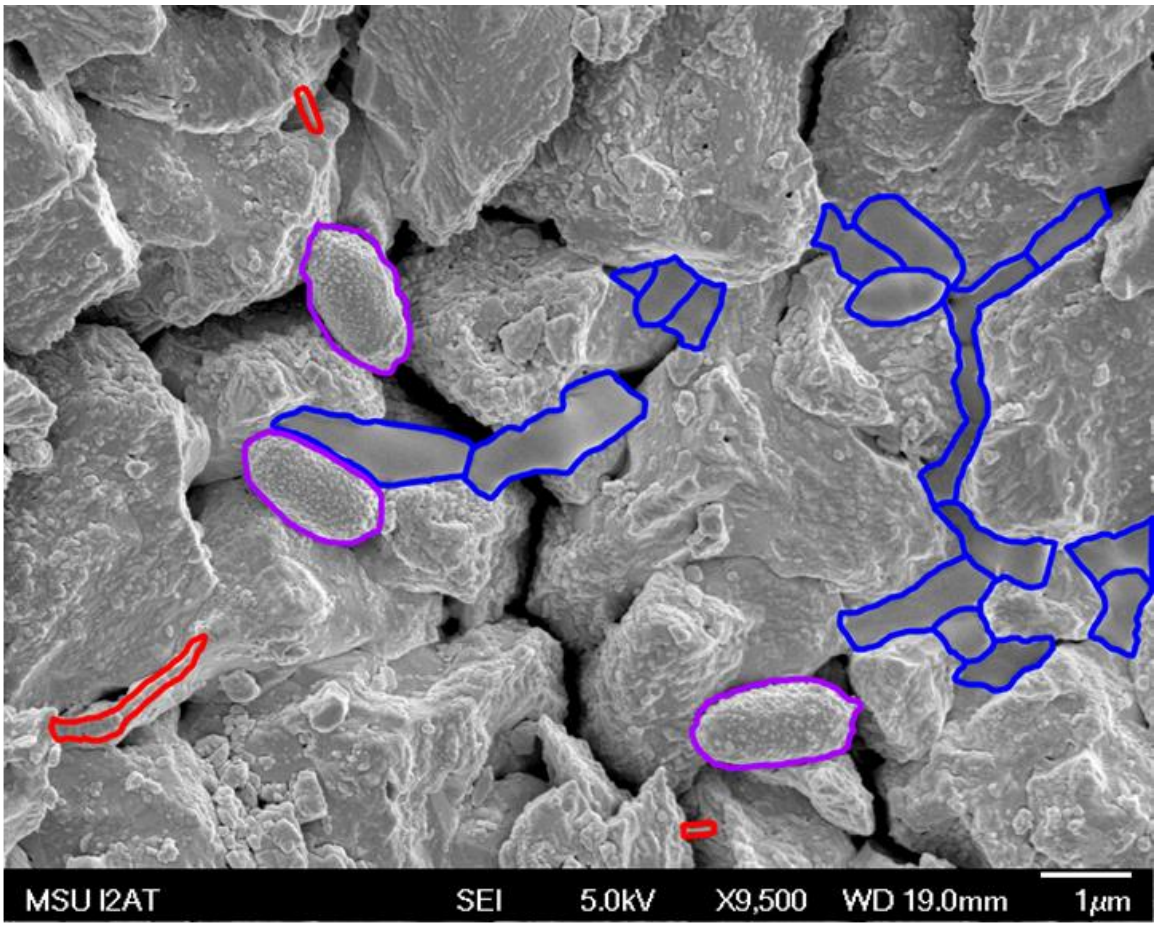

Figure 29 Outline of shapes identified in figure 28.

Red outlines the elongated, segmented tubes and filament, blue outlines the ribbon-like sheets and purple outlines the calcimicrobes

Microfacies A: Black *Renalcis*-like Layer

Description

Microfacies B is dominated by two main subfacies. Subfacies 1B is more abundant and is a dark brown, translucent, peloidal micrite that forms a wavy boundary with subfacies with 2B, a light brown fine to medium grained, porous calcite that has peloids arranged either randomly or form whispy laminations (Figure 30). Subfacies 1B make up about 50% of this piece of core. A third subfacies 3B, occurs but it is very minimal. It is blackish-brown, has an undulose shape and occurs mainly on the periphery of subfacies 1B. The boundary between subfacies 1B and 2B varies from smooth to almost wavy erratic and is readily visible because of the difference in color thus giving it its digitate appearance. Microfacies B differs mainly from microfacies A due to the absence of abundant encrusting *Renalcis*- like layers and the boundary between 1B and 2B is less sharp. Fossils present are mainly foraminiferas, ostracods and very few tube-shaped fossils. Microfacies B is present in the cores for wells: P#13472, P#15418, P#15497, P#16223B and P#16237.

Subfacies 1B is composed of fat, round peloids averaging 1mm, piling upwards in a branching pattern to form shrub-like clusters (Figure 31). The peloids in this subfacies is not very densely packed giving it a grainy appearance. Within this subfacies there are lots of voids filled with blocky calcite forming horizontally oriented vugs (0.3 to 0.5 cm) and vertically oriented veins/ fractures up to 2.5 cm in length (Figure 30).

Microfacies B

Digitate

P#13625/ 11423.4ft

Figure 30 Mapped core showing the subfacies in microfacies B (Digitate) and percentage distribution.

1B dark brown micrite (50%) and 2B coarse-grained cement (50%).

The boundary subfacies 1B forms with subfacies 2B varies from smooth and wavy in some areas to more wavy erratic in other areas giving it its digitate appearance. Fossils identified include foraminiferas, ostracods and tube shaped fossils.

Subfacies 2B represents the cavity spaces formed within the framework of subfacies 1B. The cavities are infilled with a light brown calcite, peloids, whispy laminations and remnant pieces of subfacies 1B (Figure 31). The peloids here are smaller and skinny, <1.0 mm in size, are not densely packed so it has the appearance of floating in the calcite matrix also, the peloids are generally oriented in a random pattern but sometimes as whispy laminae < 0.25 mm thick. The whispy laminations are very faint, mainly oriented horizontally with lengths of 1cm and are made up of peloids touching end to end. Fossils were present but not well preserved however, foraminiferas and tube shaped fossils were identified.

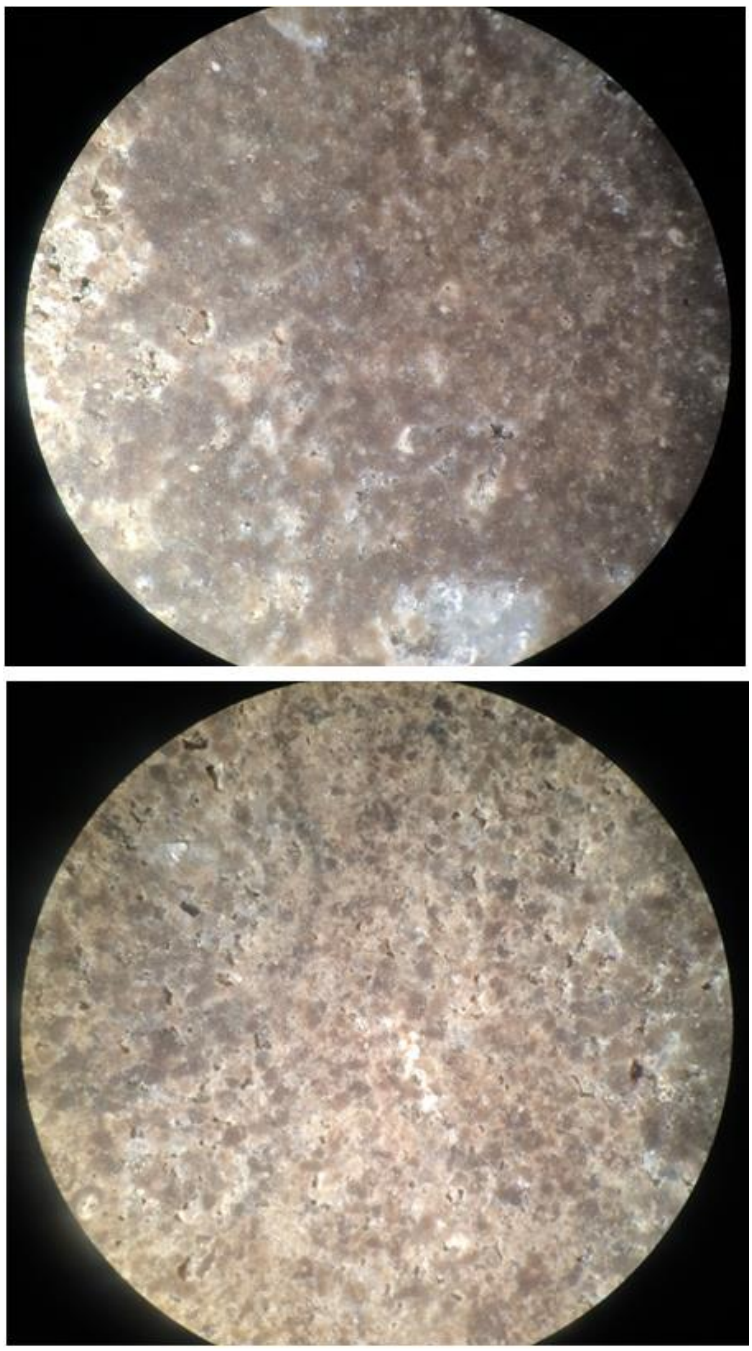

Figure 31 Photomicrograph showing the texture of subfacies 1B (above) and 2B (below).

Interpretation

Based on cross cutting relationships, it was determined that subfacies 1B formed the framework and 2B formed the cavity of subfacies B. Numerous, long, thin, vertical voids dissect microfacies 1B. These vertical voids are similar in composition to microfacies 2B. Also, cavities formed within microbial buildups usually have a smooth boundary which is evident in the lower part of the mapped core (Figure 30).

The thin section of Microfacies B was taken from the bottom of the core and contains mainly subfacies 1B and some of 2B (Figure 32). In relation to the mapped subfacies in the core, 1B's equivalent in thin section is represented by the brown, micritic peloidal area and 2D is the surrounding whitish-gray cement area. The boundary formed between 1D and 2D in the thin section is not apparent, however the brown peloids seem to float or appear suspended in the cement forming a shrubby, dendritic, branching upwards pattern in a calcite matrix. According to Folk's (1962) classification scheme it is a pelsparite.

Foraminifera, tube-shaped fossils and ostracods were identified however, microcoprolite are dominant. Generally, the fossils that are identifiable range in preservation from well to moderate, such as the foraminifera (0.25-0.4 mm) and tube-shaped fossil (0.3 mm), which were well preserved and had their shells replaced by micrite, ostracods (0.35 mm) were well preserved, and most microcoprolite (0.25-0.8 mm) were moderately preserved (Figures 33 and 34). The best preserved microcoprolites have isopachous rims (Figure 34, 4b). The allochems that comprise subfacies 1b are not densely packed. The calcite matrix that fill the void spaces between the allochems is drusy such as equigranular and blocky calcite. Some of the vugs present form touching

vug pores while other vugs form separate vug pores. Evidence of microbial presence can be seen in thin section 5b where a dendritic structure 0.6 mm in length was identified (Figure 35). Morphologically, it is made up of oval sac shapes joined together at one end and branches outwards.

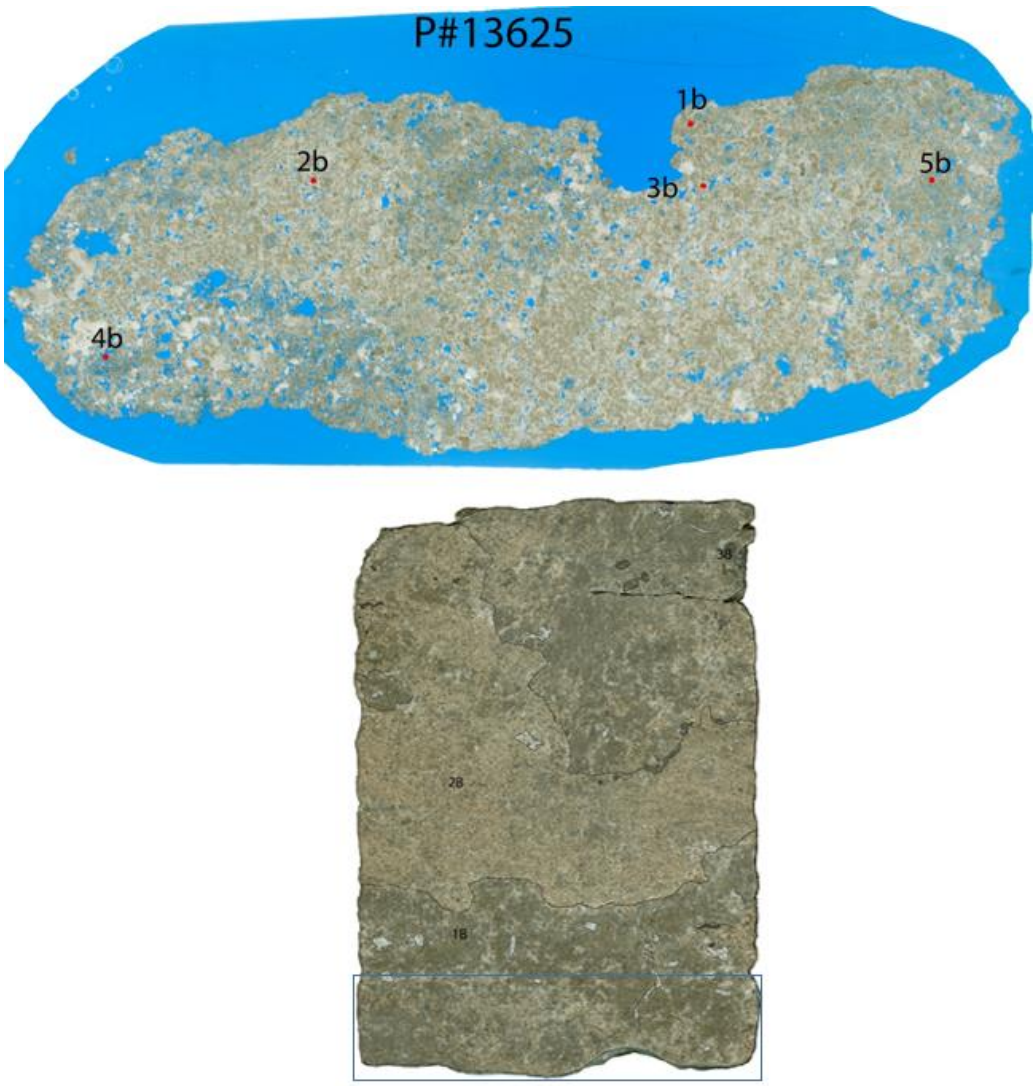

Figure 32 Thin section P#13625 was taken from the bottom of the core and mainly contains subfacies 1B and 2B.

Subfacies 1B and 2B are represented by the dark brown, building upwards peloidal area and whitish-gray matrix in thin section respectively.

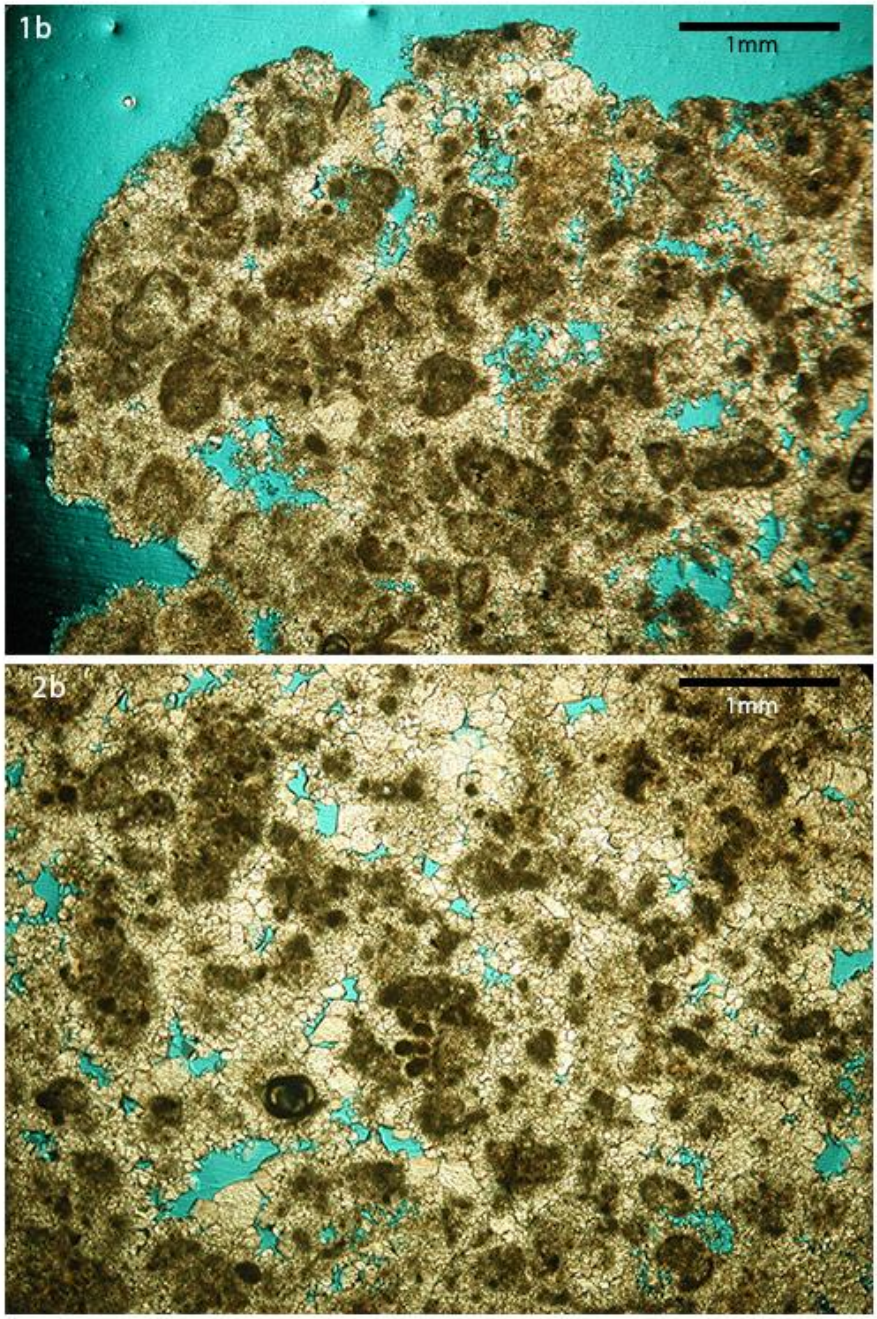

Figure 33 Thin section showing the components that makeup subfacies 1b in microfacies B.

Thin section 1b shows that the components that make up the micrite in subfacies 1B are mainly microcoprolite, peloids with few tube-shaped fossil and foraminifera. In 2b there is less allochems and they seem to float in a calcite matrix made up of drusy calcite such as equigranular and blocky calcite that occlude the vugs.

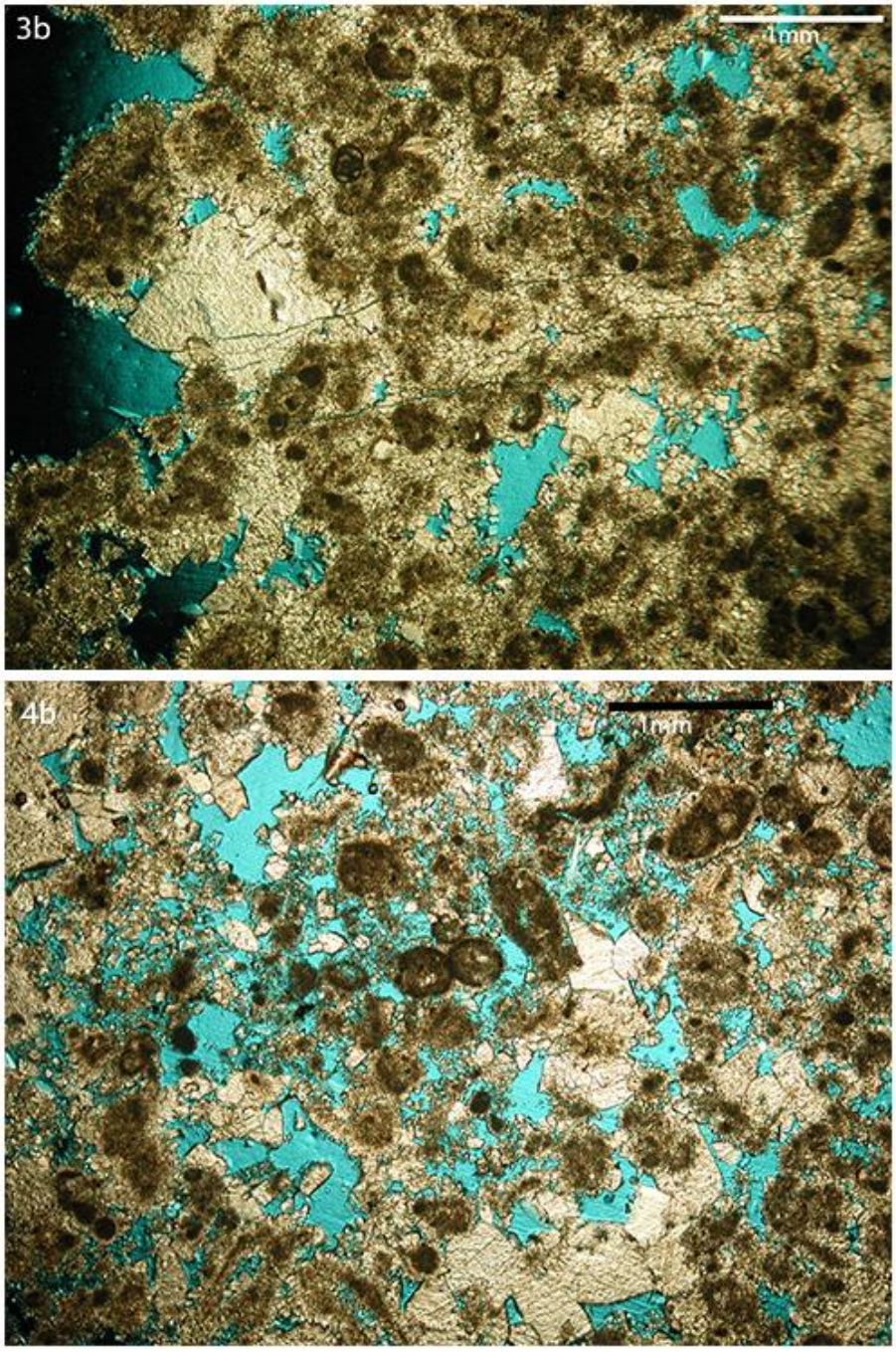

Figure 34 Thin section of subfacies 3b and 4b.

Thin section 3b horizontal fractures cut across calcite grains and micritic areas to connect some vugs. In 4b rapid cementation of the allochems form isopachous rims, vugs are infilled by drusy calcite such as equigranular and blocky to form subfacies 1B.

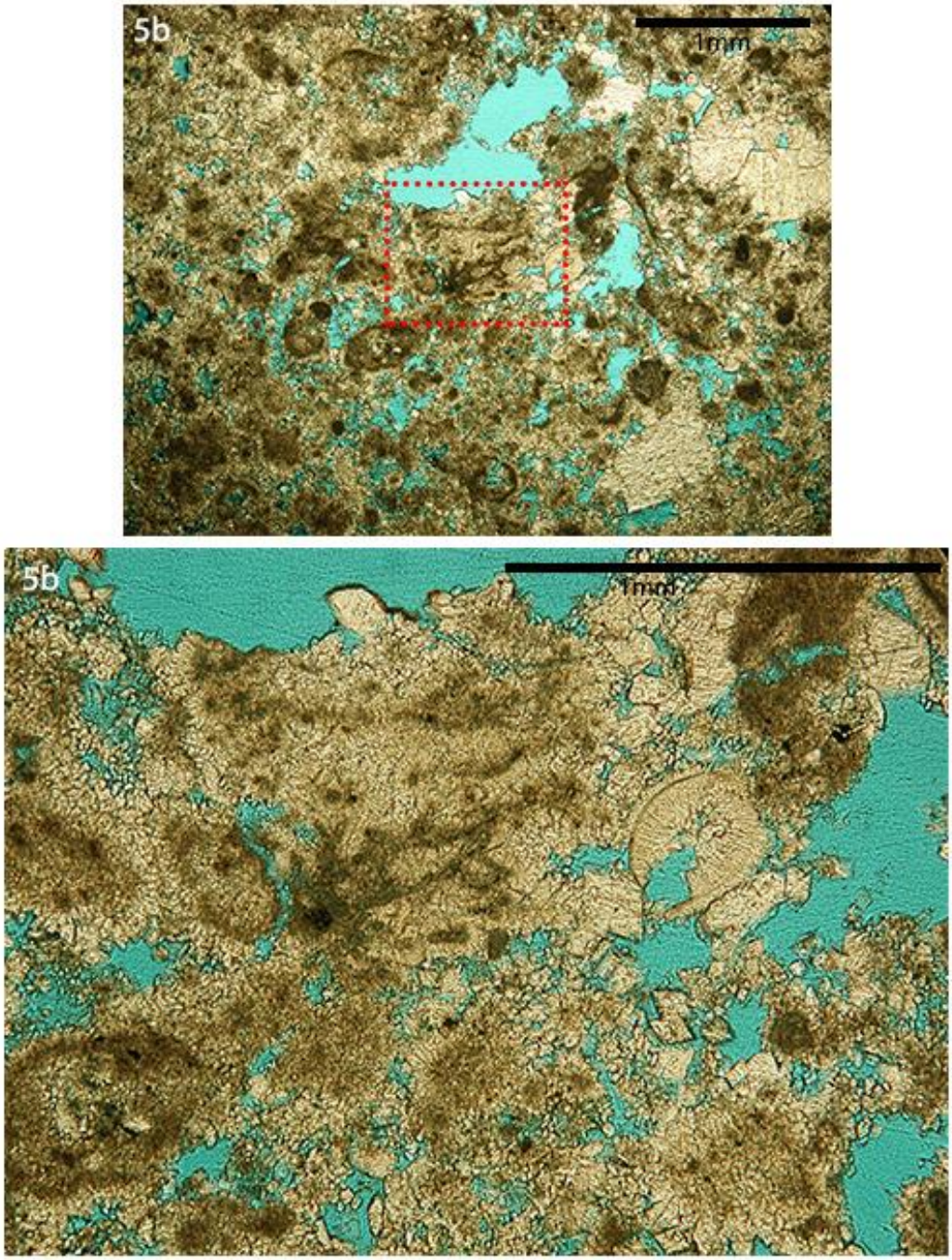

Figure 35 Inset photo of decapod fecal pellets, foraminifera, ostracods and peloids.

Red box shows a branching structure radiating from a common point. Zoomed in photo of branching structure (0.6 mm) is made up of individual elongated, sacs similar to *Renalcis*- like but linked together forming dendritic branches like *Epiphyton*- like. Euhedral dolomite rhombs that are crystal-supported are present.

Microfacies C & D: Chaotic & Brown Laminated Centimeter-Scale Cycles

Two microfacies are present in core P#16327-B and are separated by the stippled, red line (Figures 36 and 37). Microfacies D is orderly and has laminae in the cement therefore aptly named, “Brown Laminated Centimeter Scale Cycles” whereas microfacies C is not orderly, earning the name, “Chaotic”. Microfacies C formed above microfacies D and is separated by a transitional zone (between the stippled blue and red lines) which ends in an undulose boundary which is made distinct by the transition from light tan to dark gray or dark brown (Figure 36). The zone itself is described as transitional because the last orderly, layered approximately 2 cm thick cycles of microfacies D change from growing laterally to growing upward and the light pinkish-brown cement persists with large, black peloids. The location of the transitional zone in this core is in the uppermost layer of mapped subfacies 4D.

Microfacies C & D

Chaotic & Brown Laminated Centimeter-Scale Cycles

Well P#16327-B/10853.3ft

Figure 36 Mapped core showing the subfacies in microfacies D (Brown Laminated Centimeter Scale Cycle) & C (Chaotic).

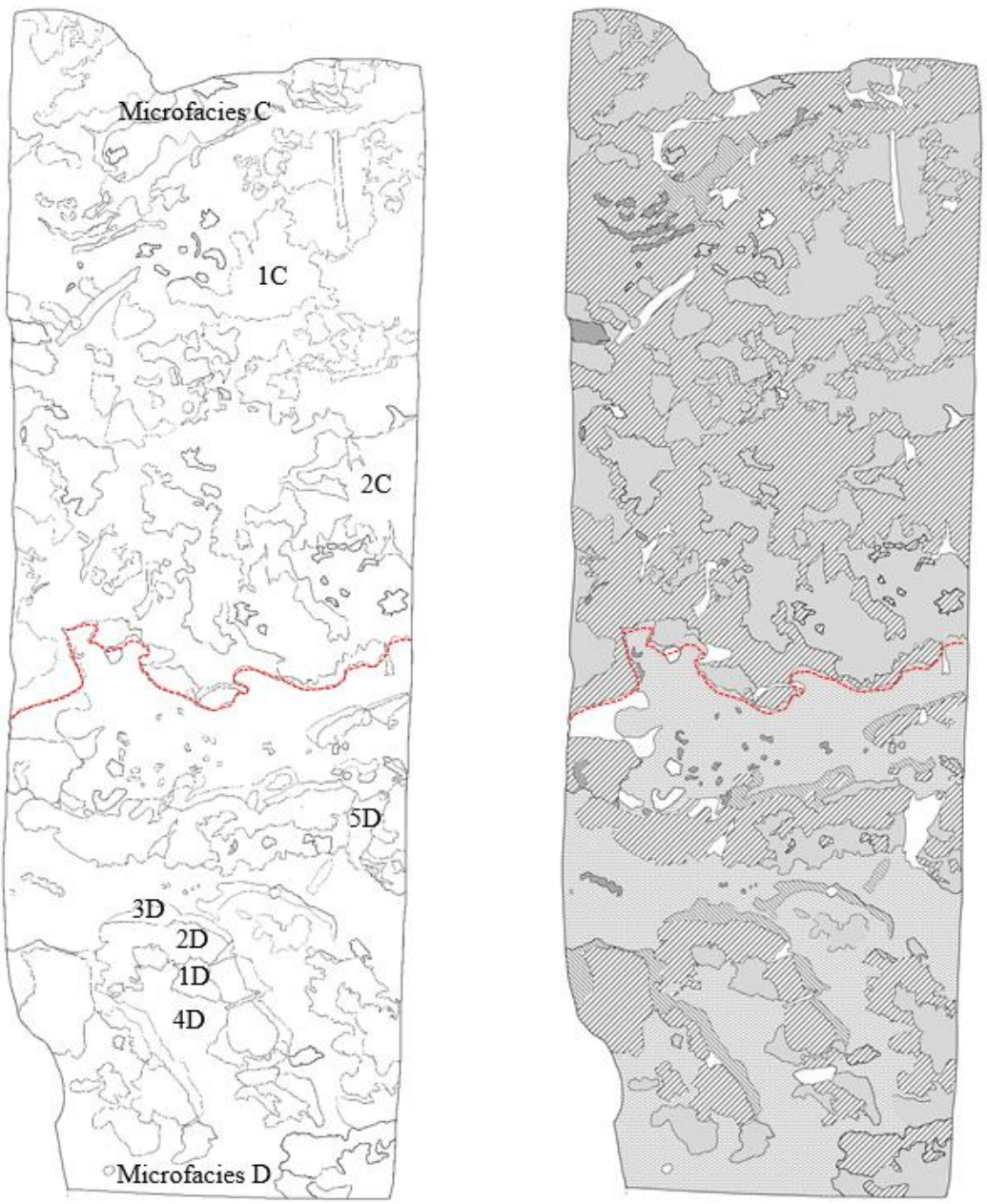

Figure 37 Mapped outline of microfacies C and D in same core.

In microfacies D the crust formed by subfacies 3D & 4D in the cavities make up more than half the rock's volume. In microfacies C the micritizing cement of 1C accounts for approximately half the rock's volume.

Microfacies C: Chaotic

Description

Microfacies C is made up of three subfacies that led to its buildup. Subfacies 1C is a grey, fine grained, dense calcite that is separated from subfacies 2C, a dark brown, dense, translucent, micritic calcite, by a definitive, but wavy undulose boundary. It is called "Chaotic" because of the pattern of growth (Figure 38).

A third subfacies, 3C was identified and accounts for less than 5% of the surface of the map made (Figure 38). It is a denser, very fine-grained, pinkish brown, homogeneous, calcite similar to crust formation in subfacies 3D of microfacies D (Brown Laminated Centimeter Scale). No fossils are present.

Subfacies 1C is similar to subfacies 1D in microfacies D. It is more prolific and better developed in Microfacies C, accounting for approximately 45% of the rock's volume (Figure 38). Fossils observed were skeletal fragments, foraminifera, some tube-shaped fossils, black rods and flecks all suspended in this dense, grey, fine-grained calcite matrix.

The dark brown micrite of subfacies 2C is similar to the one described in microfacies D, subfacies 2D, differing only in the fossil assemblage preserved within it. Fossils includes lots of foraminiferas, skeletal fragments, filamentous strands and few clusters of very small (<0.1 mm across) tube-shaped fossils (Figure 40). These filamentous strands are microbial in origin and have been identified in previous microfacies containing brown micrite with shrub-like to dendritic microfabric similar to subfacies 2C (Figure 26).

Microfacies C- Chaotic

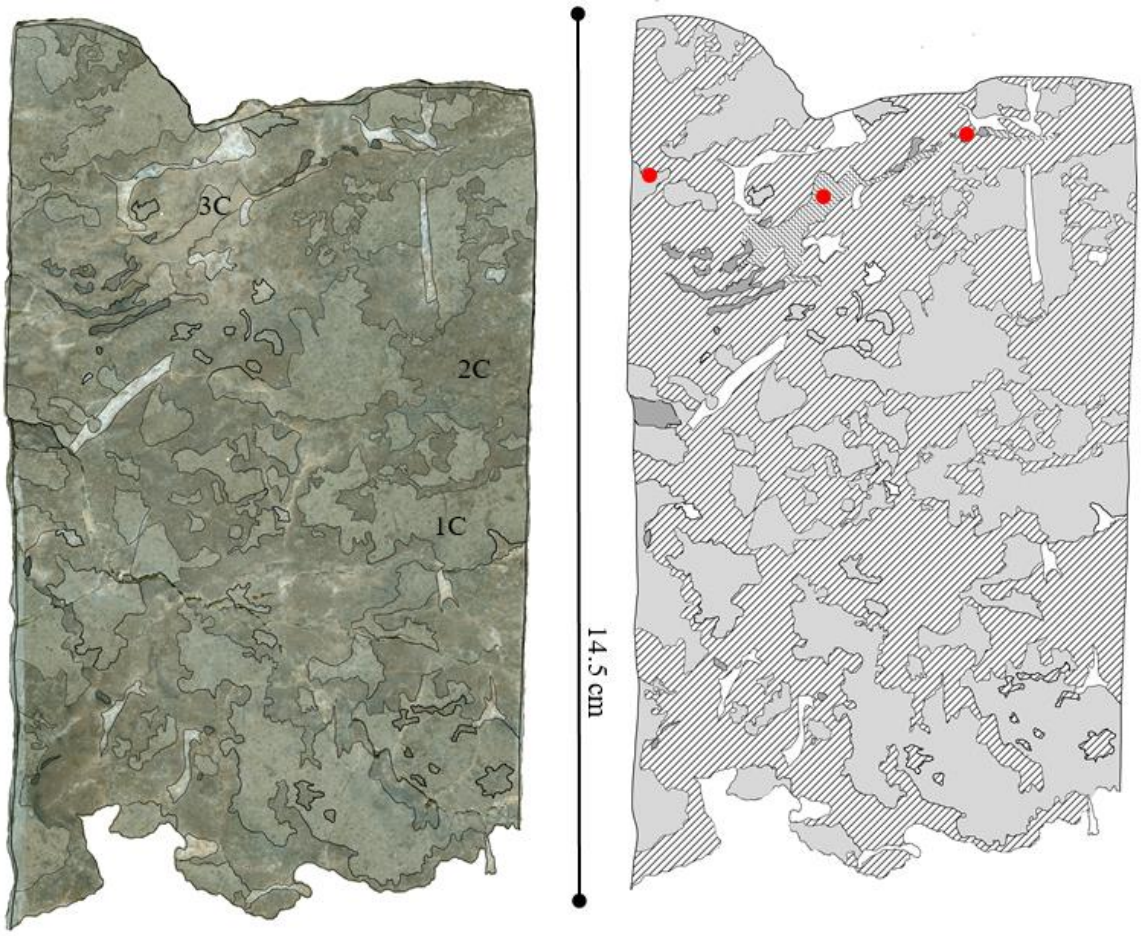

Figure 38 Core from well P#16327-B, depth 10, 853.3 feet shows polished surfaces with numbered subfacies (left) and subfacies map of the polished surface (right).

Red dots show location of photomicrographs underneath.

Interpretation

Cross cutting relationship was used to determine the order of subfacies formation. Photomicrographs show the dark brown calcite of subfacies 2C partially dissecting the grey calcite of subfacies 1C at the perimeter, infilling voids within subfacies 1C, and totally breaking up the subfacies to form smaller pieces that appear to "float" or be suspended in the dark brown micrite. Subfacies 1C would therefore be the primary framework (Figure 39).

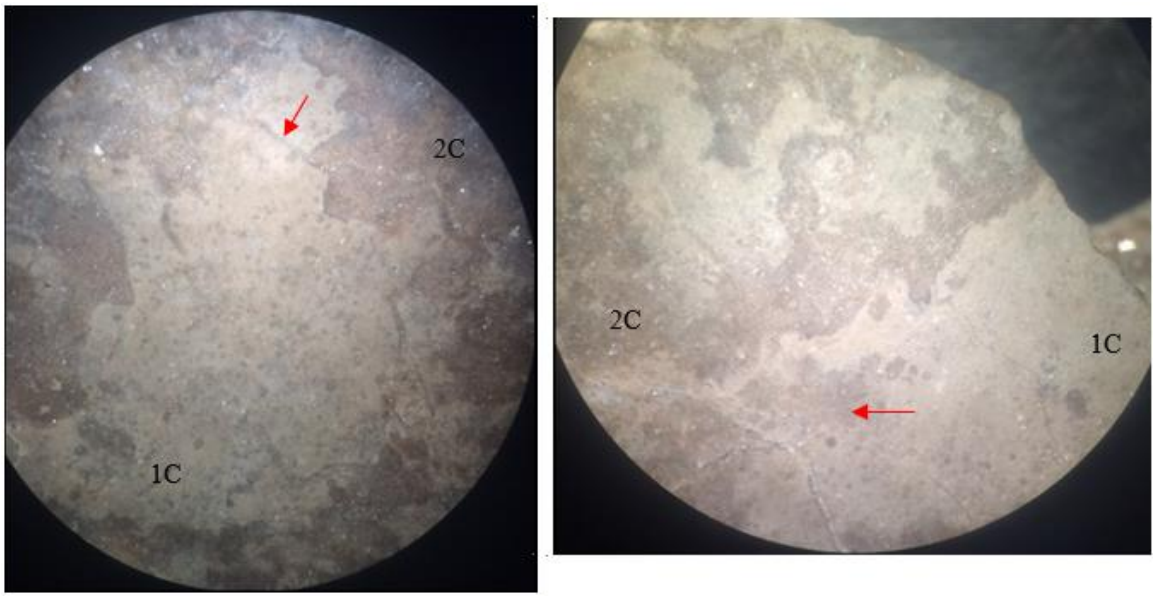

Figure 39 Cross cutting relationships in microfacies C.

Red arrows point to cross cutting relationships: partial dissection of subfacies 1C by subfacies 2C (left) and void infilling and total dissection of subfacies 1C into smaller pieces that appear suspended in 2C (right).

New to the dark brown micrite of subfacies, 2C are what appears to be clusters of juvenile, skeletal tube-shaped fossils (Figure 40). Throughout the length of the core column three entombed, preserved clusters are identified. The new environment offered in microfacies C seems suitable for recolonization. What would cause this entombment preventing propagation of this organism? Clues can be taken from the previous underlying microfacies where unraveling of the Brown Laminated Centimeter-Scale Cycle of microfacies D along with a change in direction of peloid accumulation and laminae from horizontal to vertical, maybe attributed to sea-level rise.

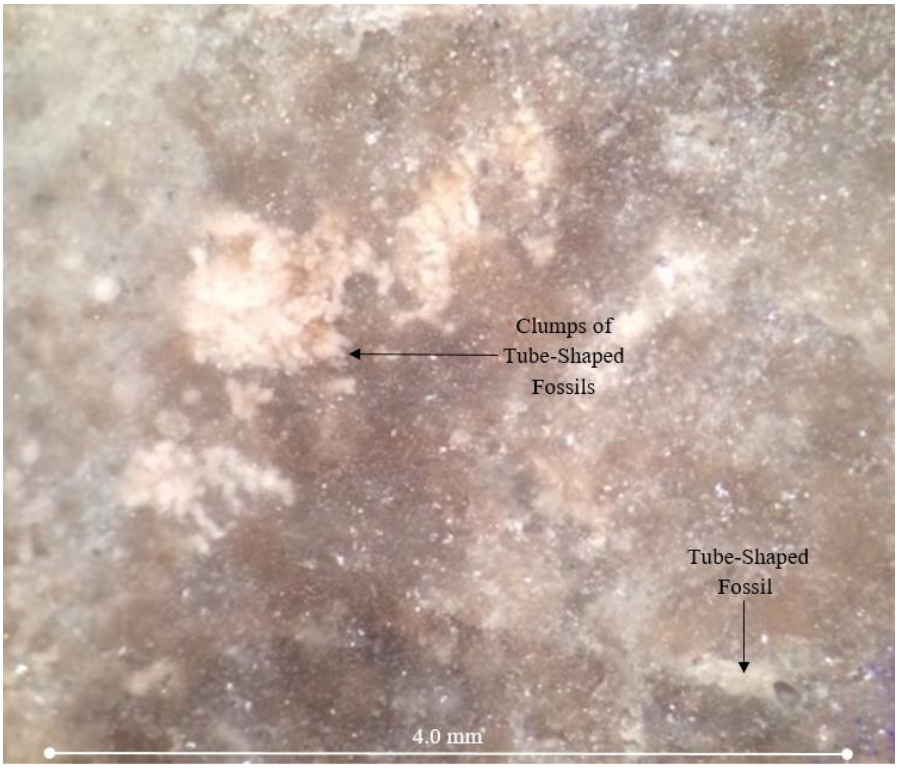

Figure 40 Photomicrograph of a cluster of juvenile tube-shaped fossils suspended in the brown micrite.

Individuals have shells that are translucent and arranged in a tube fashion. The largest cluster in the center is < 1.0 mm across.

Also, sea-level rise would explain the promotion of rapid upward microbial growth of subfacies 2C cross cutting and enveloping subfacies 1C since microbes are photosynthetic and need sunlight to metabolize. The change in depositional environment from wave-swept to relatively deeper, calmer waters may explain the close association of the two subfacies competing for sunlight and the scarcity of cavities. Tube-shaped fossils decline suggesting either preferential wave-swept environment or entombing from fast microbe growth before reaching adult stage. The rate of sea-level rise was probably rapid judging by the good preservation of clusters of juvenile along the core's length.

Of significance is the scarcity of the larger size tube-shaped fossils. A correlation can be made here based on previous observations in microfacies D whereby, as the abundance of tube-shaped fossils decrease, subfacies 1C (grey micrite) increases. This drastic decline is probably due to limited habitat in cavities, ultimately causing a temporary, mini extinction.

Subfacies 3C represents either cavity formation from fracturing after the development of subfacies 1C and 2C or a change in microbial community along a growth boundary. In effect crust formation can heal fractures preserving the denseness of the limestone.

Microfacies D: Brown Laminated Centimeter Scale Cycles

Description

Microfacies D is composed of four subfacies (Figure 41). Subfacies 1D is grey, fine grained calcite that is usually separated by sharp, but wavy boundary from 2D, a dark brown, translucent, micrite 0.25 to 1.5 cm thick. The boundary between dark brown subfacies 2D and fine grained pinkish-brownish subfacies 3D is smooth and readily visible because of the difference in color. Subfacies 3D is very fine grained, pinkish-brown, and homogeneous. Subfacies 3D is consistently encrusted by a thin < 0.05 mm, black layer. Subfacies 4D forms a transitional boundary and is composed of very fine grained, pinkish-brown calcite with brown laminae and peloids, many of which form dendritic structures giving the cement an unhomogenized appearance (Figure 41). Small amounts of medium grained, pinkish- brown calcite is present within subfacies 4D.

Subfacies 1D (grey micrite) make up about 15%, subfacies 2D (dark brown micrite) 20% and subfacies 3D and 4D (crusts) makes up about 65% of this piece of core (Figure 41). Thin, long, clear filament strands measuring 1-2 mm long were observed protruding from subfacies 4D. The dominant allochem is tube-shaped fossils. This microfacies is named centimeter-scale cycles because this distinctive pattern of repeated layers was seen throughout many (16.7%) of the cores studied. Subfacies 1D, 2D and 3D was identified with widths ranging from 1.0- 2.0 cm.

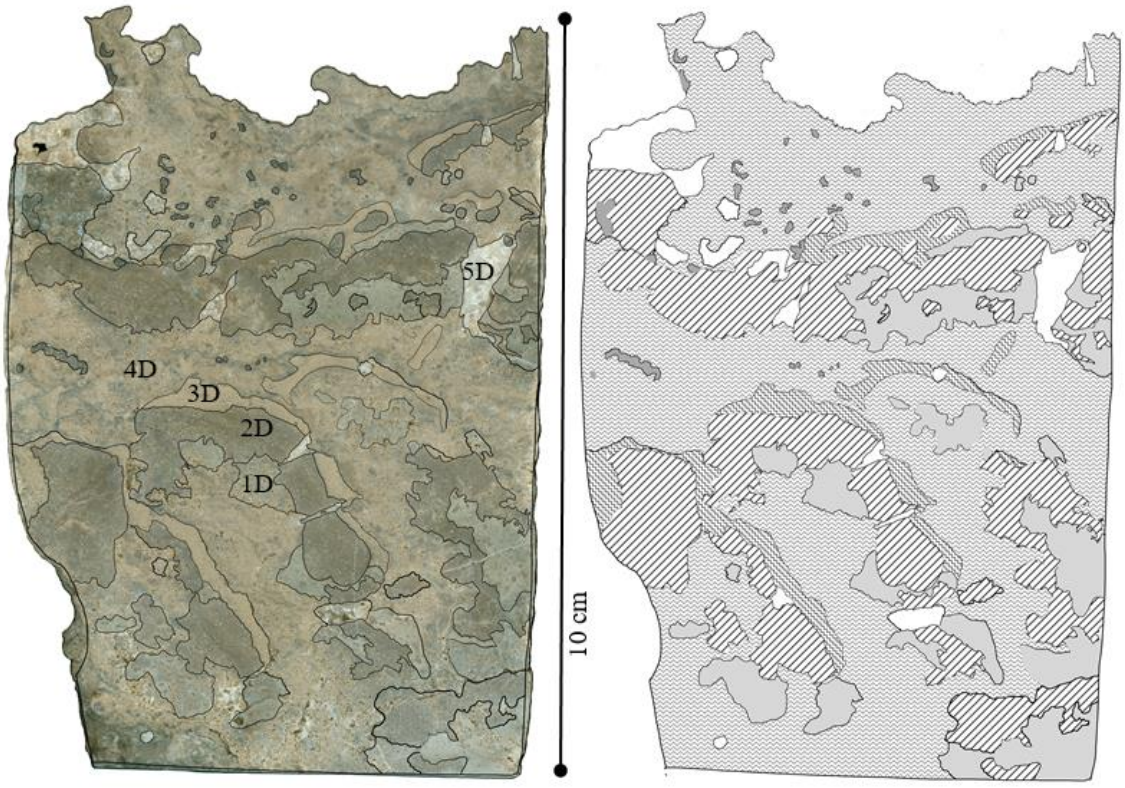

Figure 41 Mapped core showing the order of succession formation: 1D & 2D framework, 3D & 4D crust.

The crusts account for about 65% the rock's volume in this piece of core.

Subfacies 1D is a dense, very fine grained grey matrix containing remnants of skeletal fossils, approximately 30%, with a predominance of the tube-shaped fossils like the ones identified in microfacies A (Black *Renalcis*- like Layer), along with filamentous strands and disconnected, circular and elongated irregular shapes filled with brown micrite. The margin of subfacies 1D is serrate digitate, comprised of circular to clusters of circles with micritic pore centers giving it an overall fluid, wavy appearance (Figure 42).

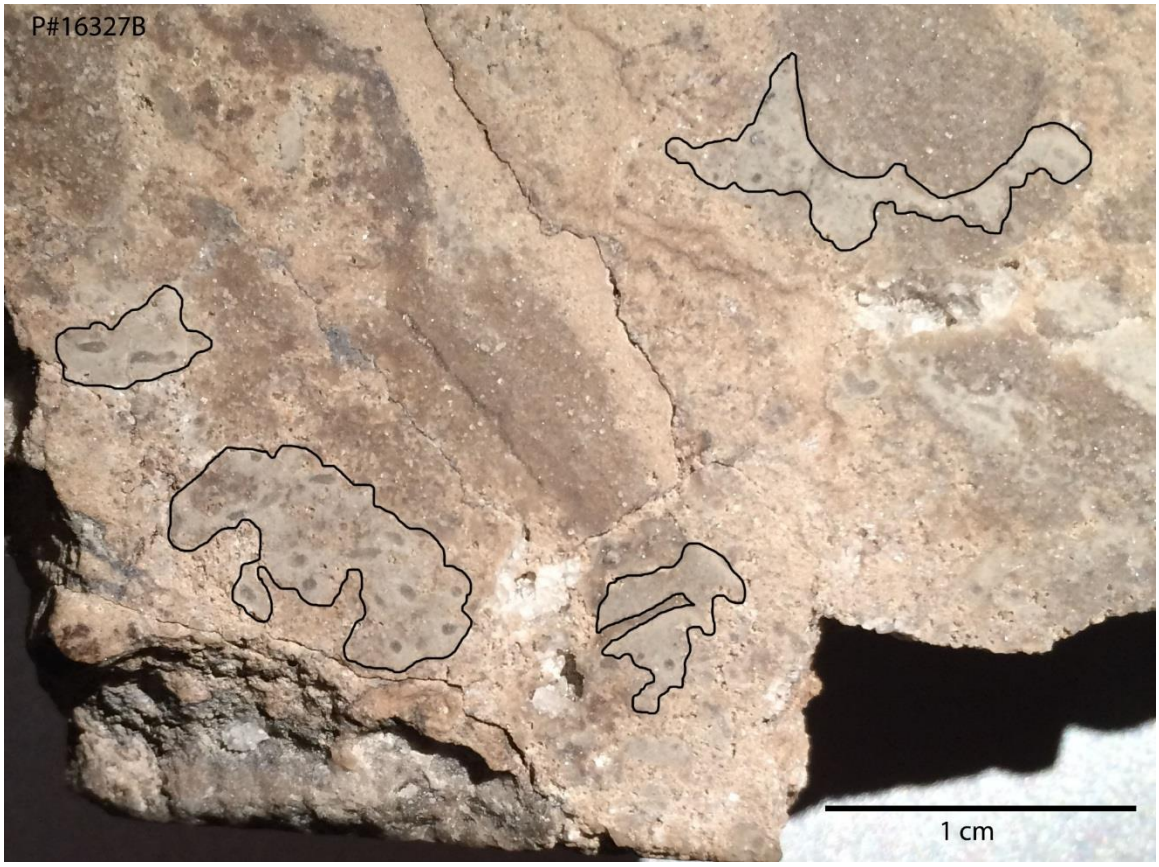

Figure 42 Outline of grey subfacies 1D showing disconnected, circular and elongated shapes filled with brown micrite.

Subfacies 2D mainly occurs above and sometimes surrounds subfacies 1D. It is a dark brown, translucent micrite similar to that in microfacies A (Black *Renalcis*- like Layer). The fossil assemblage includes foraminifera, tube-shaped fossils, but mainly skeletal fragments of the tube- shaped fossil. The fossils are evenly distributed throughout the dark brown micrite which has steeply dipping angles of 60º (Figures 42 and 43c).

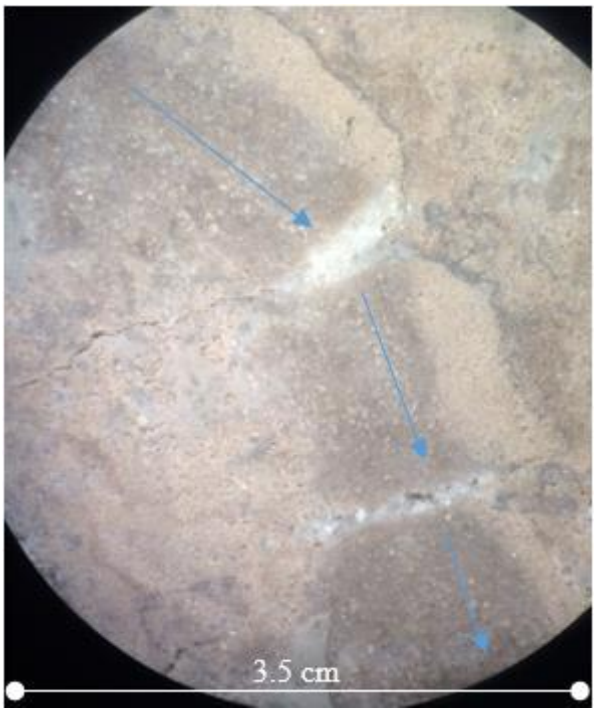

Figure 43 Photomicrograph shows allochems, predominantly tube shaped fossils within the dark brown micritic subfacies 2D.

Subfacies 2D can have steeply dipping angles of 60º (blue arrows).

Subfacies 3D is a non-skeletal, microbially precipitated carbonate that is densely packed forming a pink, fine-grained crust, not cement, 1.0- 5.0 mm thick. The calcite crystal's color and size is homogenous with no peloidal grains (Figures 43 and 44c). It mainly occurs above subfacies 2D. No fossils were found in the crust. This subfacies is consistently found in close association with subfacies 4D separated mainly by an encrusting, black, thin, clotted, peloidal to laminated microfabric.

Subfacies 4D is also a non-skeletal, microbially precipitated calcite crust with no skeletal fossils observed. It is distinguished from subfacies 3D by its greater thickness (0.5 to 2 cm), its fabric of peloids (1 mm) arranged in thin (less than 1 mm) layers of small dendritic shrub structures, and laminae (Figure 44). Overall, the calcite crust of 4D

appears inhomogeneous compared to the homogeneous crust of subfacies 3D. The thickness of subfacies 4D ranges from 0.5 up to 2 cm in the uppermost layer of this subfacies in the core.

The laminae present are multiple and sub parallel following the general orientation of the previous subfacies 3D. The peloids present mimic the orientation of the laminae either floating in the inhomogeneous crust or clinging to the black, encrusting laminae above the homogeneous crust (Figures 44a, c). The direction of growth in the case of the suspended peloids is upwards (Figure 36). This suspension of arranged peloids can be attributed to an adhesive biofilm from microbial buildups capturing the grains. Photomicrograph 43b clearly shows the crust developed at a 45ºangle to horizontal with peloids on the surface (Figure 44).

Subfacies 5D is blocky calcite that completely fill voids. The sizes of the filled voids vary from as large as 1.8 x 0.6 cm to as small as 0.2 mm. The blocky calcite is mainly found cross-cutting subfacies 1D, 2D and 3D.

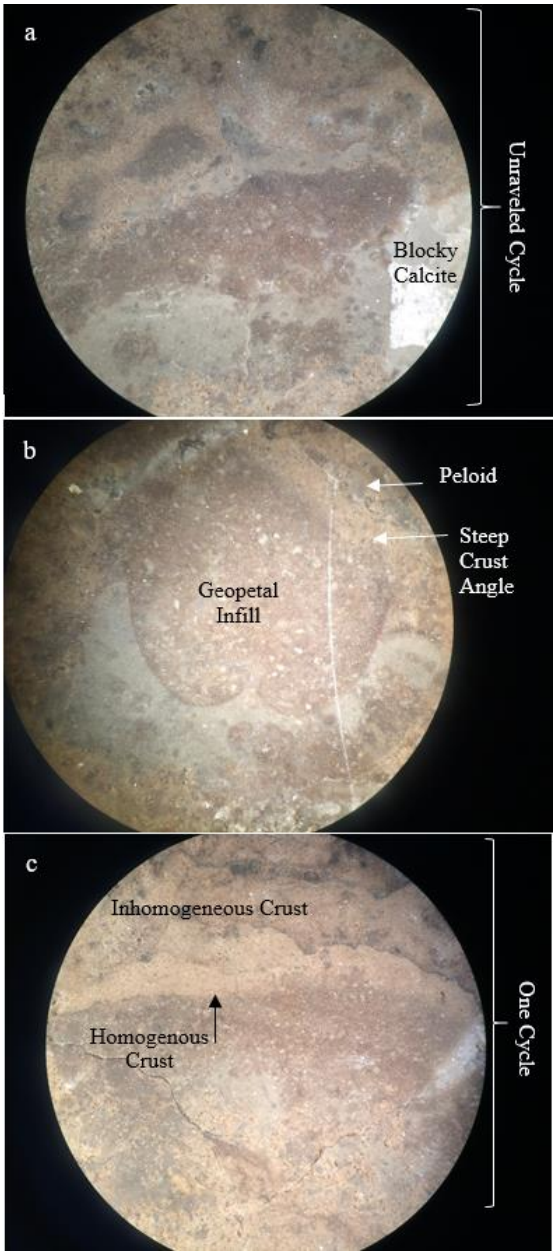

Figure 44 Photomicrographs of microfacies D.

Photomicrograph “a” represents a horizontal, unraveled cycle with light tan colored homogeneous crust and inhomogeneous crust with peloids that appear to float/suspend in the polished surface. Photomicrograph “b” is a possible infilled bivalve geopetal structure showing way up, the crust on the right of it formed at a steep 45º angle and has peloidal grains adhered to it. Photomicrograph “c” represents a normal cycle showing the boundaries between different types of crust, including the thin, black layer between the homogeneous crust and the very fine grained dendritic layer.

Interpretation

The buildup order is as follows: 1D and 2D formed the framework which created cavities for subfacies 3D and 4D to develop as homogeneous and inhomogeneous crust respectively. Subfacies 1D represents a very indistinct framework of microfacies D (Brown Laminated Centimeter Scale Cycle) and occur in close association with 2D.

In subfacies 1D (grey micrite), the arrangement of the micritic filled shapes are similar to ostium and osculum found in sponges, which are pore canals for water intake and out take respectively (Figure 42). The possibility of a sponge origin is deduced based on photomicrographs show a spicule and possibly a stomatoporoid that has been enveloped by microbes. Stromatoporids are sponges that were major reef constructors throughout the Paleozoic and the Late Mesozoic. Due to the abundance of the rasping tube fossil preserved in 1D, it can be inferred that these organisms heavily influenced the shape and rate of sponge growth due to preferential overfeeding allowing for succession 2D to develop more prominently. Another explanation of the ostium- like and osculum-like hole shapes can be due to the position the tube- shaped fossils were preserved within the grey micrite. The infilled holes could represent their interior tubes in cross section view. Together, subfacies 1D and 2D represent some sort of symbiotic relationship between sponge and microbes.

Subfacies 3D represents crust. According to Riding (2011b), crusts typically occur on wave-swept reef margins in habitats with low to no light, such as cavities and form as late stage veneers by heterotrophic community on framework skeleton at the end of active reef development. Heterotrophs cannot synthesize its own food so obtains it by feeding on other organisms or dead organic matter. In microfacies D, this cryptic habitat

formed by subfacies 1D and 2D after development, provided a home for these crust forming bacterial community to develop since it hindered competition for space from foraminifera, sponge and the tube-shaped rasping invertebrates along with other skeletal fossils which were probably eukaryotic.

Crust formation can give the true/initial size of cavities and show how interconnected they are since no more growth or buildup of the framework is occurring. This is especially true if late stage diagenesis does not influence the original cavity size and if crust only completely fill these cryptic voids since the sediment deposited would be autochthonous being supplied by microbial induced precipitation and disintegration of the surrounding framework. The homogenous crust is terminated abruptly by thin, black layer of encrusting microbes forming a sharp boundary and the less homogeneous crust of subfacies 4D begins.

Subfacies 4D is also crust. Microbially precipitated calcite completely fills the remaining space lithifying and preserving the framework. In microfacies D cavity sizes vary due to their irregular nature, ranging from 0.8mm x 1.5 cm to 8.0 cm x 2.0 cm. Originally, these cryptic habitats were probably isolated from one another but after crust formation began, disintegration of the surrounding framework successions that separated the cavities ensued, thus serving to enhance connectivity of the cavities. Also, late stage diagenesis in microfacies D (Brown Laminated Centimeter Scale), as evident from fracturing and secondary dissolutional voids that bifurcate through continuous successions of 1D and 2D, linked the cavities contributing to interconnectivity. However, in subfacies 5D, the formation of blocky calcite completely filled these secondary voids once more reducing cavity interconnectivity (Figures 41 & 44a). According to Kirkland

et al. (1998) in reference to micrites, where the surface is steep, gravity-controlled micrite may have a mucilaginous component (Figure 44b).

The peloidal arrangement observed is of importance going from being deposited at a steep then horizontal angle on adhesive biofilm then suspended by sub parallel, branching laminae in a general upwards direction, terminating in microfacies C (Chaotic) above (Figure 44). This could indicate a rise in sea-level since during this time period a transgression was taking place. According to Riding (2011b), the preferential development of crust at wave-swept reef margins probably indicates the effect of increased carbonate saturation state by intense seawater flushing. Crust formation therefore, can be a depositional paleoenvironment indicator.

A change of direction of peloidal accumulation in biofilm can be an indicator of sea-level rise and the abundance of tube-shaped fossils indicates a preferential food source and water depth in this case sponge/algae and shallow agitated water respectively where, it alters the microbial framework. It is also possible that cryptic habitat formation limited the available space for a suitable habitat thus creating competition for a shrinking space while proliferation of the tube-shaped fossil continued thus accounting for their abundance and good preservation.

The presence of medium-grained calcite very similar in color to the surrounding fine-grained crust was noted in subfacies 4D. This larger calcite was formed as a result of calcite replacement of micritic pieces from subfacies 1D (grey) and 2D (dark brown). Minute remnant pieces that were not replaced were preserved within the medium- grained replaced pieces. These remnant pieces were probably deposited into the cavities due to

the feeding activity of organisms breaking down the already semi- rigid main framework into smaller pieces.

The thin section of Microfacies D was taken from the bottom of the core and contains subfacies 1D, 2D, 4D and 5D (Figure 45). In relation to the mapped subfacies in the core, 1D's equivalent in thin section is represented by the whitish-gray area of dense, microcrystalline granular mosaic cement, 2D is the dense, brown micritic peloidal area, 4D is the porous, intercrystalline calcite sea referred to as inhomogeneous crust in the core, and 5D is the large blocky calcite grains occluding and infilling fractures and vugs. Subfacies 3D was not present in the area of the core the thin section was made from. The boundary formed between 1D and 2D in the thin section is apparent.

Figure 45 Thin section P# 16327BD contains subfacies 1D, 2D, 4D & 5D.

Thin section P# 16327BD was taken from the bottom of the core and shows three distinct areas: whitish-gray calcite, brown micrite and intercrystalline calcite sea.

According to Folk's (1962) classification scheme it is either a biosparite or pelsparite. Foraminifera, gastropod and intraclasts were identified however, peloids are more dominant. Generally, the fossils that are identifiable were well preserved and had their shells either replaced by micrite or totally dissolved to form a mold that was still able to reveal their detailed outlines (Figure 46 a, b, f and Figure 47 k, l). Compared to

Microfacies A, faunal assemblage seems to be more abundant and identifiable with three different species of foraminifera, gastropod (2.4 mm) and a preponderance of tube shaped fossils.

The thin section shows evidence of microbial influence, clearly seen in the arrangement of peloids forming a clotted, shrubby pattern around allochems (Figure 46 c, d, e, f and k). The allochems seem to act as substrate for microbial growth. This confirms the core's mapped subfacies order as subfacies 1D developing first since it acted as a substrate followed by the colonizing microbes of subfacies 2D forming the dense, dendritic peloidal, brown micrite framework. A peloidal microcrystalline cement also points to evidence of microbial buildup (Figure 46 a, f). This cement is composed of peloids and molds of foraminiferas bearing a radiating halo of micrite brought about by microbially induced precipitation (Figure 46 f).

Overall, porosity is depositional with diagenetic influence i.e. the framework (subfacies 1D and 2D) formed cavities (subfacies 4D) which became infilled or partially occluded by calcite forming vugs and voids. Generally, porosity is absent in the framework as seen from the dense, fine grained nature of the matrix and the clotted clusters of peloids. Afterwards, diagenetic processes occurred such as fractures and dissolution forming new porosity. However, blocky calcite formation served to obliterate some of the new porosity. Porosity types identified were fractures, vugs, intercrystalline, moldic and intraparticle.

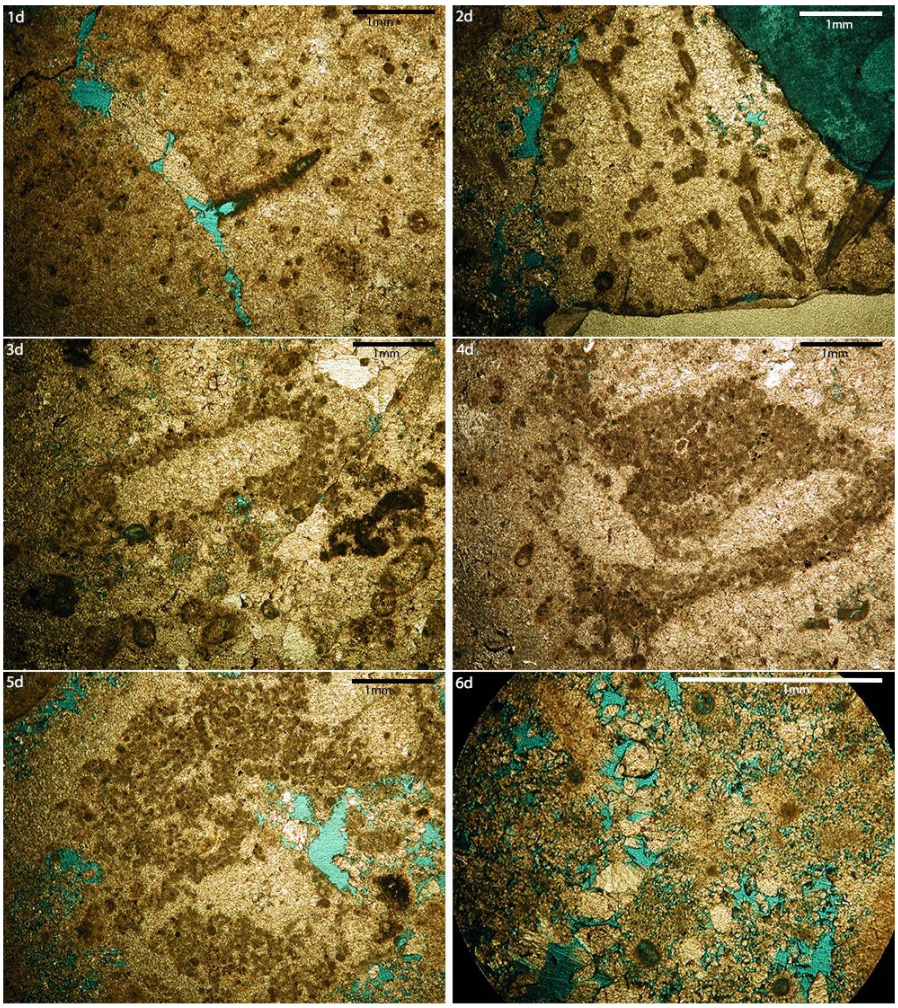

Figure 46 Evidence of microbial influence.

1d: Tube shaped fossil, foraminifera, peloids in a microcrystalline calcite cement, fracture occluded with blocky calcite
2d: Numerous micritized tube shaped fossils and foraminifera suspended in a dense calcite matrix
3d: Peloidal arrangement encrusts and radiates around an allochem outlining it
4d: Peloidal arrangement is clotted and shrub-like around an allochem acting as substrate
5d: Peloids in a dense fine grained calcite matrix
6d: Peloidal microcrystalline cement has peloids and foraminifera with intraparticle porosity, have a radiating micritic halo surrounded by granular mosaic calcite and large calcite grains within voids

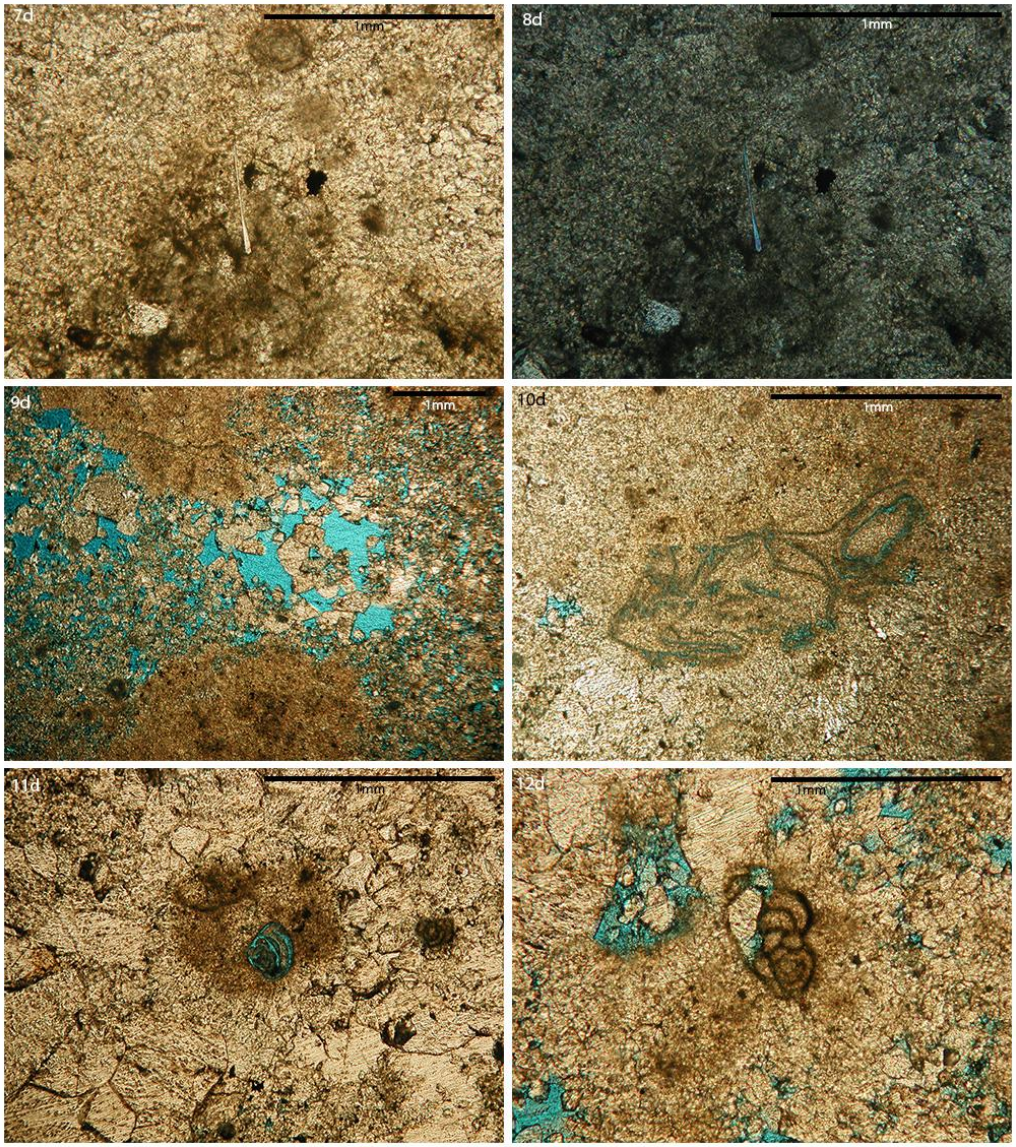

Figure 47 Preserved fossils in microfacies D.

Thin section photos 7d & 8d of a sponge spicule in a fine grained calcite matrix in plane and cross polarized light. Photos 1d, 5d, 9d, 10d/11d & k showing the different types of porosity found in microfacies B: fracture, vuggy, intercrystalline, moldic, intraparticle respectively. Overall, the process that created porosity is depositional with diagenetic influence

.

CHAPTER IV

DISCUSSIONS AND CONCLUSION

Discussion

The objectives of this study is to 1) establish the microstratigraphic successions of events that led to the formation of these buildups in the lower, thrombolitic boundstone reservoirs; and 2) to determine if freshwater or seawater influenced the distribution of the buildups. This ultimately aids in understanding the complexity of reservoir heterogeneity as well as deepens understanding of the origin of these enigmatic buildups.

To test the hypothesis that the Little Cedar Creek Field Smackover Formation buildups can be divided into microfacies and that their distribution is therefore to some extent predictable it was first necessary to gain a fundamental understanding of the origin of these mounds. To do this it was necessary to establish the microstratigraphic succession of events that formed these buildups in the lower, thrombolitic reservoir. Study of the thrombolitic buildups resulted in two significant contributions. First, distinguishing microfacies and subfacies allowed for identification of and understanding of the formation of higher and lower porosity zones. Second, an understanding of the succession of events allowed for determination of the primary event in formation of the lower thrombolitic reservoir. The first micritic component of a subfacies was considered most likely to give an original isotopic signature and answer the question of marine or non-marine origin.

Four distinct microfacies were defined from the cores: A “Renalcis-like layer”, B “Digitate”, C “Chaotic”, and D “Brown Laminated Centimeter Scale”. Variations of a single microfacies can occur as it progress through the core column along with alteration from diagenesis. As a result, obvious features that make up the thrombolite facies were used to delineate the microfacies (Table 4). These obvious features include color of the subfacies and the amount of peloidal micrite to cement to crust to black encrusting *Renalcis*-like coating.

It was found that microfacies A is composed of micrite, cement, and black *Renalcis*-like coating, no crust is present in this microfacies. It is easily recognizable by the predominant presence of the *Renalcis*-like black coating (primary encruster) that occur in multiple layers which mainly encrust the dark brown peloidal micrite framework in this microfacies. Microfacies B has no crust and is composed of peloidal micrite framework with jagged edges and cement, however the black coating is negligible to absent and was found along the perimeter of the framework. Microfacies C is mainly a dark brown and grey peloidal micrite framework with minimal to no cement, no crust and no black coating. Microfacies D has random, individual pieces of dark brown micrite with crust formation on top of the micrite only. The micrite pieces “float” in a light brown cement that contains multiple laminae giving it the appearance of a stromatolite.

Table 5 Distinctive features that aid in the identification of the microfacies.

	Distinctive Features of Microfacies				
	Black Renalcis-like Layer	Micrite	Cement	Crust	Laminae
A	Yes	Yes	Yes	No	No
B	No	Yes	Yes	No	No
C	No	Yes	No	No	No
D	No	Yes	Yes	Yes	Yes

After establishing the four microfacies, stratigraphic and structural cross sections were made along with porosity and permeability graphs which show microfacies A (Black *Renalcis*-Like layer) was the least porous and permeable with individual thicker buildups (4- 32 feet), microfacies B (Digitate) was more porous with individual thick buildups (3- 26 feet), microfacies C (Chaotic) was less porous than B and contained thinner buildups (2- 8 feet), whilst microfacies D (Brown Laminated Centimeter Scale) was the most porous and permeable with relatively thinner buildups (1- 7 feet). Generally, both microfacies A and D occurred in the higher areas.

There was an uneven distribution of the microfacies in the wells: A 52.7%, B 24.6%, C 6.0% and C 16.7%. The cross section shows that the thrombolite facies is composed of relatively high and low areas. The high areas according to the stratigraphic cross section appear to be formed by individual mound shape mainly made up of microfacies A and D and sometimes microfacies C (Chaotic). The mound shapes are separated by relatively lower areas or intermounds that is mainly composed of

microfacies B (Digitate) but can contain microfacies A and D. The mounds are built by microfacies A (Renalcis-like layer) and D (Brown Laminated Centimeter Scale) with microfacies A being more predominant (52.7%). Overall, from northeast to southwest in the Little Cedar Creek Field, the general trend is: microfacies B (Digitate) is more prevalent favoring lower areas; microfacies C (Chaotic) becomes absent; individual thicker buildups occur; and fewer types of microfacies form the buildups (mainly A and D in high areas and mainly B in low areas). Microfacies A in cores is differentiated by its black *Renalcis*-like coating that encrusts brown peloidal micrite of subfacies 1B or framework as seen in mapped core P#14270.

Based on paleogeographic reconstruction of the shoreline being 0.5- 6.75 miles (0.31- 4.2 km) away with water depths of 10- 30 feet, the higher mound areas are closer to the sea-level surface. Here, energy would be relatively higher due to for example, water oscillation/turbulence/wave action or the elements prompting encrustation growth of the *Renalcis*-like layer to form preferentially, in effect forming and protecting the framework and enhancing its rigidity. Protection of the peloidal, micritic framework from diagenesis should be noted here since Microfacies B (Digitate) is similar to microfacies A but lacks black *Renalcis*-like encrustation.

In these areas current energy was probably relatively lower, therefore, it was not necessary for black, sturdy encrustations to develop. In mapped cores, of microfacies B, the peloidal micritic buildups of subfacies 1B (framework) contained long, vertical, infilled veins and jagged boundaries in some parts. Compare this to microfacies A with smooth boundaries and small infilled voids. A deduction can be made that layers of

encrustations can offer its substrate (subfacies 1A framework) protection from the elements and affect the degree of diagenesis.

Porosity and permeability log plots were available for only six of the ten wells. Measurements of each microfacies from each well was recorded in a table and plotted on a graph (Table 4 and Figure 17). Porosity values ranged from 2% to 16.83% and permeability values ranged from 0.087 to 930 millidarcies. Microfacies A (Black *Renalcis*- like Layer) generally had the lowest porosity and permeability values and microfacies D (Brown Laminated Centimeter Scale Cycle) generally had the best values. Overall, the majority of the data points on the graph clustered below 100 millidarcies but with a wide range of porosity values.

In cores and thin sections, the classification of pore type encountered are as follows: microfacies A (Black *Renalcis*- like Layer) contained fracture, fenestral, intercrystalline, and vuggy; microfacies B (Digitate) contained mainly vuggy, intercrystalline and negligible moldic; microfacies C (Chaotic) no thin section was made and microfacies D (Brown Laminated Centimeter Scale Cycle) contained vuggy, moldic, intercrystalline, interparticle, and fracture. Vuggy porosity is common in the different microfacies. Microfacies D contained more types of porosity probably accounting for its better values, its better permeability values can be explained by touching vug pores i.e., vugs were connected by intercrystalline porosity. Microfacies B (Digitate) had a lot of separate vug porosity but intercrystalline porosity connected some vugs accounting for its increase in permeability.

Microfacies A had mainly separate vug pores with little connectivity via intercrystalline and fracture pores because of drusy calcite infilling. There was no

preference for a specific porosity type in the microfacies. It was also difficult to determine a clear trend in porosity and permeability of individual microfacies by looking at all the wells. However, a trend was found in the porosity and permeability of individual microfacies in individual wells (Table 4). It was found that microfacies A in all wells, presented itself as a potential barrier or baffler since it is relatively less porous and permeable, sandwiching microfacies that are relatively more porous and permeable. Overall, finding a trend in permeability and porosity values of microfacies in the field was difficult due to varying degrees of diagenesis from well to well but it is possible to find microfacies trend within individual wells. Of importance also is the percentage of dark brown micrite quantified in each microfacies. Microfacies A and C had the most micrite and generally had the lowest porosity whereas, microfacies B and D had the least amount of micrite and had relatively better porosity values.

The microbial origin of these buildups was established with evidence collected through core description, thin section, and SEM. Both core description of polished slabs and petrographic analysis were used to delineate the thrombolite facies into microfacies and subfacies. Thin sections reveal ostracods, gastropod, and foraminifera. Four sponge spicules in total were found in microfacies D (Brown Laminated Centimeter Scale) in different thin sections taken from wells P#16223, P#16237 and P#16327B (Figure 48). These three wells were drilled in the same mound in the northeastern part of the field (Figures 14 and 16). Features diagnostic of preserved sponge bodies in cores were very vague, such as ostium/osciculum, mammilion.

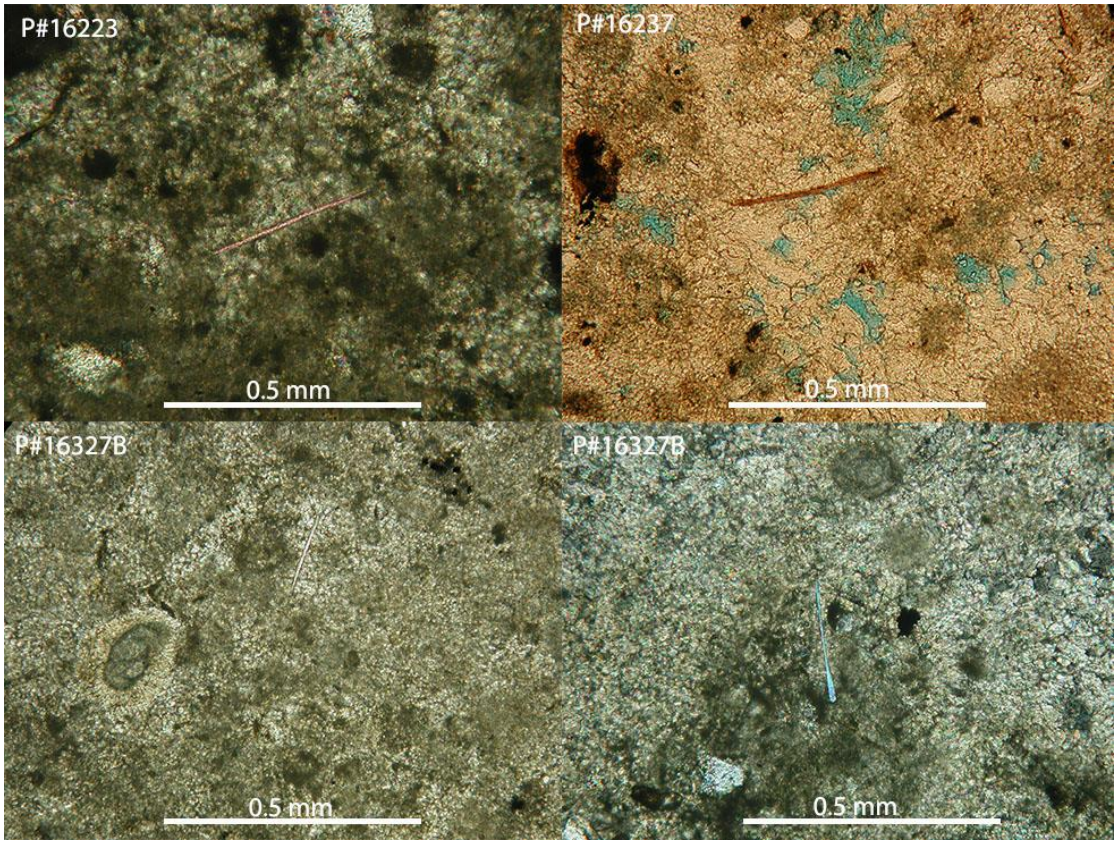

Figure 48 Four spicules were found in thin sections taken from microfacies D. Thin section P#16237 is not in cross polarized light. The spicule sizes range from 0.25 to 0.375 mm.

In these same thin sections, peloids arranged in dendritic patterns encrust leached substrates similar in shape to stromatoporoids were identified, but because the original internal morphology of the substrate was totally destroyed leaving only its outline, it is impossible to determine definitively. In any event the evidence for sponges and stromatoporoid in this buildup was minimal.

In contrast, abundant evidence suggests a microbial origin for this thrombolithic buildup. The most abundant microbial component are peloids (size mm), many of which are arranged in vaguely or clearly dendritic structures which, branch upwards. These

form local patterns and in some places clusters producing shrub growth forms of which all are indicative of microbial influence. The shrub growth forms are densely packed peloids that branch upwards. This pattern occurs because the microbes when alive were composed of a colony of unicellular, soft bodies wrapped in a soft to sticky mucilaginous sheath which either trapped peloids or created and environment conducive to their precipitation. That sticky mucilaginous sheath also tapped small organisms that lived in the water column. As the microbes grew upwards or towards sunlight, it continuously produced peloids and captured organisms.

After death of the microbes, its soft body deteriorated leaving behind the typical dendritic arrangement of the preserved building blocks that were once held suspended in the mucilaginous sheath. In polished sections of core, other microbial building blocks visible included nodules of tangled, spaghetti-like filamentous strands similar to the calcimicrobe, *Giravanella*. Another calcimicrobe- like feature identified in polished slab and in thin section are *Renalcis- like* distinct stacked, saccate chambers with alternating bands separating each chamber. Also of microbial or algal origin were laminae forming stromatoids layers that encrusted random pieces of peloidal micrite between laminae layers. Stromatoids refers to the component laminae of stomatolites i.e. sets of laminae, not to the stromatolitic head (Monty, 1977).

The modern analogies for these microbial structures include green algae growing in lakes, which result in laminated layers. Another analogy is from the deep ocean where mineralized “rusticules” on the bow of the sunken Titanic is precipitated by microbes (Figure 49). These analogies can help explain microfacies D (Brown Laminated, Centimeter-Scale Cycle) lacey appearance formed by the multiple laminae layers and its

good porosity. On the lake's surface the algae appears puffy and denser however, in the water the algae is net-like or lacey and very porous giving it a low biomass. When it becomes mineralized in the water column it may have a similar appearance to microfacies D. The lake is shallow and is a low energy environment. The "rusticules" on the Titanic are made of layers of delicate, porous, knob-like mounds of rust that look like icicles. The rusticules were also formed in a low energy environment, over two miles underwater. The similar lacey appearance of microfacies D to the rusticules and lake algae suggests a low energy environment of deposition for this microfacies.

Figure 49 A possible explanation for the formation of microfacies D (Brown Laminated Centimeter Scale Cycle) using modern analogies of algae in lake (right) and microbes in the deep ocean (bottom left).

Additional evidence for a microbial origin includes cores with crust. The distribution of crust on top of dark brown, peloidal micrite framework indicative of heterotrophic bacteria that either mark the end of active microbial framework development by forming as late stage veneer on the micrite framework or growth in cryptic habitats forming firstly a veneer of non-skeletal, clean, homogeneous, fine-grained calcite crust on the microbial framework before secondly, transitioning into more peloidal crust stacked in a vague dendritic pattern (Figure 50). Each stage of crust development is separated by laminae. Thin, long, clear filament strands (1-2 mm long) were present protruding from the crust.

Cryptic habitats can be isolated to semi-isolated enclosed cavities formed by voids within the microbial framework where illumination is poor. Heterotrophic bacteria is restricted to cryptic habitats because they can use organic compounds scavenged from living hosts or dead organic matter as an energy source since light as an energy source for organisms (photophilic) is low to absent in cryptic habitats. Studies on preserved crusts found on coral reef in SE Spain and coral-algal- microbialite reef in SW Tahiti determined that the non-skeletal, fine-grained microfabric with minor allochthonous silt-sized peloids and local microbial filaments, infer a bacterial origin for the crusts (Riding, 2011b).

Crust formation in cryptic habitats according to this study, was due to competition for substrate/framework space by photophilic eukaryotic organisms, relegating heterotrophic bacteria to available dark, framework cavity space. Also, the position of crust overlying a succession of increasingly sciaphilic (shade-loving) skeletal organisms

marks the closing stage of framework growth. Crusts can therefore strengthen microbial framework and reduce cavity volume.

The crust from microfacies D (Brown Laminated Centimeter Scale) and the above mentioned study were compared (Figure 50). Similarities found in crust in microfacies D are: fine-grained non- skeletal microfabric, subordinate peloids, microbial filaments, crust form as overlying veneer on microbial framework, two types of crust (homogeneous and peloidal), sub-parallel laminae separating each type of crustal development, and crust reducing cavity volume.

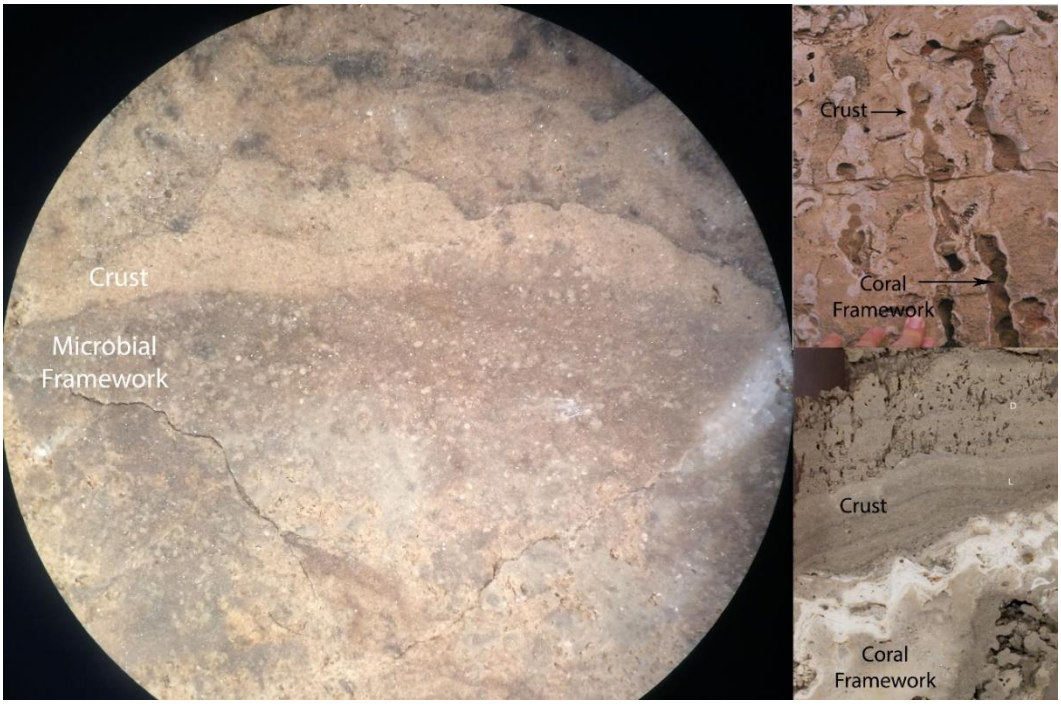

Figure 50 Crust in all the photos were produced by heterotrophic bacteria.

Left, crust in microfacies D forms a veneer on microbial framework and infills available cavity space. The crust transitions from homogeneous calcite to crust with peloids and laminae. Both crusts are separated by a thin, black layer. Top right, strengthening of framework by crust forming veneer on dissolved *Porites* coral branches. Bottom right, cavity volume reduction by two types of crust, dendritic (D) and laminated (L) growing on framework (Photos on right taken from Riding, 2011).

Lastly, in well P#14270 SEM imaging was able to capture what appear to be individual calcimicrobe spheres that are oval-shaped, have a rough, mottled texture that looks clotted and measure approximately 1µm. This texture on calcite's surface is associated with bacterial activity as previously explained by Frankel and Bazylinski (2003) whereby, biomineralization is stimulated in microbial carbonates due to the secretion of metabolic byproducts by bacteria extracellularly such as on the cell walls or exopolymers (slimes, sheaths, biofilms) to precipitate minerals randomly on the external cell walls. The fabric of the limestone will be clotted and finely peloidal (Flügel, 2010). Also found in association with the spheres were bare filament strands linking broken pieces of mottled calcite and an exposed, segmented, 3µm long algal tubule mold partially encased by mottled calcite. The algal mold may represent calcite-filled tubules that formed as endolithic borings. Algal tubules are indicative of the photic zone and form by precipitating a sheath of calcite around filaments.

A tangled filament nodule identified in core P#14270 microfacies A, was compared in thin section, core, and SEM image to strengthen microbial identification in the various medium used (Figure 51). The nodules in longitude view both in core and thin section had similar features such as a compact base, long tangled filament strands, and micritic rim surrounding the filaments. Core photographs of the same nodule in cross section and longitudinal view both show the outer micritic rim however, in cross section view of the filament nodule, it appears as a micritic rim surrounding a white calcite area with numerous holes. The diameter of the holes are similar in size to the width of a filament strand suggesting the strands formed the holes. In SEM image, holes and filament are present and maybe related to similar features found in core and thin section.

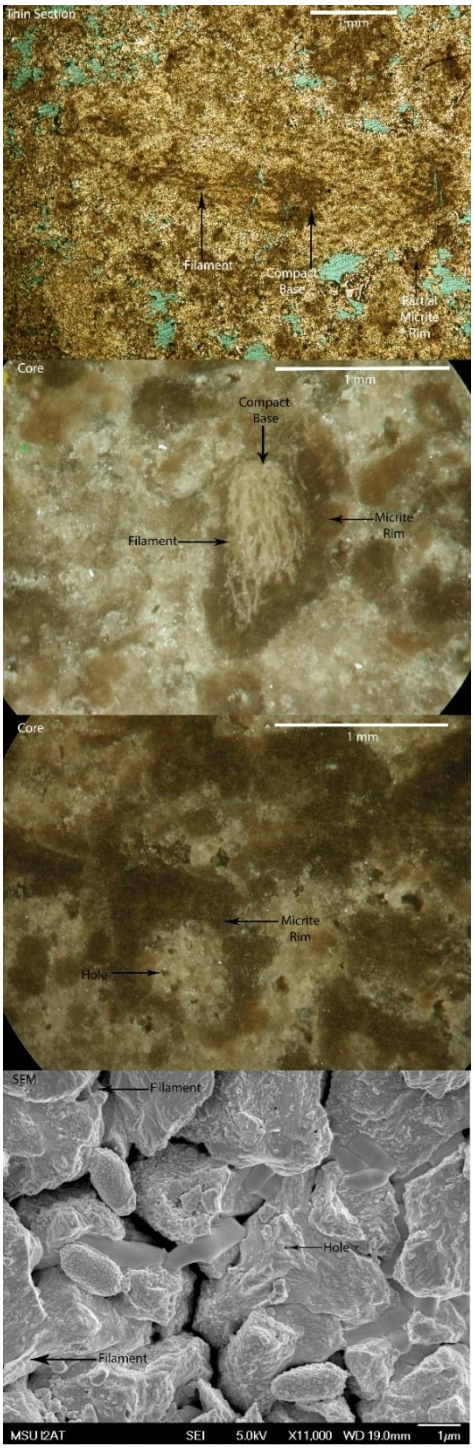

Figure 51 Filament nodule's appearance in different mediums (thin section, core, SEM).

The ability to observe the filament nodule in these different mediums (thin section, photomicrographs and SEM) have been helpful in being able to identify the nodules in different views such as, longitudinal and cross section view also, how the nodules interact with the surrounding calcite in 2D and 3D. All of this evidence points heavily to microbial influence for the thrombolite buildup.

The final and strongest evidence for a marine origin of these buildups is in the form of isotopic data that shows a marine origin for the earliest components of these buildups. The two objectives in this study were demonstrated through core, thin section, SEM, and isotope analysis. The first objective was to retrieve milled samples from the cores for oxygen and carbon isotope analysis to determine if the microbial buildups were influenced by fresh water or sea water. Isotopic ^{18}O and ^{13}C data show that thrombolite buildups are marine in origin since the samples taken from the established primary framework and microbial building blocks had ratios that plotted on Hudson's 1977 diagram in region 8, as common marine limestone.

The depleted or negative ^{18}O values of -4.0, -2.4, -4.1 and -5.1 (‰ VPDB) imply a relative increase in the lighter isotope ^{16}O associated with decreasing salinity and higher temperatures. During the Jurassic "greenhouse" climate governed this period, globally glacial and ice sheet melt waters enriched in ^{16}O had already been deposited into seawater circulation from the last glacial period. Also, a regional transgression brought about by oceanic crust emplacement in the Gulf of Mexico was occurring, this probably improved connectivity and sea water circulation between the restricted embayment and the emerging gulf thus accounting for the salinity decrease. The ^{13}C values of 4.0, 3.8, 3.1 and 3.2 (‰ VPDB) are positive or enriched with the heavier ^{13}C isotope which is

close to sea water ^{13}C values of near 0‰ suggesting precipitation near isotopic equilibrium of the original sea water.

These positive values are also reflective of marine shell dissolution values. In cores foraminifera, ostracods, and tube-shaped fossils which once habited this water, stored this isotopic data in their shells. Also, in thin sections microcoprolite produced by *Thallasinoides* shrimp, would have passed along these isotopic signatures from their diet and onto their fecal organic matter. Lastly, the photosynthesizing microbes would have preferentially taken up the lighter ^{12}C isotope therefore contributing to ^{13}C enrichment. The negative oxygen and positive carbon isotopic ratio of the samples clearly shows that sea water was responsible for the thrombolite buildups.

Conclusion

The results from the microfacies delineation supports the hypothesis that the thrombolite buildups in the Smackover Formation in the Little Cedar Creek Field can be divided into four microfacies based on petrographic analysis. Their distribution is predictable to some extent based on porosity and permeability data and the occurrence of mounds and intermounds.

1. Four dominant microfacies were identified and given descriptive names: Microfacies A- Black *Renalcis*-like Layer, Microfacies B- Digitate, Microfacies C- Chaotic, Microfacies D- Brown Laminated Centimeter Scale Cycle. For the core described, the percentage of microfacies is: Microfacies A (Black *Renalcis*-like Layer) 52.7%, Microfacies B (Digitate) 24.6%, Microfacies C (Chaotic) 6.0%, and Microfacies D (Brown Laminated Centimeter Scale Cycle 16.7 %.

2. The thrombolite mound that makes up the Little Cedar Creek field consist of high (mounds) and low areas. Mounds are mainly made up of microfacies A (Black *Renalcis*-like Layer and D (Brown Laminated Centimeter Scale Cycle) which constitutes 52.7% and 16.7% respectively of the core described. Mound thickness varies from 39 to 50 feet based on cross sections. The range of thickness for individual microfacies that makeup the mounds are: microfacies A (Black *Renalcis*-like Layer), 3 to 32 feet; microfacies C (Chaotic), 2 to 8 feet and microfacies D (Brown Laminated Centimeter Scale Cycles), 1 to 8 feet. Low areas between the mounds are mainly made up of microfacies B (Digitate) which has thicknesses of 3 to 26 feet.

3. Porosity and permeability data shows a range of 2 to 16.83% and 0.087 to 930 millidarcies respectively. Microfacies A: 2.2 to 9% and 0.087 to 60 millidarcies. Microfacies B: 2 to 16.83% and 5 to 930 millidarcies. Microfacies C: 6.25% and 0.17 millidarcies. Microfacies D: 10.4 to 11.3% and 115 to 592.3 millidarcies. Microfacies A (Black *Renalcis*-like Layer) was the relatively least porous and permeable, acting as a potential barrier to flow in contrast to other overlying and underlying microfacies that are relatively more porous and permeable. Microfacies D (Brown Laminated Centimeter Scale Cycles) was the most porous and permeable. Also, the greater the amount of dark brown micrite a microfacies contains, the lower its porosity.

4. Thin section, cores and SEM confirm evidence of microbes responsible for each microfacies buildup. Microfacies A (Black *Renalcis*-like Layer): peloids arranged in dendritic structures, tangled filamentous nodules, long filament strands, mottled calcimicrobe spheres, and algal tubules. Microfacies B (Digitate): peloids arranged in dendritic to clotted shrubby structures, *Renalcis*- like to *Epiphyton*-like saccate, dendritic structure. Microfacies C (Chaotic): long filament strands. Microfacies D (Brown Laminated Centimeter Scale Cycles): peloids arranged in clotted shrubby structures around substrate, long filament strands, and heterotrophic bacterial crust.

5. Micritic components of the rock determined by sequential or crosscutting relationships to be primary constituents were sampled for isotopic analysis and isotopic ratios show depleted or negative values for ^{18}O ranging from -2.4 to -5.1‰ VPDB and enriched or positive values for ^{13}C ranging from 3.1 to 4.0 ‰ VPDB, suggesting a marine origin, which is consistent with observed fossils and microbial structures.

REFERENCES

Ahr, W.M., 2009, Microbial Carbonates as Hydrocarbon Reservoirs. American Association of Petroleum Geology.

An Overview of the Little Cedar Creek and Brooklyn Fields, Geological Survey of Alabama, State Oil and Gas Board, 2012, http://www.gsa.state.al.us/documents/misc_ogb/lcc_overview.pdf (accessed March 17, 2016).

Arkansas Oil and Gas Boom Towns, American Oil and Gas Historical Society, 2015, http://aoghs.org/states/arkansas-oil-and-gas-boom-towns (accessed March 17, 2016).

Arp, G., Reimer, A., and Reitner, J., 2001, Photosynthesis- induced biofilm calcification and calcium concentrations in Phanerozoic oceans. Science 292, p. 1707- 1704.

Baria, L., 2011, Abstract: A Status Report on Little Cedar Creek Field, Conecuh County, Alabama, The Largest Smackover Field Discovered in the Last 40 Years. Mississippi Geological Society, v. 59, no. 8, p. 5.

Baria, L. R., and Heydari, E., 2012, Late Jurassic Microbiolite Reservoirs of Southwestern Alabama, Little Cedar Creek Field: A Core Presentation. AAPG Hedberg Conference Microbial Carbonate Reservoir Characterization, Houston, TX.

Bawden, T.M., Einaudi, M.T., Bostick, A.M., Wooden, J., Norby, J.W., Orobona, M.J.T., and Chamberlain, C.P., 2003, Extreme 34S depletions in ZnS at the Mike gold deposit, Carlin Trend, Nevada: Evidence for bacteriogenic supergene sphalerite. Geological Society of America, v. 31, p. 913- 916

Benson, D.J., 1985, Diagenetic controls on Reservoir development and quality, Smackover Formation of Southwest Alabama. Gulf Coast Association of Geological Societies Transactions v. 35, p. 317-326.

Broecker, W.S., 1982, Glacial to Interglacial Change in Ocean Chemistry. Progress in Oceanography, v. 11(2), p. 151-197

Couradeau E, Benzerara K, Gérard E, Moreira D, Bernard S, Brown Jr., G.E, and Lopez-Garcia, P., 2012. An early-branching microbialite cyanobacterium forms intracellular carbonates. Science. V.336, p. 459–462.

Crevello, P.D., and Harris, P.M., 1984, Depositional models for Jurassic reefal buildups: *in* Proc. Of the Third Annual Research Conf., Gulf Coast Section, Soc. Econ. Paleontologists and Mineralogists: Jurassic of the Gulf Rim, p. 57-102.

Day, K.L., and Parcell, W.C., 2013, Development of Upper Jurassic microbialite buildups in the Little Cedar Creek and Brooklyn Fields and possible embayment wide microbolite buildups in southwest Alabama. Geological Society of America, v. 45, p.106

De Wet, Carol, B., Frey, Holli, M., Gaswirth, Stephanie, B., Mora, Claudia, I., Rahnis, Michael, and Bruno, Caroline, R., 2004, Origin of Meter-Scale Submarine Cavities and Herringbone Calcite Cement in a Cambrian Microbial Reef, Ledger Formation (USA). Journal of Sedimentary Research, v. 74. No. 6, p. 914- 923.

Dunham, R. J., 1962, Classification of carbonate rocks according to depositional texture. In: Ham, W. E. (ed.), Classification of carbonate rocks: American Association of Petroleum Geologists Memoir, p. 108-121.

Flugel, E., 2010, Microfacies of Carbonate Rocks, Berlin Heidelberg, Springer, p. 984

Folk, R.L., 1974, Petrology of Sedimentary Rocks, Texas, Hemphill Publishing Company, p. 190.

Frankel, R. B., and Bazylinski, D.A., 2003, Biologically induced mineralization by bacteria. Reviews in Mineralogy and Geochemistry 54.1 (2003): 95-114.

Galloway, W.E., 2009, Gulf of Mexico: GeoExPro, v. 6

Haddad, S.A., and Mancini, E.A., 2013a: Reservoir Characterization, modeling, and evaluation of Upper Smacker microbial carbonate and associated facies in Little Cedar Creek field, southwest Alabama, eastern Gulf coastal plain of the United States. AAPG, V.97, NO. 11, p. 2059-2083

Haddard, S.A., and Mancini, E., 2013b, Little Cedar Creek Field: Reservoir Characterization to Simulation. A Geologic and Engineering Case Study of an Upper Jurassic Microbial Carbonate Reservoir in Southwest Alabama. AAPG, v.97/11, p.2059-2083.

Hazzad, R.T., 1939, Notes on the Comache and Pre-Comache? Mesozoic formations of the Ark-La-Tx area, and a suggested correlation with northern Mexico: Shreveport Geological Society Guide Book to 14th Annual Field Trip, p. 155-178.

Heydari, E., and Baria, L., 2005, A Conceptual Model for the Sequence Stratigraphy of the Smackover Formation in the North-Central U.S. Gulf Coast. Gulf Coast Association of Geological Societies Transactions, v. 55, p. 321-340.

Heydari, E., and Baria, L.B., 2006, Reservoir Characteristics of the Smackover Formation at the Little Cedar Creek Field, Conch County, Alabama. Gulf Coast Association of Geological Societies Transactions, v. 56, p. 283-289.

Hudec, M.R., Norton, I.O., Jackson, M.P.A., and Peel, F.J., 2013, Jurassic evolution of the Gulf of Mexico salt basin: AAPG, V.97, P. 1683-1710

Hudson, J.D., 1977, Stable Isotopes and Limestone Lithification. Journal of the Geological Society of London, v. 133, p. 637- 660

Kirkland, B.L., Dickson, J.A.D., Wood, R.A., and Land, L.S, 1998, Microbialite and Microstratigraphy: The Origin of Encrustations in the Middle and Upper Capitan Formation, Guadeloupe Mountains, Texas and New Mexico, U.S.A. Journal of Sedimentary Research, vol. 68, p. 956-969

Lieber, R.B., 1989, Abstract: Practical model from the Smackover Formation: Gulf Coast Association of Geological Societies Transactions, v. 39, p. 183-186.

Mancini, E.A., Mink, R.M., Bearden, B.L., and Wilkerson, R.P., 1985, Norphlet Formation (Upper Jurassic) of southwestern and offshore Alabama: Environments of deposition and petroleum geology: American Association of Petroleum Geologists Bulletin, v. 69, p. 881-898.

Mancini, E.A., M. Badali, T.M., Puckett, T.M., Parcell, W.C., and Llinas, J.C., 2001, Mesozoic carbonate petroleum systems in the northeastern Gulf of Mexico, Petroleum Systems of Deep-Water Basins: GCS-SEPM Foundation 21st Annual Research Conference, p. 423-451.

Mancini, E.A., Lil, P., Goddard, D.A., and Zimmerman, R.K., 2005, Petroleum Source Rocks of the Interior Salt Basins, North Central and Northeastern Gulf of Mexico: American Association of Petroleum Geologists, v. 55, p. 486-504.

Mancini, E. A., Parcell, W.C., and Ahr, W. M., 2006, Upper Jurassic Smackover Thrombolite Buildups and Associated Nearshore Facies, Southwest Alabama. Gulf Coast Association of Geological Societies Transactions, v. 56, p. 551- 563

Mancini, E.A., Parcell, W.C., Ahr, W.M., Ramirez, V.O., Llinas, J.C., and Cameron, M., 2008, Upper Jurassic updip stratigraphic trap and associated Smackover Microbial and nearshore carbonate facies, eastern Gulf Coastal Plain, USA: American Association of Petroleum Geologists Bulletin, v.92, p. 49-434.

Monty, C.L.V., 1995, The Rise and Nature of carbonate mud-mounds: an introductory actuality approach, *in* Monty, C.L.V., Bosence, D.W.J., Bridges, P.H., and Pratt, B.R., eds., Carbonate Mud- Mounds; Their Origin and Evolution: International Association of Sedimentologists, Special Publication 23, p. 11-48

Nagarajan, R., Sial, A.N., Armstrong-Altrin, J.S., Madhavaraju, J., and, Nagendra, R., 2008, Carbon and Oxygen Isotope Geochemistry of Neoproterozoic Limestones of the Shahabad Formation, Bhima Basin, Karnataka, Southern India. Revista Mexicana de Ciencias Geologicas, v. 25, p. 225- 235

Nelson, C.S., and Smith, A.M., 1996, Stable Oxygen and Carbon Isotope Compositional Fields for Skeletal and Diagenetic Components in New Zealand Cenozoic Nontropical Carbonate Sediments and Limestones: A Synthesis and Review. New Zealand Journal of Geology and Geophysics, v. 39, p. 93-107

Oehler, J.H., 1981, Abstract: Carbonate source rocks in the Jurassic Smackover trend of Mississippi, Alabama, and Florida: Houston Geological Society Bulletin, v. 23, p. 4- 4.

Parcell, W.C., 1999: Stratigraphic Architecture of Upper Jurassic (Oxfordian) Reefs in the Northeastern Gulf Coast, U.S. and the Eastern Paris Basin, France: Gulf Coast Association of Geological Societies Transactions, v. XLIX

Pickering, K.T, and Owen, T.A., 1997, An Introduction to Global Environmental Issues- Second Edition. Publisher: Routledge, p. 51-52

Prather, B.E., 1992, Evolution of a late Jurassic carbonate/evaporate platform, Conecuh embayment, northeastern Gulf Coast, U.S.A.: American Association of Petroleum Geologists Bulletin, v. 76, no. 2, p. 164-190.

Pratt, R. Brian, 1984, Epiphyton and Renalcis- Diagenetic Microfossils From Calcification of Coccoid Blue-Green Algae: Journal of Sedimentary Petrology, v. 54, no. 3

Prothero, R. Donald and Schwab, Fred, 2004, Sedimentary Geology Text Book, Mcmillan Publisher, p. 225.

Rezende, M.F., Tonietto, S.N., Pope, M.C., 2013: Three-dimensional pore connectivity evaluation in a Holocene and Jurassic microbialite buildup. AAPG, v. 97, p. 2085-2101.

Riding, R., and Toomey, Donald Francis, 1972, The sedimentological Role of Epiphyton and Renalcis in Lower Ordovician Mounds, Southern Oklahoma: Journal of Paleontology, vol. 46, no. 4.

Riding, R., 1991, Calcified Algae and Bacteria, A.Y. Zhuravlev and R. Riding, The Ecology of the Cambrian Radiation, New York: Columbia University Press, p. 445-473.

Riding, R., 2000, Microbial carbonates: the geological record of calcified bacterial-algal mats and biofilms. Sedimentology (2000) 47 (Suppl. 1), 179-214.

Riding, R., 2011a, Calcified cyanobacteria. *Encyclopedia of Geobiology.* Encyclopedia of Earth Science Series, Springer, Heidelberg, pp.211-223.

Riding, R, 2011b, Reefal microbial crusts In D. Hopely (ed.), Encyclopedia of Modern Coral Reefs. Encyclopedia of Earth Sciences Series, Springer, Heidelberg, p. 911-915

Riding, R., 2012, A hard life for cyanobacteria. Science, v. 336, p. 427-428.

Rindsberg, A.K., and Kopaska-Merkel, D.C., 2013, Paleoecology and Diagenesis of Parafaverina ziczac isp. Nov., a Crustacean Microcoprolite from the Upper Jurassic (Oxfordian) Smackover Formation of Alabama. Bulletin Alabama Museum Natural History 31, v.2, p. 74-93.

Salvador, A., 1987, Late Triassic-Jurassic paleogeography and of Gulf of Mexico basin: AAPG, v. 71, p. 419-451.

Salvador, A., 1991, The Geology of North America: The Gulf of Mexico Basin. The Geological Society of America, v. J, p. 128-180, 389-444.

Schlager, W., 1992, Sedimentology and sequence stratigraphy of reefs and carbonate platforms.-Continuing Education Course Notes, 34, 71pp.

Tedesco, W.A., 2003, An Eolian Facies within the Upper Jurassic Smackover Facies Formation, Tchula Lake field, Mississippi. American Association of Petroleum Geologists.

Tonietto, S., and Pope, M., 2013, Pore Type Characterization, Petrophysical Properties, and Diagenesis of Jurassic Thrombolite Reservoirs. American Association of Petroleum Geologists: Geoscience Technology Workshop, Revisiting Reservoir Quality Issues in Unconventional and Conventional Resources: Techniques, Technologies and Case Studies, Austin, Texas.

Tonietto, S.N., Smoot, M.Z., and Pope, M., 2014, Pore type characterization and classification in carbonate reservoirs. American Association of Petroleum Geologists.

Wade, W.J., and Moore, C.H., 1993, Jurassic Sequence Stratigraphy of Southwest Alabama. Gulf Coast Association of Geological Societies, v. 43, p. 431-443

Wurster, M. C., Patterson, P.P., Cheatham, M.M., 1999, Advances in micromilling techniques: a new apparatus for acquiring high-resolution oxygen and carbon stable isotope values and major/minor elemental ratios from accretionary carbonate. Computers and Geosciences 25 (1999), p.1159-1166.